FABRICATION OF METALLIC GLASS $Fe_{81} B_{13.5} Si_{3.5} C_2$ RIBBONS AND STUDY OF ITS THERMAL STABILITY

A Thesis Submitted
in Partial Fulfilment of the Requirements
for the Degree of
MASTER OF TECHNOLOGY

by

PRATAP **KUMAR** ROY

to the
MATERIALS SCIENCE PROGRAM
INDIAN INSTITUTE OF TECHNOLOGY KANPUR
August 1986

BAPI, MA ''!

স্মানেব চোন শেষ নাই,
শানাব চেষ্টা বৃথা তাই॥

' হীবক বাবাব দেশে '
সত্যজিৎ বায়

Source of Knowledge will Never be Dry
No Point Giving it a   Useless Try

' Hirak Rajar Deshey '

Satyajit Ray
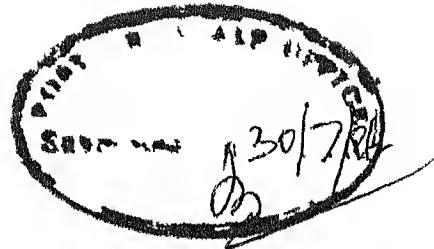
CERTIFICATE

Certified that this work on 'FABRICATION OF METALLIC GLASS $Fe_{81}B_{13.5}Si_{3.5}C_2$ RIBBONS AND STUDY OF ITS THERMAL STABILITY' has been carried out under our supervision and that it has not been submitted elsewhere for a degree

D C Agarwal
Assistant Professor
Material Science Program
I I T Kanpur

K.P Gupta
Professor
Material Science Program
I I T Kanpur

Date July 30, 1986

ACKNOWLEDGEMENT

LIST OF FIGURES

FIGURE NO   FIGURE   PAGE

FIGURE NO   FIGURE   PAGE

LIST OF TABLES

ABSTRACT

Fe-B-Si-C metallic glasses are both scientifically and technologically important However the research as well as the use are often handicapped by already processed material received from other sources without known previous thermal history or the very narrow ribbons prepared in the laboratory

In the present study, reasonably wide ribbons have been produced using an existing single roller melt spinning aparatus and the process has been standardized The range of different process parameters have been identified The time and temperature path difference between the state of molten metal and the final amorphous state seems to be important in achieving an amorphous state The jet turbulence of the molten metal, on the other hand affects the physical properties of the prepared ribbons

The prepared ribbons have been tested with X-ray and TEM to confirm their amorphous nature.

The prepared ribbons have been subjected to both isothermal and dynamic heat treatments They have been tested by both calorimetric and electrical resistance vs temperature experiments It has been found that the crystallization process is passing through a series of multistep,

overlapping reactions   The melt spun ribbons have not
been found to be crystallized even after annealing well
beyond crystallization temperature for several minutes
Contrary to general belief, structural relaxation has been
found to enhance the crystallization temperature   It also
affects the crystallization process itself   Relaxed samples
show up either some old intermediate reactions already
present but are camouflaged by structural disorder or are
passing through new intermediate reactions   It has also been
found that even after a high annealing to 310oC for 25 minutes
the relaxation of the as melt spun sample is negligible   On
the contrary a 60 minuite anneal at the same temperature almos
relaxes the sample   Moreover even a single thermal cycle
through a temperature near but below crystallization start
temperature relaxes the sample completely   The samples,
subjected to different heat treatments do not loose the
ductility   The structural relaxation helps in increasing the
magnetization process as well as increass the Curie temperature

Two and most probably a third fine, reversible chang
similar to CSRO, have been found below crystallization
temperature

LIST OF CONTENTS

CHAPTER I

INTRODUCTION

To enquire the limits of non-equilibrium crystallization, Paul Duez and his co-workers first started the technology of metallic glass preparation in 1960 in a rudimentary way   After this, it went into hybernation till 1973, when commercial production of metallic glasses started in pilot plants in U S A and Japan   The advent of technology started the curiosity of both technologists and scientists and it reached skyhigh limits during the later part of '70s and early '80s, as is evident from the number of personnel involved in research and the number of conferences organised From a technologist's stand point, the presence of high hardness coupled with high tensile strength, remarkable resistance to corrosion makes this class of materials an important conter der for future use   Particularly in case of magnetic metallic glasses, the easy and high magnetization, coupled with low magnetic loss, makes it and ideal and potential candidate in all the spheres where soft magnetic properties are useful Future use, among others, envisages the miniaturization of airborne transformers and lucrative space use. From scientific point of view, the field holds intellectual challanges to find out the nature of magnetization processes involved in amorphous systems, the process of work hardening, the nature

of structural and internal disorders and provides an oppor-
tunity to test whether all the laws developed for crystalline
materials, particularly the age old concept of dislocation
movement, hold good for amorphous systems too Or in other
words, the study of amorphous state opens up the possibility
of finding out the fundamental nature of these laws and if
not, developed a more unified and fundamental concept

Even though the most common and favourite process
of metallic glass formation, the single roller melt spinning
process, seems to be a relatively simple one, the number of
process parameters involved, the short time of fabrication,
the achievement of severe quenching rate of more than 10^6oC/
minute, till now makes it extremely difficult to produce
standard, continuous and wide metallic glass ribbons Hence
the field still offers enough challenge to produce standardized
glasses as well as enquire the effects of different process
parameters The extreme thinness, of the order of 25 to 80
microns and the severe quenching rate produce in the amor-
phous metallic material inherent instability and throws up
interesting effects in the properties For any practical use
the nature and the limits of such instabilities and the ways
to overcome them cannot be over emphasized These structu-
ral relaxation can produce important changes in the properties
and behaviour of the material For example, all the literature
involving the crystallization behaviour of metallic glasses,
assumes a structurally relaxed state just prior to crystalli-
zation. It is important to investigate whether this is really

so and if not whether the structural relaxation affect the
crystallization and to what extent   During such structural
relaxation, changes involving topological short range order
(TSRO) and chemical short range order (CSRO) have been obser-
ved for many metallic glasses

In this work, first it has been tried to
produce reasonably wide, continuous and uniform metallic
glass ribbons of Fe_{81} $B_{13\ 5}$ $Si_{3\ 5}$ C_2 equivalent to Allied
Chemical's Metglas 2605Sc Secondly   crystallization as
well as structural relaxation behaviour, the effect of latter
on the former, have been studied with as melt spun metallic
glasses with or without different types of heat treatment
The instability and consequent structural relaxation of the
metallic glass ribbons, have been studied using DSC and
electrical resistance techniques   Magnetic properties namely
Curie temperature and magnetization have been studied using
the Vibrating Sample Magnetometer   And of course the amor-
phous nature has been confirmed by TEM and X-ray analysis

Chapter II deals with the literature survey
involving metallic glass preparation, the crystallization
behaviour and structural relaxation involving TSRO and CSRO
Chapter III deals with the experimental conditions used
Chapter IV gives the experimental observation and finally
Chapter V discusses the results obtained.

CHAPTER II

LITERATURE SURVEY

II 1   Fabrication of Metallic Glass Ribbo

There are several ways to melt spin an alloy to produce amorphous metallic ribbons   One of the most common methods employs a single roller chill block on which a jet of molten metal is made to impinge   Generally the material is heated to or above the liquidous temperature in a quartz or ceramic crucible having a suitable orifice at its end   The molten metal is forced through the orifice of the crucible on to a rotating chill block, generally made of copper or steel   Under appropriate process conditions a glassy metallic ribbon is formed by the solidification of jet at the rotating substrate   Fig 1 describes the essential process

The broad principles of glass formation appear to be as follows   The fabrication technique should cool the glass forming melt at a rate faster than its'critical quench-ing rate' so that crystallization can be avoided   It also should cool the melt to a final temperature which should be at least lower than its crystallization temperature or pre-ferably below its glass transition temperature (T_g) The first principle ensures that an amorphous state is achived   The second ensures that the glass is recoverable at room temper-ature   Several attempts have been made to explain the modes
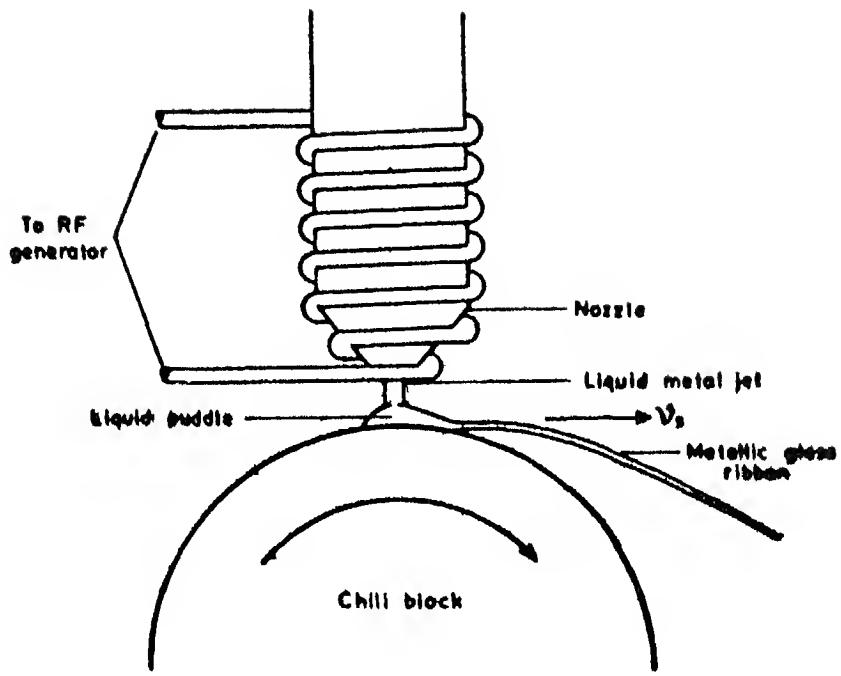
Figure 1   Schematic view of melt spinning apparatus

of ribbon formation and their correlation with the available experimental data [1]   Kavesh [2] has described two possible modes of ribbon formation, namely, (i) transport dominated ribbon formation and (ii) energy equilibrium ribbon formation   In transport dominated ribbon formation two limiting cases and a mixed case have been distinguished   These are (a) thermal transport being the controlling factor (b) momentum transport being the controlling factor and(c) a coupled thermal and hydrodynamic regime controlling the ribbon formation   If thermal transport is much faster than momentum transport, a solid boundary layer will form adjacent to the chill surface and propagate into the melt puddle to form the ribbon   In this case the materials within the frozen layer will be in motion with the chill surface   Outside the frozen layer a sharp velocity transition zone will exist   Finally in the outer zone, there will be a slight momentum transport If momentum transport from the chill surface is much faster than thermal transport, a liquid boundary layer will be dragged out of the melt puddle by the moving substrate to solidify further downstream   The velocity gradient will be continuous across the depth of the puddle

In energy equilibrium mode the ribbon is formed by the wetting of the substrate   The dimensions of the molten puddle and therefore the ribbon dimensions, are determined by the equilibrium of kinetic energy, surface energy and viscous dissipition of the jet, puddle, chill surface

and the air boundary layer in motion with the chill surface

In the laboratory scale, the formation of glassy metal and the ribbon geometry depend mainly on the material parameters and process parameters   In the material parameters, the selection of suitable alloy system is the most important criterion for metallic glass formation   A single parameter which is shown to be useful in expressing the glass forming Tendency (GFT) of an alloy system is the reduced glass transition temperature(T_{gr}) which is the ratio of the glass transition temperature T_g and melting point T_m Davis [3] has shown that the alloy which has a $T_{gr} > 0.45$ can be cast to metallic glass successfully   Pure metals with $T_{gr} < 0.25$ can not be quenched to glassy state under the usually achieved cooling rates (10^4-10^8oC/ second)   Davis [4 and 5] reported that at a cooling rate of more than 10^{10} oC/ second, partly glassy Ni foils can be produced only if Ni has a trace of oxygen in it   Glass formation in the case of alloys appears to be favoured if the compositions are near eutectic compositions   Glass forming binary alloys, mainly transition or noble metals, containing 15 to 30/ semimetals or alloys of inter-transition metals such as Nb-Ni and Cu-Zr have been studied extensively   All the glass forming alloys seem to have two common features, a negative heat of mixing indicating a strong interaction between constituent atoms and relatively low melting temperature   In case of binary alloys the critical quenching rate seems to be around 10^6oC/ second or higher   Addition of a third of a fourth alloying

element, which exibits different crystalline symmetry, enhances
to a great extent the ease of formation of glasses mainly by
lowering the melting point (Table 1). For example Pd-Cu-Si,
Pd-Ni-P, Pt-Ni-P alloys having a critical cooling rate of
10^2 oC/ second [6] can be cast in glassy rod form of 1 to 3mm
diameter   Table 1 lists some of the glass forming alloys

In the process level, the important parameters
which control the formation of glassy state seem to be the
cooling rate, the decree of supercooling (i e , the initial
temperature of molten jet and the final temperature of the
substrate) and heterogenious nucleation rate. These factors
in turn are governed by the volumetric flow rate of the melt
through the nozzle, length of the nozzle, distence between
chill surface and nozzle tip, surface velocity of the chill
block, polish and cleanness of the chill surface [7-9]
Libermann [7] has given an emperical relationship   Q=Wts
applicable for a low value of volumetric flow rate upto
4×10^3 mm/ second where W is the width of the ribbon (mm), t is
the thickness of the ribbon (mm), s is the linear speed of
rotating chill block (mm/second) and Q is the volumetric flow
rate (mm^3/ second)   At higher values of Q, upto 7×10^3
mm^3/second, the relationship between ribbon dimension and
casting conditions can be best explained by Kavesh's [2]
energy equilibrium model   Q is varied by varying orifice
length   Pavuna [1] and Libermann [7] have shown that the
relationship of W and Q is linear   This linearity has been

TABLE 1

Metallic glass forming systems

Group	Representative system	Typical composition (atom %)	Typical system	T_m (oC)	T_g (oC)	T_x (oC)	$r_{A,B}$
Early transition metal/noble metal + metalloid	Pd–Si,Co–P, Fe–P–C, Ni–P–B, Au–Si,	15–25 metalloid	$Au_{81}Si_{19}$	1336	290	280	0 92
Early transition metal + late transition metal/ Cu	Zr–Cu,Y–Cu, Ti–Ni,Nb–Ni, Ta–Ni,	30–65 Cu 40–65 Ni 30–40 late transition metal	$Cu_{60}Zr_{40}$	1800	740	760	1 23
Early transition +Li, Mg group	(Ti Zr) Be	20–60 Be	Zr–Be	2050	–	–	0 73
Actinide +early transition metal	U–V,V–Cr	20–40 (early transition metal)	–	–	–	–	–
Ternary systems	–	–	$Au_{78}Ge_{14}Si_8$	632	297	305	–
	–	–	$Pd_{77}Cu_6Si_{17}$	1009	636	675	–
	–	–	$Pt_{56}Ni_{24}P_{20}$	770	485	642	–
	–	–	$Fe_{80}P_{13}C_7$	1220	720	710	–

T_x = Crystalization temperature oC

$r_{A,B}$ = Ratio of the diameter of tne bigger atom to that of the smaller atom

9

verified(Fig 2) by Agarwal and Chalachary [10] Pavuna [1]
also noted that Q has to be kept constant in a given melt
spinning run so that the ribbon edges do not become uneven

Fig 3 shows the effect of ejection pressure on
the glass formation for the $Fe_{14}B_5Si_3C_1$ alloy system [11]
The figure indicates that the square root of ejection press-
ure is directly proportional to ribbon thickness and ribbon
surface finish and after a limiting value, which is dependent
on nozzle slot breadth, the ribbon thickness is maximum and
the pressure has no further effect on the formation of glass
The ejection pressure is generally applied just after the
required heating of the melt   Agarwal and Chakachary [10]
have found that with a circular orifice diameter greater
than 1 mm the ejection of melt takes place before the press-
ure is applied

During practical experiment to produce
metallic glass ribbons, the problem of oxidation during melt
spinning in air is very important, As pointed out by
Agarwal and Chakachary [10], the major factor which governs the
oxidation of melt spun ribbon is the distance between the chill
block and the nozzle   They hold the view that the above ment-
ioned distance at the upper bound is limited by the chance of
melt oxidation and freezing during the flow of the molten
metal from nozzle to substrate   At the lower bound, the
distance is limited by the chance of nozzle end hitting the
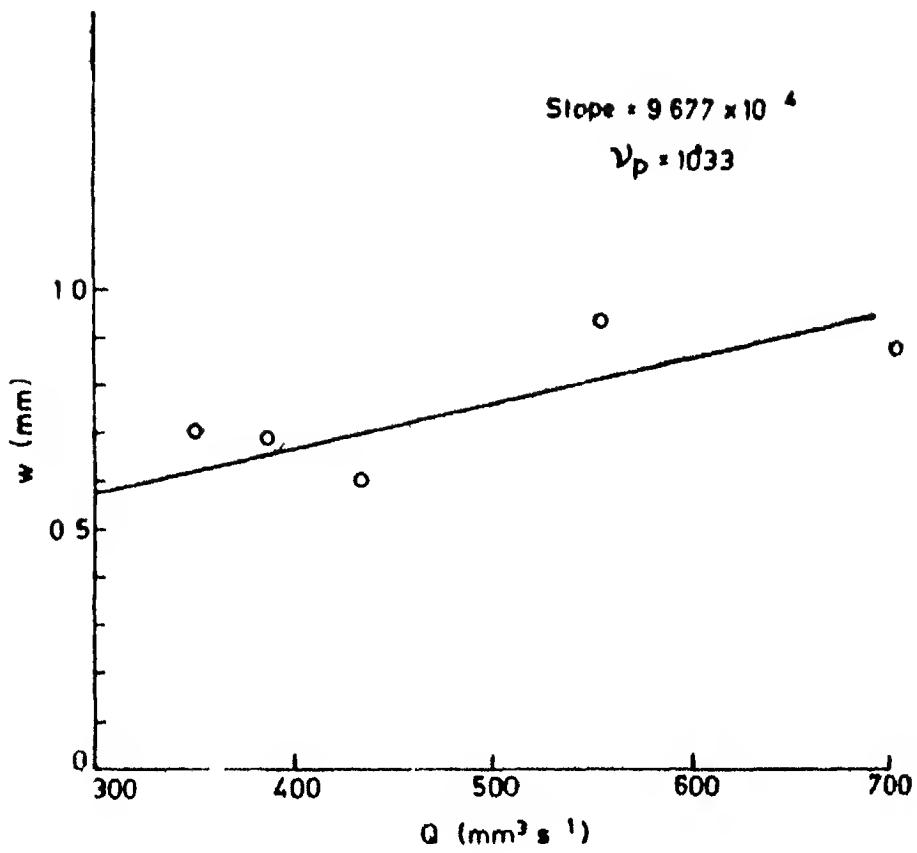
Figure 2   Effect of the volumetric flow rate on
the width of the ribbon
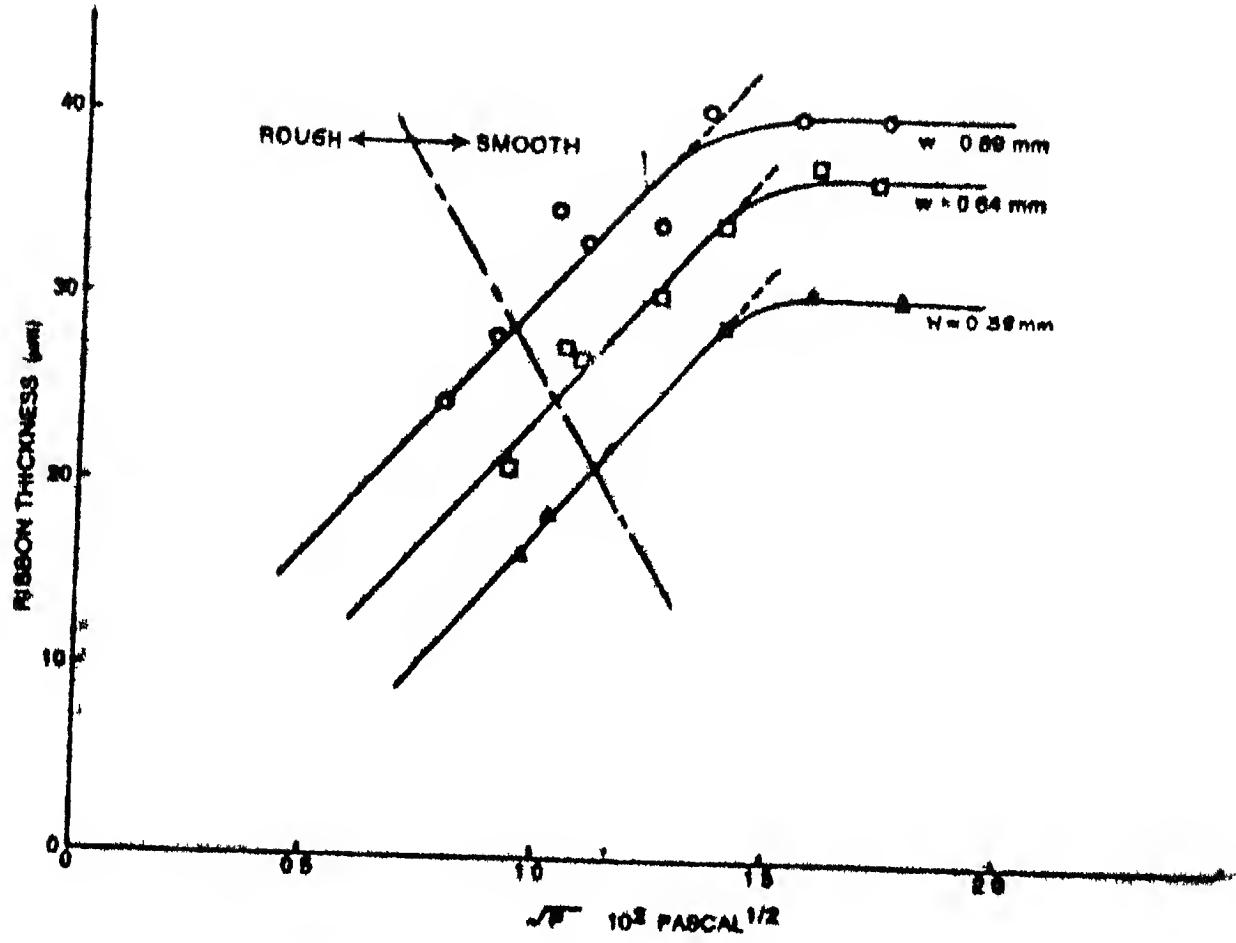
Fig 3   Ribbon thickness and ribbon surface finish
as a function of the squared root of ejection
pressure P, measured in three nozzle slot
breadth w

substrate because of the vibrations present in the wheel

On the basis of the above observation, Agarwal and

Chakachary [10] have recommended an optimum distance of

1 mm between the nozzle tip and the rotating substrate   For

circular nozzles,Pavuna [1] has given a thumb rule for

optimum distance to be equal to four times the diameter of the

orifice of the nozzle

The jet impingement angle or more specifically

the angle of the nozzle to the wheel surface is maintained

at 90o   Libermann [7] has shown that if the angle is changed,

it only results in the reduction of the width of the ribbon

without any other compensating advantage   Pavuna [1] has

shown that the chill surface has to be clean in order to avoid

the possibilities of heterogeneous nucleation   This observa-

tion of Pavuna has been supported by Agarwal and Chakachary [

II 2 Crystallisation

From a technological standpoint, thermal
stability of metallic glasses is an important parameter
for their use   More recently the interesting properties
of microcrystalline alloys have also focussed the attention
on crystallization of amorphous metallic alloys   There is
also the fundamental interest in developing a uniform theory
of amorphous and crystalline states   All these have generated
an interest in the study of amorphous to crystalline transfor-
mation of metallic glasses

Experimental evidence points to the fact that amor-
phous to crystalline transformation occurs through nucleation
and growth and is essentially a diffusion controlled process
Depending on the amount of chemical species present, the tran-
sition from amorphous to crystalline state can occur in any
of the three modes   1) Polymorphic   2) Eutectic or Eutectoid
and   3) Primary [12,13]   The nature of the diffusion can
be short range, intermediate or long range [13]

Polymorphic transition   In the Fe-B system,
for B concentration more than 16 atomic percent, the trans-
formation of amorphous $Fe_{75}B_{25}$ to Fe_3B is a Polymorphic
transformation (Fig 4c) [14]   In these cases the parent
amorphous phase $Fe_{75}B_{25}$ is transforming to Fe_3B without a
marked change in concentration   The product, in general,
may be in a supersaturated stable or metastable state   The

(a)

$a-Fe_{86}B_{14}$

primary crystallization

(b)

$a-Fe_{80}B_{20}$

eutectic crystallization

(c)

$a\ Fe_{75}B_{25}$

polymorphous crystallizaton

$\alpha-Fe$

$\alpha-Fe\ Fe_3B$

Fe_3B

$\alpha-Fe$ Fe_3B

Fe_2B $\alpha-Fe$ $\alpha-Fe$

crystallization
of Fe-B alloys
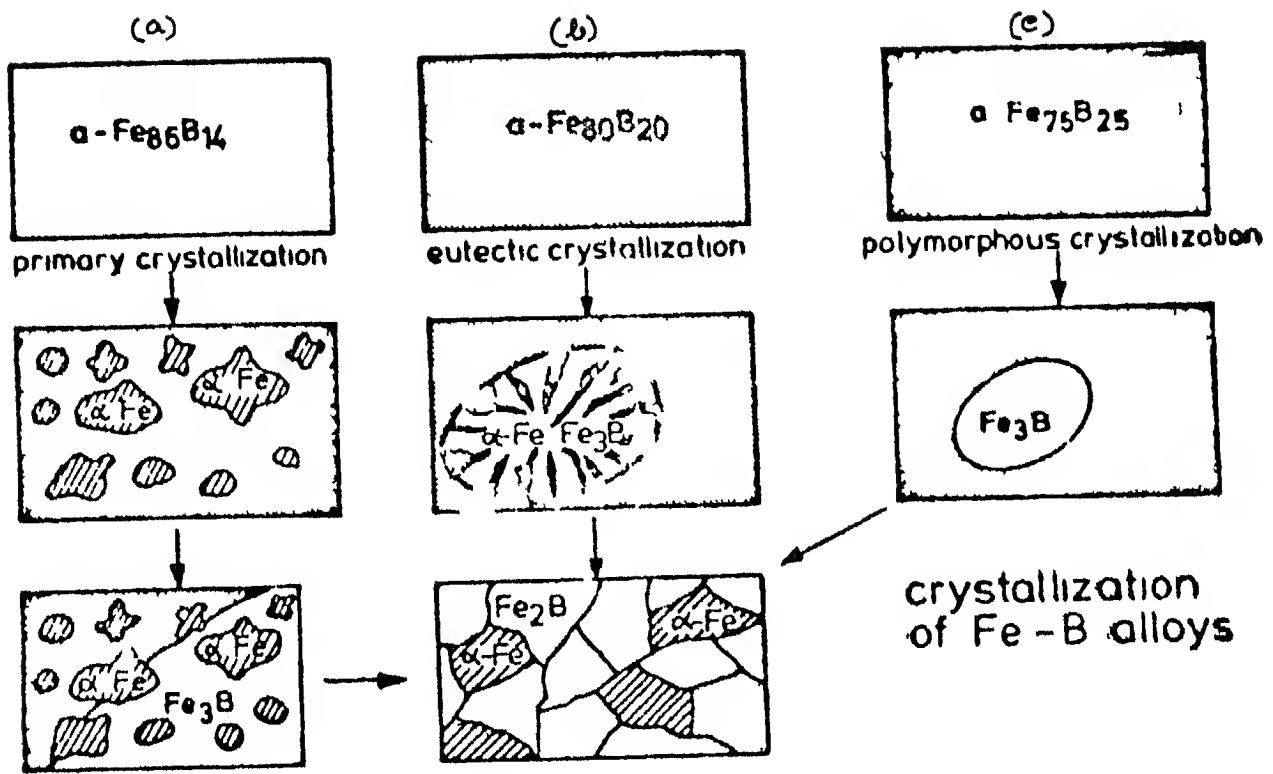
Figure 4   Schematic diagram of typical crystallization
modes in Fe-B metallic glass alloys depending
on chemical compooition on the parent amorphous
phase

diffusional atoms are jumping across the transformation
front   Hence, a short range diffusion is taking place
In general the polymorphic type of transformation occurs
in the concentration range of pure elements or stoichio-
metric compounds

Eutectic/ Eutectoid transformation   In
Fe-B system with B concentration 17-20 atomic percent, α-Fe
and Fe_3B precipitate out simultaneously from amorphous
matrix at 500oC [14]   At higher temperatures, further break-
down of Fe_3B occurs   In analogy to the transformation of
crystalline material into two product phases simultaneously,
the transformation of an amorphous phase $Fe_{80}B_{20}$ into two
product phases α Fe and Fe_3B (Fig 4b) is called a Eutectoid
or Eutectic type of transformation   Here an intermediate
range diffusion of atoms is taking place   Hence, this process
is slower than polymorphic transformation

) Primary transformation   In Fe-B system,
with B concentration less than 16 atomic percent, the cryst-
allization behaviour can be explained by primary crystall-
ization   The amorphous $Fe_{86}B_{14}$ alloy initially precipitates
α-Fe between 300oC to 450oC [14] (Fig 4a) At a higher
temperature of 550oC, Fe_3B starts to crystallize from B
enriched matrix   At a still higher temperature, the Fe_3B
crystals decompose into α-Fe and Fe_2B In general, in this
type of transformation, the product crystalline phase is

substantially different from the parent amorphous phase

In the as produced amorphous metallic state, it is expected that the material is highly unstable and on heating it should go through some changes and finally crystallization should occur In considering the crystallization process, an ideal metastable state i e a state of complete structural relaxation is generally assumed to have been achieved before reaching the crystallization temperature Hence, at least, theoratically, the effect of quenching rate, state of stress etc ,are not expected to influence crystallization behaviour When the amorphous materials are subjected to dynamic tests such as DTA,DSC and measurement of change in electrical resistance with change in temperature etc , the factors like state of stress, effect of quenching rate etc,, however are expected to influence crystallization The time elapsed before crystallization, which depends on the heating rate employed, may not be sufficient to take the specimen to an ideal metastable state before crystallization It has been observed that in majority of the cases, the investigators work with specimens obtained from sources like Allied Chemicals, U S A Depending on the manufacturing conditions such as quenching rate, superheating etc and storage time, the specimens of the same composition may show somewhat different crystallization characteristics The effect of the above mentioned parameters on the crystallization process as well as on the structure and stability of metallic glasses have

not been thoroughly investigated Higher quenching rate and
higher superheat are expected to increase the level of ther-
mal stress as well as chemical and structural disorders
Hence, an acceleration in crystallization is to be expected
Contary to this expectation, however, crystallization in
$Fe_{40}Ni_{40}B_{20}$ glasses do not start from the ribbon surface which
was in contact with the cold substrate [15] In this case,
crystallization starts from the free surface which is less
severely quenched than the surface in contact with rotating
substrate This somewhat unexpected recrystallization
behaviour obtained in $Fe_{40}Ni_{40}B_{20}$ metallic glass ribbon has
been suggested to be due to the lack of critical size and
number of quenched in nuclei This state of quenched in
nuclei is important since these act as a trigger in the
crystallization process

The crystallization of amorphous $Fe_{81}B_{13.5}Si_{3.5}C_2$
(Metglas 2605Sc) has been studied extensively [16 to 19]
since it is an important material from engineering point of
view. The Fig 5 illustrates the DSC data obtained by
Swartz et al [16] on Metglas 2605Sc The heating rate used
in this experiment is 10oC/ minute The dip in the DSC trace
near 377oC has been interpreted to be due to Curie tempera-
ture The two distinct exothermic peaks, at 497oC and 532oC
indicate at least a two stage crystallization in this material
The X-ray diffraction results of Swartz et al [16] are shown
in Fig 6 The X-ray patterns are obtained with several
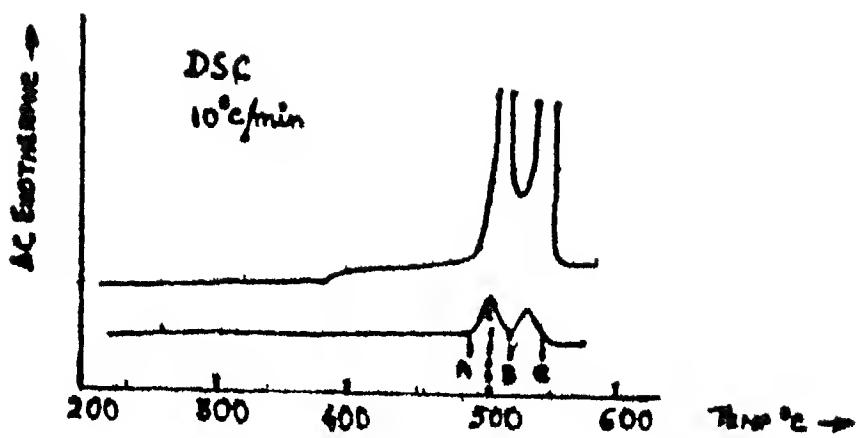
Figure 5   DSC recording of as received Metglas 2605 Sc
(The upper trace is a 10 fold expansion of
lower one)
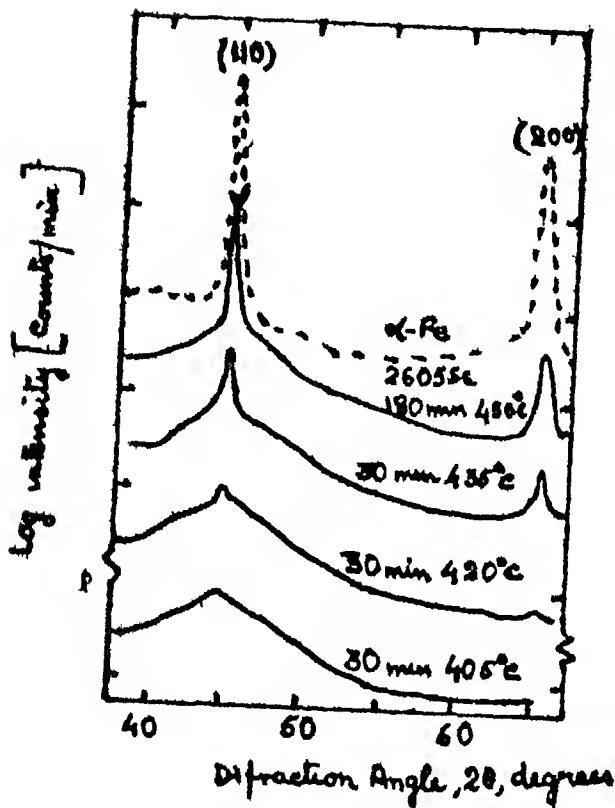
Figure 6   X- ray diffraction spectra of isothermally
annealed samples of 2605 Sc along with an α-Fe
pattern for comparison

Metglas 2605Sc specimens annealed for 30 minutes at diff-
erent temperatures   Fig 6 also indicates an X-ray diff-
raction pattern of pure α Fe   The amorphous state of the
as obtained material is characterized by the appearence of
a broad intensity maximum between 40o to 50o diffraction
angles (2θ)   The results indicate that on 30 minute annea-
ling α Fe peaks begin to appear and even after 3 hours
annealing at 450oC, the broad peak due to amorphous state
does not completely vanish   However, after 7 hours of
annealing at 450oC, the diffraction pattern show   complete
crystallization with the appearance of only α Fe and Fe_3B
diffraction lines   On the basis of DSC and XRD data,
alongwith TEM and coercivity data Swartz et al [16] propo-
sed that α Fe is the first phase to crystallize , Then Fe_3B
nucleates heterogeneously and consumes the remaining amor-
phous matrix   Saegusa and Moris [17,18] studied Metglas
2605Sc, using Mossbauer technique after isochronally annea-
ling the specimens from room temperature to 487oC (20 minutes
to reach 487oC from room temperature) and upto 722oC (50
minutes to reach 722oC)   Their results can be summerized
as follows   The Curie temperature is reported to be 397oC
(397$\pm$ 2oC)   At 417oC, the first crystallization product,
Fe and 4 atomic percent Si precipitates out   Between 432oC
and 437oC, a quasistable amorphous phase, with composition
$Fe_{75\ 2}B_{18\ 2}Si_{3\ 2}C_{2\ 4}$ has been reported   At 442oC, the
second crystallization of Fe_2B starts and the amorphous

matrix, within the temperature range of 442oC to 457oC,
assumes another quasistable state   The composition of this
quasistable state is somewhat uncertain but it has been
suggested to be $Fe_{76\ 0}B_{17\ 3}Si_{3\ 0}C_{3\ 7}$ In the event of
complete precipitation of C as Fe_3C, the composition of
the quasistable state may also be $Fe_{16}B_{20\ 3}Si_{3\ 8}$ The
amount of Fe_3C however, is too small to be detected Above
457oC, the crystallization continues till it is completed
at 507oC Above 527oC, an ordering transformation in the
crystallized Fe + 4 atomic percent Si occurs   The final
crystallized product have been suggested to be Fe + 7 atomic
percent Si, Fe_2B and Fe_3C, the amount of Fe_3C being too small
Bhanu Prasad and Bhatnagar [19] have studied the crystalliza-
tion behaviour of Metglas 2605Sc, employing DTA, electrical
resistivity with change in temperature and Mossbauer studies
DTA results(Fig 7)show that crystallization occurs at around
452oC, in agreement with what has been observed by Swartz
et al (Fig 5)   But unlike Swartz et al Bhanu Prasad et al
find that crystallization process give rise to three
thermal effects between 452oC to 627oC The first two peaks
at 487oC and 507oC are the most prominent ones and a third
peak is at 577oC The first two peaks appear at   slightly
lower temperatures than what has been found by Swartz et al [16
Fig 8 shows the dependence of electrical resistivity relative
to ρ_{2oC} Initially electrical resistivity increases linearly
with temperature   At 452oC, the temperature around which
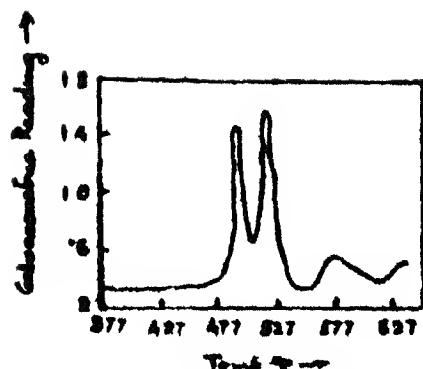
Figure 7 DTA of Metglas 2605Sc over temperature
range of 377oC to 627oC
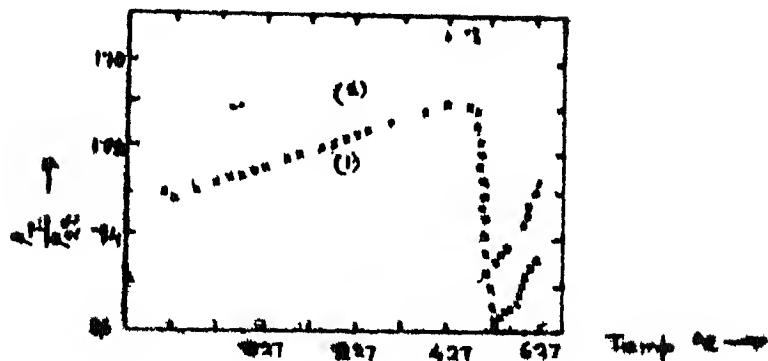
Figure 8 Resistivity ratio (T)/ (2) vs temperature(oC)
of Metglas 2605Sc
(Curve (b) represents the reproducibility of
curve (a) when repeated with a fresh sample).
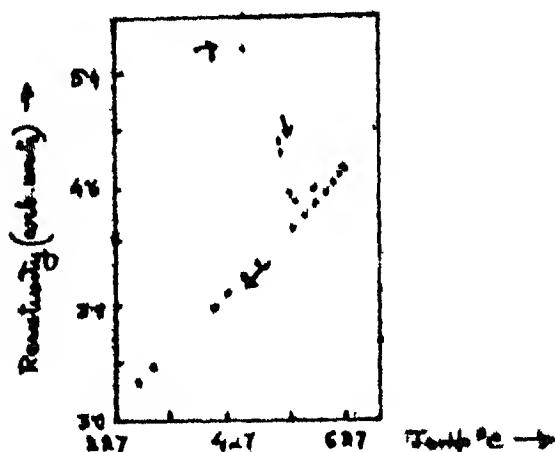
Figure 9 Electrical resistivity as a function of
temperature for Metglas2605Sc between 227oC to627oC.

crystallization begins, a rapid change of slope occurs and
from about 477oC, relative resistivity decreases very rapidly
with increase in temperature   At around 535oC, the tempera-
ture at which the second peak in DTA occurs, the relative
resistivity again begins to increase   A further change in
slope of relative resistivity vs temperature occurs at
$\smile$ 552oC which corresponds to the temperature at which the
third DTA peak begings   After crystallization, when the
specimen is cooled, ρ (T) follows a different path as shown
in Fig 9 which is typical of crystallized samples   Through
Mossbauer studies and XRD work Bhanu Prasad et al have tried
to interpret the observed thermal effects and electrical
resistivity changes in terms of formation of specific
products during crystallization process   The thermal
effect in the temperature range of 452 to 507oC has been
attributed to the precipitation of pure α-Fe phase till a
compositionally stable amorphous phase is achieved   (The
α phase, in the terminology of Sageusa and Moris [17] as
well as Bhanu Prasad et al [19] means almost pure α Fe [20].
The second peak in DTA trace, approximately between 507o
and 537oC is attributed to crystallization of the composi-
tionally stable amorphous phase   It is observed that the
two DTA peaks almost overlap each other   This may be
interpreted in the following way   As soon as pure α-Fe
is precipitated the remaining amorphous phase starts crysta-
llizing which is completed at 537oC   The third peak at 577oC
is possibly due to the precipitation of pure α-Fe or a new

$Fe_{100-X} Si_X$ phase   The final crystallization products are given to be α Fe, Fe_2B and a magnetic $Fe_{23}(CB)_6$ or an alloy of $Fe_{100-X}Si_X$ alongwith a small amount of Fe_3C. The Curie temperature for Metglas 2605Sc has been given to be 425oC ($\pm$1) which is comparatively higher than that determined by Swartz et al [17]

II.3 Structural Relaxation

A very high quenching rate, generally of the order of 10^4oC per second or more   is employed in preparing metallic glasses   This high quenching rate enables the alloy to bypass crystallization and attain an amorphous state   During quenching, the atoms have insufficient time to relieve the high temperature atomic configurations   As a result, the as quenched alloy remains in a highly metastable state   When this highly metastable amorphous alloy is heat treated, the quenched in structure will tend to relax to a more stable state   Several concepts to describe the features of atomic process involved in structural relaxation have been proposed [21-25]

The concept of excess free volume is a very well known and common concept to describe structural relaxation in polymorphic glasses [21-23]   The free volume in glassy state is analogous to the concept of vacancy in crystalline state   The equilibrium free volume present in glassy state is directly proportional to temperature and is related to viscosity   As the liquid is cooled, the free volume is

decreased with an increase in viscosity However the decrease in free volume requires time as the 'excess free volume' somehow has to reach the surface [21-22] Hence the rate of change of viscosity, which is dependent on diffusivity, determines the rate of annealing out of the excess free volume If the temperature is dropped quickly to or below glass transition temperature (T_g), a high viscosity, usually 10^3 poise at T_g, is reached Because of the high viscosity and insufficient time, all the free volume can not reach the surface As a result, excess free volume will remain trapped in the structure During structural relaxation, the excess free volume is expected to anneal out

        Egami [24], however has disputed the above concept of structural relaxation of metallic glasses through 'annealing out of excess free volume' process proposed by Turnbull and Cohen [25] In a study of $Fe_{40}Ni_{40}P_{14}B_6$ glass, Egami has shown that well below T_g, a rather extensive atomic rearrangement, involving collective movement of a large number of atoms, takes place Inspite of this large rearrangement of atoms, the corresponding change in volume is very small [24] On the basis of the above consideration, Egami has introduced the concept of structural defects, more or less analogous to crystalline metals, to explain structural relaxation In this concept it has been assumed that below T_g, the excess free volume captured in the glassy system collapses leaving internal strains around it. The centre

of these strains is considered equivalent to defects in crystalline materials For structural relaxation, the mechanism proposed assumes that the defects go on trans-forming and redistributing themselves to more stable low energy configurations, probably by splitting up into smaller and more stable defects Ultimately they become a part of the stable amorphous structure This change is an irrever-sible and exothermic change

Using energy dispersive X-ray diffraction (CDXD) analysis of $Fe_{40}Ni_{40}P_{14}B_6$ glasses, Egami [24] has shown that the structural relaxation involves an extensive change in short range order of basic structural units which are consi-dered to remain unaffected themselves except for some slight distortions The change in short range order thus involves only change in relative configuration of these units with respect to each other It is not dependent on the chemical identities of the atoms in each structural unit Hence this type of short range order has been called topological short range order (TSRO) Available information [24-29] suggests that the relaxation due to TSRO is slow and occurs over a wide range of temperature TSRO results in the reduction of creep and stress relaxation rates [26-27], decrease in internal friction [28] as well as densification of the alloy [29]

In amorphous metallic alloys, another kind of change in short range order with change in temperature is

observed   This is due to a change in short range correlation
of different chemical species   In contrast to the irrever-
sible, relatively slow relaxation characteristics of TSRO,
the chemical short range order (CSRO) is found to be rever-
sible, and relatively fast   It usually occurs within a
relatively narrow temperature range [30,31]   However, the
existance of CSRO, has not been proved directly since the
conventional X-ray diffraction techniques are rather diffi-
cult to use for this purpose [24]   The evidence of the
presence of CSRO is through indirect means such as property
changes observed during magnetic transition, electrical resis-
tivity, and elastic modulus measurements   For example, it
has been found that if $Fe_{27}Ni_{53}P_{14}B_6$ is cyclically annealed
for 60 minutes at $250oC$ and 30 minutes at $300oC$, a change in
Curie temperature (T_c) is observed [32]   The change in T_c
is totally reversible for eight annealing cycles (Fig 10)
[32]. Electrical resistance measurements as a function of
temperature has been done for a large number of systems
These are classified in three groups, namely metal-metal
system, multimetal-metalloid system and monometal-metalloid
system   The electrical resistance change with temperature
is shown in Fig 11 [33] for a large number of metal-metal
systems   Similarly the electrical resistance change with
temperature is shown for a large number of multimetal-meta-
lloid systems, in Fig 12 [33]   In all the systems studied
(Figs 11 and 12) a variation of relative resistance with
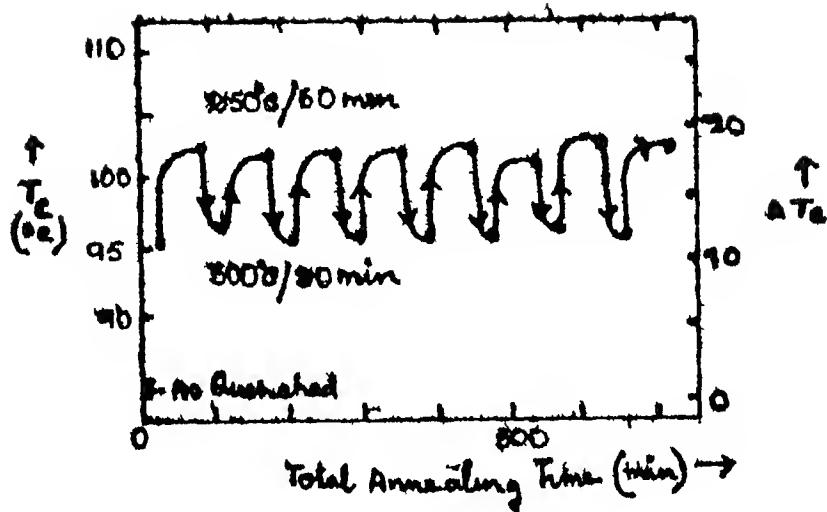
Figure 10   Changes in Curie temperature of $Fe_{27}Ni_{53}P_{14}B_6$ during cyclic annealing at $300^{\circ}C$ for 30 minutes and $250^{\circ}C$ for 120 minutes over eight cycle indicating that the changes are totally reversible
(Curves connecting data points are guides for the eye and does not represent the true kinetics of change)
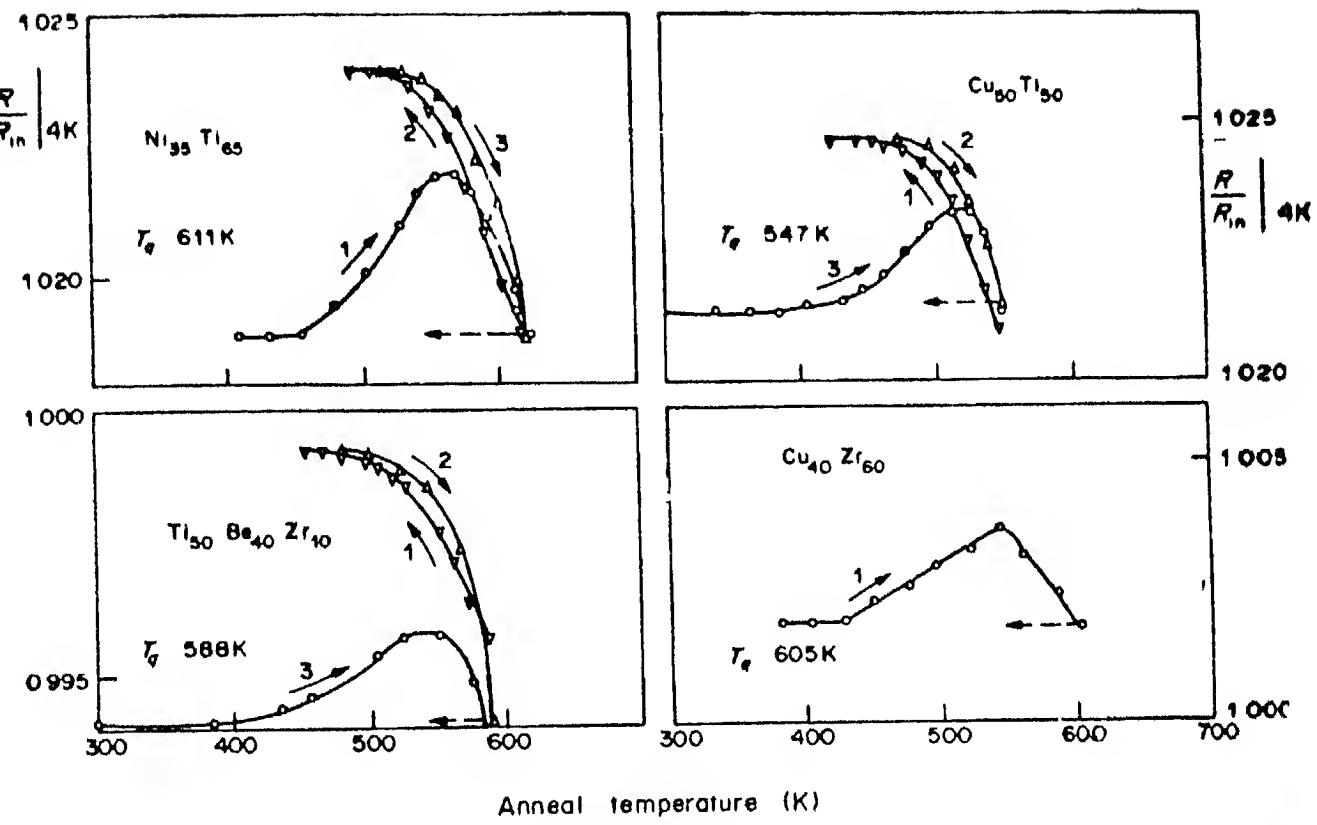
Fig. 11 Evolution of the electrical resistance during isochronal up and down temperature cycles or heat up anneals after a quench from the maximum temperature preceded by a ten minute anneal at this temperature (All curves were normalised with respect to the initial resistance in the as received condition The duration of every anneal is 10 min The symbols ∇ and Δ are for anneals conducted at decreasing and increasing temperatures respectively in this figure)
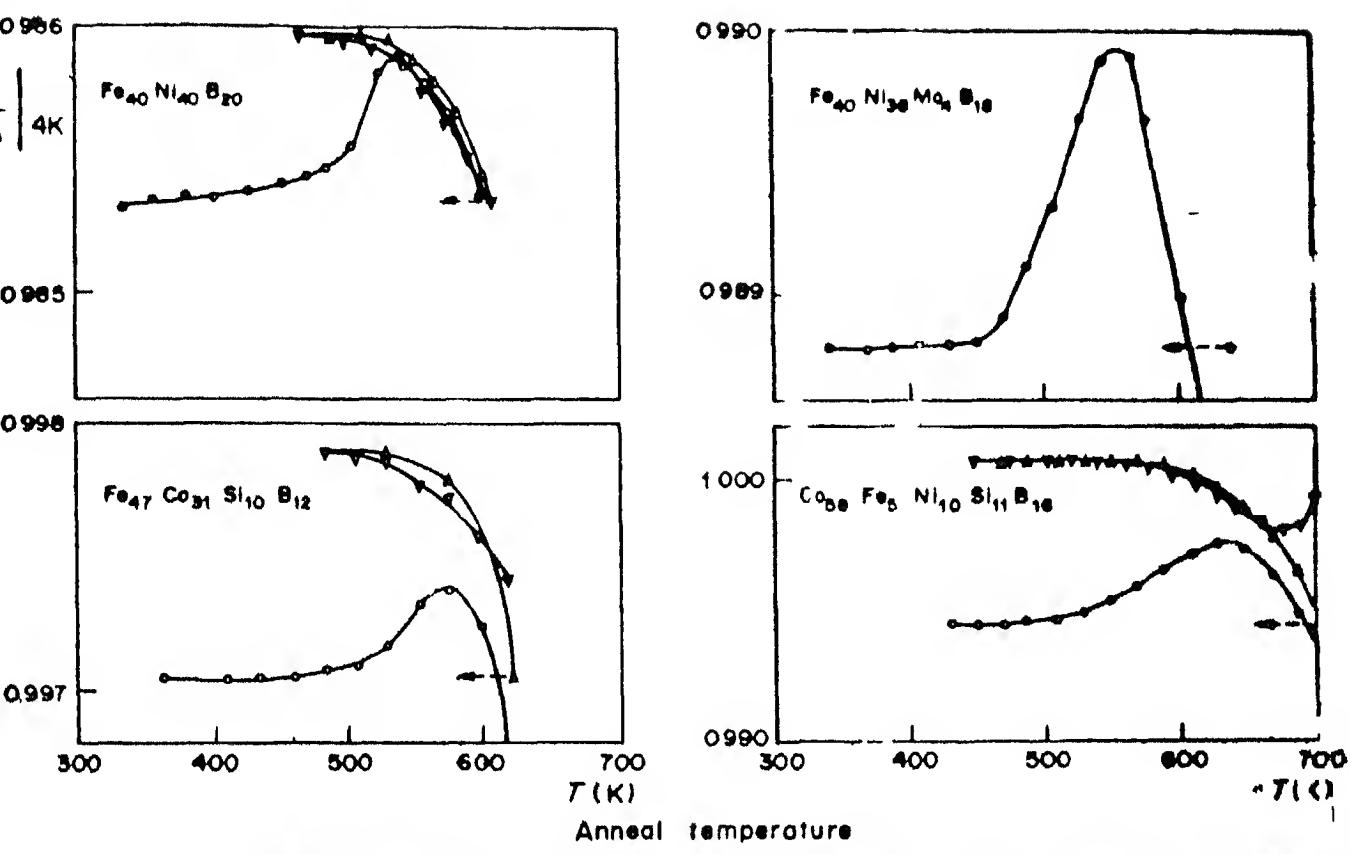
Fig 12 Evolution of the 4 K resistance of some metal–metalloid glasses during 10 min isochronal anneals conducted after a prestabilization (10 or 30 min) treatment at the maximum temperature indicated on the figure

temperature on isochronal annealing of the alloys is observed. Clearly a reversible effect is found for both metal-metal and multimetal- metalloid systems. On the basis of above experiments, Balanjat et al [33] have surmised the following. In case of systems which show reversible effect, the common factor is the presence of two metal species regardless of whether a metalloid is present or not. The Faber-Ziemann theory [34] also postulates a change in electrical resistivity with CSRO in amorphous alloys. On the basis of above observations, the presence of a CSRO in amorphous metallic alloys have been accepted. Egami [35] proposed a two process model to account for CSRO-TSRO change in amorphous alloys. Chen [36] proposed a one process model to account for both reversible and irreversible change in amorphous alloys.

In the case of monometal-metalloid alloys, there is no basis for a common factor to explain the reversible changes. For example, $Fe_{80}B_{20}$ does not show a reversible effect whereas $Fe_{81.5}B_{14.5}Si_4$ shows it [33]. Similarly, $Pd_{82}Si_{18}$ shows a reversible effect [37] whereas $Pd_{80}Si_{20}$ does not [33]. However, one thing is common for the alloys which show a reversible effect in monometal-metalloid systems. The reversible effect is found to be very small in magnitude [33]. Another important conclusion is that all the monometal - metalloid systems showing reversible effect deviate from the 80 atomic percent metal-20 atomic percent metalloid compositions. For example, $Fe_{80}B_{20}$ and $Pd_{20}Si_{20}$ do not show a

reversible effect whereas $Pd_{82}Si_{18}$ shows it   Balanjat
et al [33] have postulated that in metallic glasses, the
available interstitial sites are around 0 2 atomic fraction
The metalloid atoms occupy the interstitial position   Hence
not much atomic rearrangement will be possible at 20 atomic
percent metalloid composition   All the interstitial sites
will be occupied   Some authors [33] have also suggested that
in certain system the reversible change may be insensitive to
electrical resistivity   Hence they have stressed the need
for further experimentation with calorimetric and other tests
In general CSRO causes a change in Curie temperature, seggre-
gation [38] and change in field induced magnetic anisotropy
[39]   However some of these property changes may be affected
by TSRO too and vice versa [24,32,35,40]

TSRO and CSRO may be superimposed on each other.
This makes their detection difficult   Fig 13 and Fig 14
show the electrical resistance change for two systems when
subjected to several heating and cooling cycles The rever-
sible effects are shown by a bump in the resistivity curve
of Fig 13   The vertical shift of the curves also shows that
TSRO is changing for each cycle   If the equilibrium state
of CSRO was highly sensitive to TSRO, then it would not have
been possible to realize a reversible process

When amorphous alloys are subjected to the
effect of time and temperature, another kind of internal
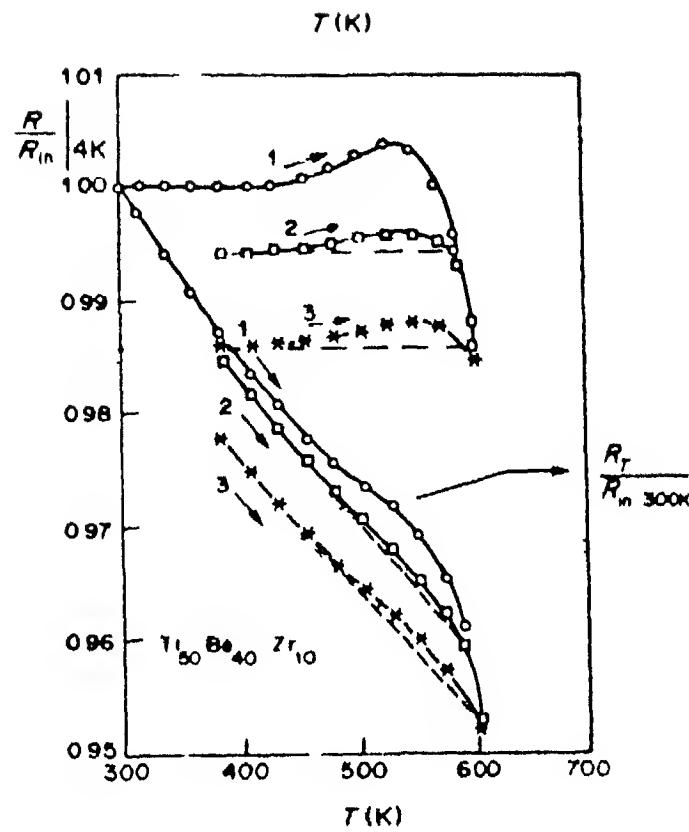
'Figure 10 Temperature dependence of the electrical resistance of $Cu_{50}Ti_{50}$ and $Ti_{50}Be_{40}Zr_{10}$ measured at the end of every isochronal anneal during the first heat up sequence of specimens originally in the as received condition (The short range (reversible) ordering manifests itself by a bump in the $R(T)$ curves)
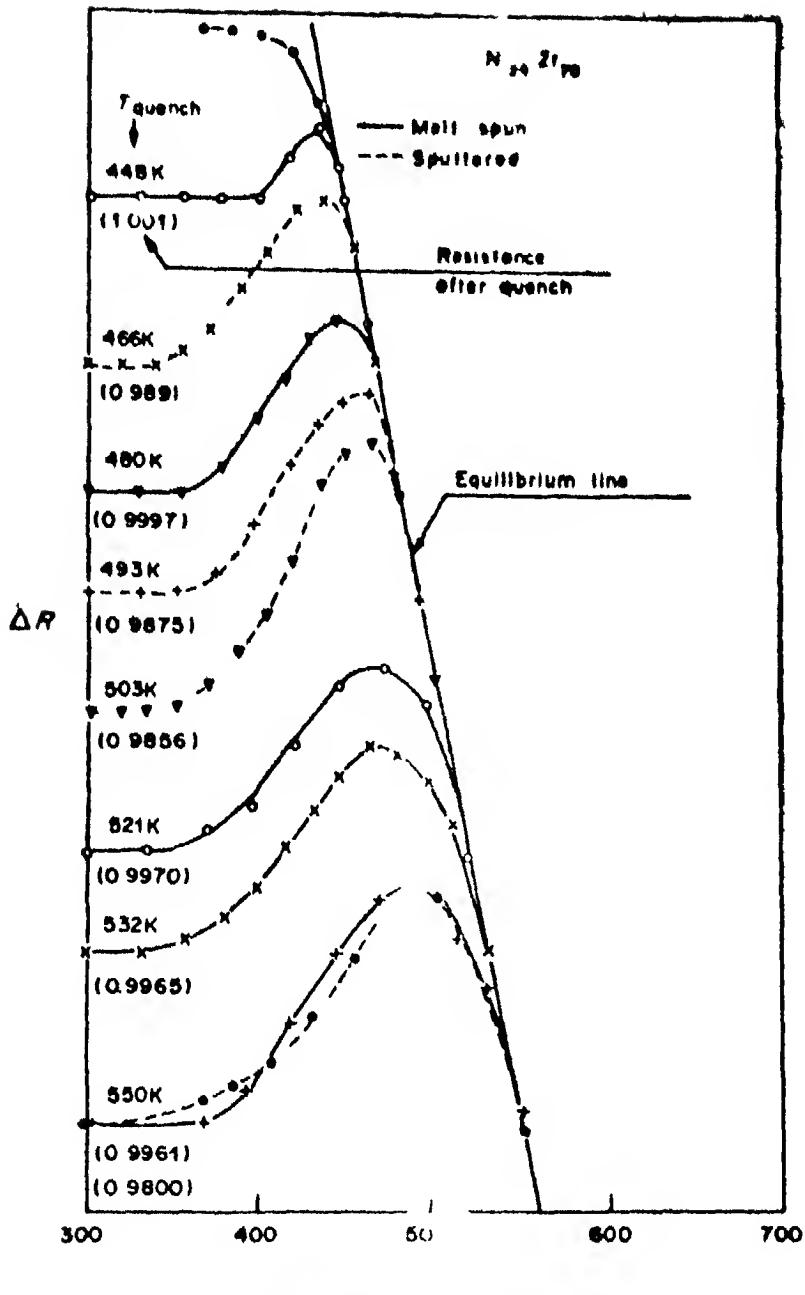
Fig. 14 Reversible resistance effects in $Ni_{24}Zr_{76}$ (There is obviously an irreversible decrease in resistance super imposed on the reversible effect as indicated by the resistance values reported on the figure In the figure the curves for the various annealing cycles have been shifted upwards to compensate for the irreversible resistance decrease)

stress relelving may take place   If the as quenched
amorphous alloy is subjected to mechanical working,
internal stresses are stored in the alloy   The residual
stresses at low temperature annealing get rellved by the
diffusion of structural defects [32].   These residual stress
effects result in change in stress induced magnetic aniso-
tropy and stress relaxation [41]   Somctimes they affect the
magnetic properties too   Lubrosky et al [42] have shown a
remarkable change in remanance, Curic temperature and
decrease in saturation field by relieving stresses at a
temperature slightly below Γ_g

A harmful effect of heat treatment is that in
some cases [43] the alloy bocomes brittle   Davis group
[44] has shown thal the embrittlement occurs in those cases
where the final product after crystallization is B C C or
H C P When the final crystallized product is FCC, the
embrittlement does not occur   The relationship between the
final crystallized phase and the relaxed amorphous phase is
not well understood at present   But the investigation shows
that there probably is a relation

Structural relaxation behaviour of Metglas
2605Sc has been studied by Mossbauer spectroscopy by Sageusa
and Moris [18] Metglas 2605Sc was isochronically annealed
at various temperatures using different heating rates   The
Mossbauer spectra were recorded On these basis, the authors
suggested that structural relaxation in Metglas 2605Sc to

take place in three different stages   Annealing before
crystallization of the as melt spun sample appears to
produce no substantial change upto 127oC   In the temper-
ature range of 127oC and 347oC an increase in short range
ordering has been observed   This may be topological or
chemical   In interpreting magnetic properties of $Fe_{27}Ni_{53}P_{14}B_6$
glass, Egami [32] has proposed a pairing of Fe-Fe atoms
Sageusa and Moris [18] concluded that for a similar pairing
to operate in 2605Sc, an increase in the average Fe^{57} hyper-
fine field is expected in Mossbauer study   They observed the
required increase in the Metglas 2605Sc   This led to the conc-
lusion that enhancement of short range Fe-Fe pair ordering
is taking place in the temperature range of 127oC to 347oC.
However they are not sure of this observation In the region
of 347oC to 417oC, a different kind of ordering has been
observed   The crystallization studies of Metglas 2605Sc
suggested [18] that the first crystalline product precipi-
tating out at 417oC is α phase containing 4 atomic percent Si
This observation led them to conclude that in the tempera-
ture range between 347oC and 417oC atomic rearrangement may
be producing atomic clusters which later help the formation
of nucleii containing Fe- with 4 atomic persent Si A two
step structural relaxation doesnot appear to be peculiar
to Metglas 2605Sc $Fe_{40}Ni_{40}P_{14}B_6$ glass also appears to
show two stage relaxation process [45]

CHAPTER III

EXPERIMENTAL PROCEDURE

III.1 Fabrication of Metallic Glass Ribbon

Fabrication of metallic glass ribbon involves the following steps

    i) Preparation of nozzle

    ii) Preparation of the alloy and

    iii) Melt spinning

Each of these steps are discussed in detail in the following section

i) Preparation of the nozzle   For preparing nozzles to inject molten metal onto a rotating substrate quartz tubes are utilized   The induction coil of the melt spinning set up was suitable for holding only 10 mm internal diameter and 12 mm outer diameter quartz tubes   One end of the quartz tubes is to be sealed and formed into a suitably shaped nozzle   For this a graphite die is needed into which the sealed end of the quartz tube can be blown to form the nozzle shape   An orifice is then cut at the closed end of the quartz tube to produce the nozzle suitable for melt spinning

The die is hard fabricated using a graphite block   The one end open die cavity is shaped using

jewellers file and the die cavity surface is polished
Different dies are prepared to give differ nt nozzles as
given in the results One end of a 12 mm O D quartz
tube is sealed in oxyhydrogen flame The closed end of the
quartz tube is then heated to its softening temperature,
pressed vertically in the die cavity and Argon gas pressure
is applied at its open end so that the softened quartz glass
fill the die cavity providing uniform wall thickness. For
proper filling of the die cavity the pressure of Argon gas
used is O 3 Kg/cm^2. The tip of the closed end of the nozzle
where orifice is to be made is thinned slowly by rubbing it
against belt surfacer and 4/O emery paper, taking care
that the nozzle does not break due to vibration The flatte ⊢
ning of the nozzle tip as well as its thinning is continued
till a hole is about to develope. The nozzle is then mounted
on the bed of a circular diamond saw cutting m/c (Microslice
2, Metals Research Ltd , Cambridge, U K) The line joining
the two opposite walls of the quartz tube is kept parallal
to the cutting surface With few rotation of the cutting
wheel a rectangular orifice is made. The sharp edges ofthe
nozzle are polished with a 4/O emery paper Then the nozzle
are finally stressrelivevd by annealing This procedure
produce serration free orifice The alternate procedure of
orifice making, namely,first cutting the orifice followed
by thinning the nozzle by emery polishing usually produce
undesirable serrations at the orifice The nozzles produced

are of approximately 6 mm in orifice length

ii) Preparation of the alloy Preparation of Fe_{81} $B_{13.5}Si_{3.5}C_2$ alloy is done in two steps a) First a master alloy of Fe and C is prepared by induction melting and b) Then the Fe-B-Si-C alloy is prepared by arc melting Fe,Fe-C alloy, B and Si The materials used for alloy preparation are 99 999/ pure Fe 99/ B, 99 9/ Si (all from Alpha Products USA) and C powder obtained from graphite rod trimmings

a) Preparation of Fe-C alloy An alloy to contain ultimately 2 at/ C is prepared by induction melting of weighed quantities (50 gm or 100 gm) of Fe and baked graphite powder taken in a recrystallized alumina crucible Weighed quantities of Fe and C are induction melted in Argon atmosphere using a graphite crucible as a suscepter and is homogenized just below the melting point of the alloy for 30 minutes The prepared Fe-C alloy is cut into pieces and is inspected under an optical microscope at a magnification of 500X It ensures that there is no undissolved C present in the alloy The alloy is cleaned by polishing with emery paper and cut in small pieces

b) Preparation of Fe-B-Si-C alloy Appropriate amounts of pure B,Si and Fe-C alloy are weighed to produce about 20 gms of $Fe_{81}B_{13.5}Si_{3.5}C_2$ alloy   Each batch of alloy is melted thrice in an arc furnace in Argon atmosphere to ensure proper homogenization   The pellets from arc melting

are polished clean and broken by a pneumatic hammer. 10 to
15 gms of the above alloy is cleaned by using a mild solu-
tion of 1 0 part by volume of hydrochloric acid and 2 parts
by volume of water   The cleaned alloy pieces are then taken
in an one end sealed quartz tube of 10 mm O D to premelt
the alloy pieces to form a single cylindrical specimen of
  8 mm O D   This is done to have maximum amount of material
for melt spinning using the existing apparatus and to prevent
possibility of cracking of the quartz nozzle   The quartz tube
along with the charge is then successively evacuated and
flushed with high purity Argon (IOL grade Iolar -2) three
times to ensure complete removal of oxygen from quartz tube
The alloy is then melted in the same induction heater used
for final melt spinning by keeping the variac control of the
generator at 68 divisions   The melting and the solidifica-
tion is done thrice to ensure complete homogenization The
power input corresponding to the melting becomes fixed in
second and third melting   The quartz tube is then broken
to remove the cylindrical alloy rod of about 8 mm O D
The alloy rod is cleaned successively with hydrochloric acid,
distilled water and methanol just before using for melt
spinning.

                iii) Melt spinning   The experimental set up
for melt spinning is schematically shown in Fig 15 A rolled
copper disc of 10 cm diameter and a rim width of 2 5 cm is
mounted on a 'Wolf' lathe grinder assembly it serve the

Induction furnace

Transformer coil

Cu-wheel

Spraying nozzle

Drying column

Pressure gauge

Crucible furnace

Fused CaCl$_2$ tower

Gas line

Valve

Argon gas inlet

Y direction

X direction
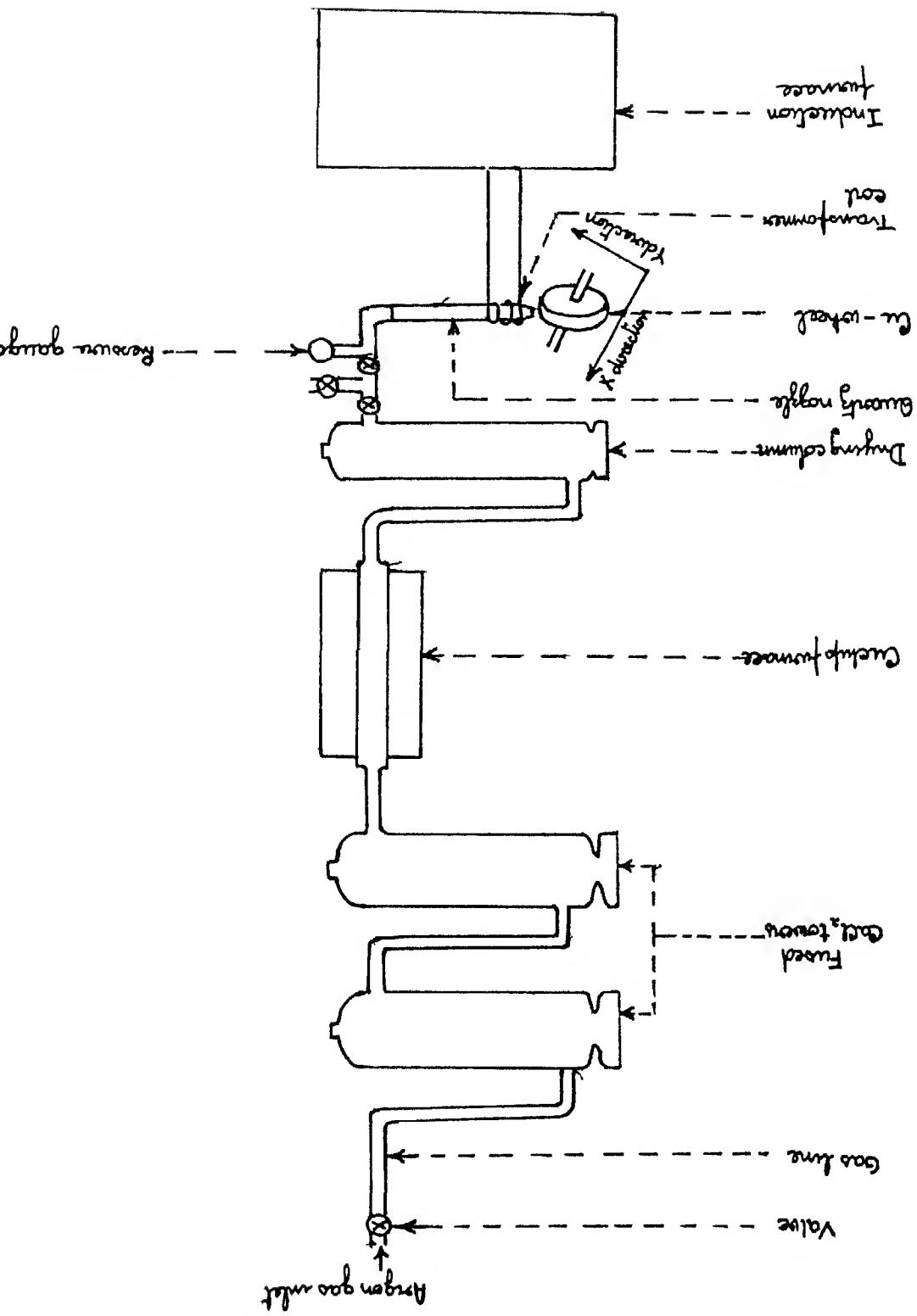
Figure 15   Experimental Meltspinning set up

purpose of the rotating cold substrate   The lathe grinder
is mounted on a X-Y control table for easy and accurate
placement of the substrate below the nozzle   The speed of
the copper disc can be varied by using an autotransformer
and adjusting the AC input voltage   The motor speed is
calibrated using a tachometer against the applied voltage
Before each run the copper disc is cleaned by 4/0 emery
paper to give it a matte finish   The connection at the other
end of the silica tube is so that it can be connected either
to a rotary vacuum pump (Precivac Engineering Co , Calcutta)
or to a high purity Argon gas cylinder connected with a gas
purifying train (Fig 15)   It should be mentioned that
the vacuum pump is used only for alloy preparation described
before and not during actual melt spinning   A 3KW, 450KHz
R_f generator (Pal Industries, Ghaziabad) is connected with
a custom made transformer to provide a high current at low
voltage output   The induction coil is locally made   The
coil characteristics are as follows

> Diameters of tube = 2 mm
>
> Coil diameter= 15mm
>
> Coil height=20 mm
>
> Number of turns/length = 3
>
> Coil material=refrigeration Cu tube
>
> Gap of coil and quartz tube =0 5 mm

The power and hence the temperature of the charge in the
R_f coil is varied by controlling a variable voltage

transformer   Since there is no power meter provided with the equipment, the standardization of melting and melt spinning process has been done in turns of the dials reading (maximum reading 100) of the adjustable transformer

The nozzle is cleaned with distilled water and methanol and dried in hot air   The prepared charge, weighing 10 to 15 gms as described in the material preparation, is taken in the nozzle   The open end of the nozzle is connected with Argon and the whole system is flushed with pure dry Argon for few minutes   A weak flow of Argon is maintained till ejection of the melt to prevent chances of oxidation of the charge   The nozzle is placed inside R_f coil vertically above the rotating surface of the Copper wheel   The distance of the nozzle tip to the surface of the copper wheel is varied from less than 1mm upto 2 mm, even though the smaller gap is generally preferred   Care is taken to see that the R_f coil does not touch the nozzle and a uniform gap between the nozzle tip and the R_f coil is maintained   The nozzle is so placed in the R_f coil that the lowest end of the nozzle tip, with a small fraction of the sample, is kept slightly outside the R_f coil at the chilled block end   The maximum part of the sample **at the** other end, is kept inside the R_f coil   The above arrangement has important consequences which will be discussed later   The loaded nozzle is then heated up, slowly at first increasing by 2 divisions of the adjustable

transformer upto 30 divisions   After 30 divisions the
charge is heated up quickly   Near about 60 divisions the
alloy reaches its melting temperature While the charge is
heated to 40 divisions of the adjustable transformer the
chill block is set in motion   The temperature is raised
quickly at this point,transformer adjusted at the rate of
30 divisions per second to reach the desired superheat
value of 75 divisions of the transformer   At this point
the melt is held for 1 second and the ejection pressure,
which is preset between 0 6 to 1 2 Kgf/cm^2 , is applied
The molten metal ejects out on the rotating Cu substrate
to produce the ribbons   Five to six metre long, six to seven
milimeter wide ribbon of average thickness 30 micron can be
obtained

III 2 Characterisation

The metallic glass $Fe_{81}B_{13.5}Si_{3.5}C_2$ produced
by melt spinning technique is subjected to two different types
of physical studies (i) Study of the melt spun ribbon from
the process point of view and (ii) studies related to
thermal stability of amorphous ribbons. For the first kind
of studies metrological, X-ray and TEM techniques are used
to study the macroscopic as well as microscopic nature of
the material Whereas for the latter kind of studies change
in electrical resistance with temperature and differential
scanning calorimetry (DSC) are used   Since the alloys are

useful for their magnetic properties, to a limited extent magnetic properties are tested using a vibrating sample magnetometer

1) Study of melt spun ribbons from process point of view The metallic glass ribbons produced in laboratories are generally not much wide. Hence for precise measurement of dimensions, a Carl-Zeuiss MP-320 shodowgraph is used It is essentially an optical projector with 100X magnification and is fitted with a micrometer to read the dimensions directly from the enlarged shadow of the sample Thickness is measured using a micrometer screw gauge Both X-ray TEM are used to determine whether the melt spun ribbons are crystalline or amorphous

A Phillips Transmission Electron Microscope EM 301, operated at 100 KV is used The samples are first cleaned successively in tiichloroethylene (TCE) for degreasing, followed by acetone to remove TCE and finally washed in methanol The samples are then thinned by electrochemical thinning A bath of 5/ perchloric acid + 95/ methanol is prepared The solution is explosive above 20oC Hence it is cooled by an ice bath to keep it at a temperature below 10oC Platinum is used as a cathode and the sample as anode The thinning conditions are 30V at 8o -12oC for 4 to 5 seconds Apperance of small holes on the immersed part of the sample indicates completion of sample thinning The prepared sample is kept immersed in methanol, till putting in TEM,

to prevent oxidation

A Rich-Seifert Isodebyflex 2002 twin tube diffractometer fitted with Cr target tube is used for X-ray diffraction   The specimen is prepared by cutting the melt spun ribbons in 2 54 cm long pieces   The cut pieces of the ribbon are cleaned successively in trichloroethylene, acetone and methonol   These are attached to a computer card/piece of 2 54 cm x 2 54 cm size using quickfix   The whole card board space is completely covered with two layers of ribbons The two layers of ribbon pieces are found necessary to comp-lectly cut off the diffraction pattern due to computer card The prepared specimen is mounted on the diffractometer stage and a diffraction pattern is recorded using the following diffractometer conditions-

Slit size = 2 mm   Scanning speed =9/min

Receiving slit = 0 3 mm   Chart speed = 3 cm/min

Voltage = 40 KV   Time constant = 2 sec

Current = 30 mA   Range = 10 K counts/min

Angles scanned (2θ) =10o to120o

ii) Study related to thermal stability a) Sample preparation   Sample preparation procedure for thermal stab-ility tests and magnetic tests are the same   The melt spun Fe-B-Si-C ribbon seemsto have a fine layer of oxide forming very soon after its formation So these oxide layers are cleaned by lightly polishing the surface with 4/0 emery paper, followed by successively cleaning with trichloro-ethyline acetone and methanol   After cleaning some of the

specimens are given specific heat treatments before testing
The tests carried out along with specific heat treatment
given to the specimens are detailed out below

Test type I - A single run of the melt spun specimen to
crystallization

Test type II- A specimen is continuously heated from room
temperature to a fixed temperature below the crystalliza-
tion temperature and then furnace cooled to room temperature
This heat treatment cycle (called 'runs' in latter part
of the discussions) is repeated several times for some speci-
mens This is followed by a final run to crystallization

Test type III- A specimen is given an isothermal treatment
at a fixed temperature of $100oC, 310oC, 600oC$ for fixed times
e g 10 minutes, 25 minutes and 60 minutes for stabilizing
the material A stabilized sample is then subjected to
either of the following tests- Test type III a) The stabili-
zed specimen is taken to crystallization from room temper-
ature at a fixed rate of heating via single run or test type
III b) The stabilized specimen is heated to a fixed temper-
ature below crystallization at a fixed rate of heating
followed by furnace cooling This heating and cooling
cycle is repeated several times followed by a final run
to crystallization

        In measuring electrical resistance, either of
the test types I and II are employed The sample used is

of uniform width and having no pores or oxide scale An
existing apparatus to measure electrical resistance as a
function of temperature has been made use of   A thermally
insulated furnace controlled by a programmable temperature
controller is heated at a fixed rate of 1oC or 2oC /minute
A standard four probe method of electrical resistance
measurement is used   The current passed through the sample
is kept constant by a HP constant current source   A diff-
erential method of potential measurement is utilized to make
use of high sensitivity ranges of a Keithley microvoltmeter
A balance potential is provided by a L and N potentiometer
The unbalanced emf is continuously recorded by a two pen
strip chart recorder which also simultaneously record the
temperature of the specimen   A sensitive range of 30µV full
scale is used to detect very small changes in electrical
resistance Balancing emf of the potentiometer is to be
changed frequently to keep the recorder pen within chart
span   Each time the balancing emf is adjusted and noted
so that the potential drop across the specimen can be
calculated   A Pt vs Pt + 10/ Rh thermocouple is used to
measure the specimen temperature

Before starting the electrical resistance
measurement the sample chamber is flushed with purified
Argon gas   Standard Argon gas is passed through a gas
purification train containing gas drying columns and hot
Cu and Ti chips to remove moisture, Oxygen and Nitrogen

The purified gas is passed through the sample chamber at
a rate of 2 to 3 bubbles per minute   The programmable
controller is turned on and the difference emf is conti-
nuously traced on the chart paper In this apparatus the
specimen can not be cooled at any desired rate because of
heavy thermal insulation of the furnace   The typical
testing conditions for electrical resistance measurement
with increasing temperature are as follows

> Chart speed = O 3 cm/min
>
> μV meter range = 30μV,100μV or 300μV
>
> Heating rate = 2oC/min
>
> Measuring Current = 1 milliamp
>
> Argon gas flow = 2 bubbles/min

A dupont 910 DSC is used for thermal analysis
of the ribbons for DSC work   Test types I,II and III are
employed small pieces of cleaned ribbon weighing approxima-
tely 15 to 25 miligrams are put in small aluminium pans
provided by the manufacturer for use as crucibles   A second
empty aluminium pan is used as a reference   To protect the
sample from oxidation, pure Iolar - 2 Argon gas is passed
through the DSC cell   The gas inlet of the DSC cell is
connected to the gas cylinder fitted with a sensitive pre-
ssure regulator and needle valve   The outlet is connected to
an oil bubbler so that the flow rate can be controlled as
well as monitored.   A gas flow rate of 2 to 3 bubbles per
minute is used throughout the experiment.   The heating

cycle is programmed The specimen is first heated to 50oC at a rapid rate and the DSC is brought to a standby position No DSC data are recorded below 50oC. From this temperature the specimen is heated to the desired temperature as required in different test types at a heating rate of 10oC / min. The measurement are made at different sensitivity levels of the DSC and the recorder On the DSC, two sensitivity ranges 1X and 10X are available The chart recorder sensitivity can be chosen from 0 01, to 10V full scale The measurements are made in 'DSC Calibrated' mode of the equipment Base line adjustment are made at the start of a set of experiments but no adjustments are made in between runs to avoid the change in DSC peak characteristics In the highest sensitivity ranges, namely combination of DSC 10X and chart 01V full scale, the base line is found to change slightly after 3 or 4 runs and it is nonlinear Hence from time to time base line traces are made A two pen strip chart recorder is used to record against time Q, the heat evolved or absorbed,and dQ/dT, the latter is found very helpful in detecting small thermal effects Specimen temperature is displayed by a digital mV meter and noted manually on the strip chart recorder One typical experiment for example uses the following conditions

Heating rate = 10oC/min

Argon flow rate = 2 to 3 bubbles/min

Initial temperature = 50oC

Final temperature = 333oC

Range for Q = 0 1 mV full scale

Range for dQ/dT = 0 01 mV full scale

DSC sensitivity = 10X

DSC in calibrated mode

The cleaned samples are used in the high temperature assembly of a vibrating sample magnetometer (VSM) to measure magnetic moment as a function of temperature in the residual field of a Varian electromagnet The residual field is 40 Oe The specimen is heated at a slow rate approximately at 5oC/minute The magnetic moment vs temperature curve is used to determine the Curie temperature The saturation magnetization of the cleaned specimen is determined at room temperature by keeping the long axis of the specimen parallal to the field

CHAPTER IV

RESULTS

IV 1 Fabrication of Metallic Glass Ribbon

Metallic glass ribbons are prepared in the laboratory using an existing single roller melt spinning apparatus   The effect of different process parameters both on ribbon formation and the quality of the ribbons produced are investigated   This section gives the result of different process parameters and their effects

Nozzle length   The Fig 16 shows the meaning of different terms used   Quartz tubes of outside diameter 12 mm and inside diameter 10 mm are taken and nozzles are made   The orifice lengths are kept same but the angle with horizontal is varied   The other conditions during melt spinning are kept constant   Table 2 gives the results obtained with different nozzles   The best results are obtained with nozzle C

Ejection pressure   Keeping the other conditions fixed, ejection pressure is varied   The results are given in Table 3

Distance between chill block and nozzle   Table 4 describes the effect of this distance on ribbon formation and chara-cteristics   In all the experiments described in Table 4 a pressure of 1 Kgf/cm^2 to 1 2 Kgf/cm^2 is applied
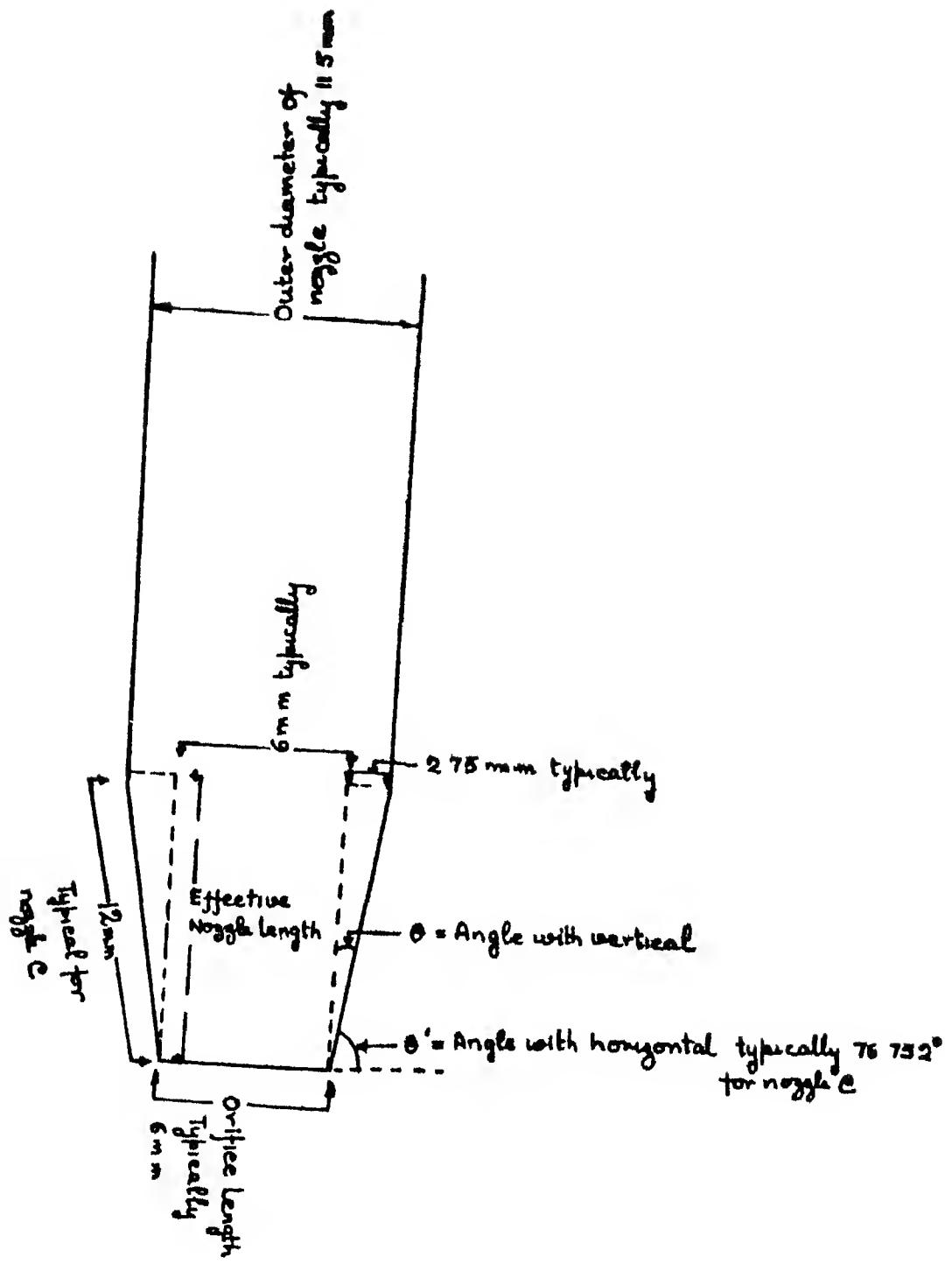
Figure 16   Quartz nozzles for meltspinning

TABLE 2

The effect of nozzle length on ribbon formation

Nozzle	Orifice length (mm)	Angle with horizontal (Θ°)	Effective nozzle length (mm)	Ribbon Characteristics
A	6	89	85 7	Uneven and discontinuous ribbons
B	6	80	15 8	Even edge, continuous ribbons
C	6	76	11 6	Even edge, continuous ribbons
D	6	60	4 8	Even edge, continuous ribbons
E	6	35	1.9	Uneven and discontinuous ribbons

TABLE 3

The effect of ejection pressure on ribbon formation

Ejection pressure (Kgf/cm^2)	Ribbon characteristics
0 05	Uneven, discontinuous ribbon formation
0 1	Uneven, discontinuous ribbon formation
0 6	Uniform, continuous ribbon formation
0 8	Uniform, continuous ribbon formation
1 0	Uniform, continuous ribbon formation
2 0	Quartz nozzle bursts

Degree of super heating   The number of turns of the input
power of the transformer in the induction furnace versus
ribbon characteristics is given in Table 5   The ribbons are
best produced within the range of 68 to 80 divisions of the
input power

Surface velocity of the substrate   Four velocities are tried
keeping the other experimental conditions fixed and the
surface velocity vs the ribbon characteristics are shown
in Table 6

Orific geometry   The orifice is a rectangular hole with
the length being controlled and the width the same as that
of the cutting wheel

Several sketches of the good and bad nozzles
with different orifice geometry are shown in Fig 17   In
nozzle (1) , serration occur when the nozzle is first cut
in the cutting wheel and then thinned during preparation .
In nozzle (2), the orifice is extended to both the sides
of the nozzle   In nozzle (3), the width of the nozzle
is more than the cutting wheel thickness   In nozzle (4),
the orifice is not extended throughout the length of the
nozzle   Nozzle (5) is the best nozzle

Summery of important parameters to produce
best metallic glass ribbons under the existing conditions
and one particular value to produce continuous and reson-
ably wide (six to seven milimeters) ribbons are given in
Table 7

TABLE   5

The effect of supperheating on ribbon formation

Superheating Number of turns of the divisions power (divisions)	Ribbon characteristics
60-64 (melting point)	Partially crystalline ribbons
62-68	Completely glassy ribbons,edges sometimes brittle
68-80	Completely glassy ribbons, edges not brittle
85-95	Partly crystalline, and sometimes oxidized ribbons
90-100	Mostly crystalline, often burnt out and sometimes metal globule formation

TABLE 6

The effect of chillblock surface velocity on
ribbon formation

Voltage (V)	Linear speed (m/minute)	Thickness of the ribbon (micron)	Ribbon characteristics
120	297 0	30-40	Crystallized and brittle
200	480 8	30-35	Uniform and continuous
210	514 3	25-35	Uniform and continuous
270	-	-	Burnt out and semi crystallized

ORIFICE LENGTH

ORIFICE WIDTH

THICKNES O GLASSHA L

NOZ LE 1

NO ZLE 2

N ZLE 3

NOZZLE 4

NOZZ E 5
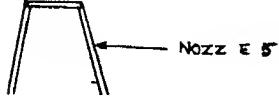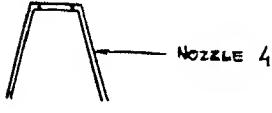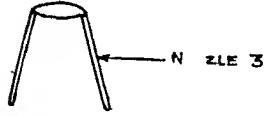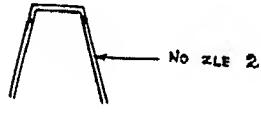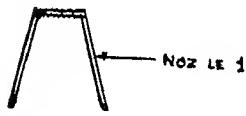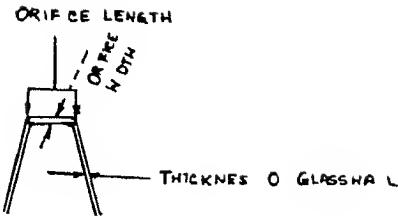
Figure 17   Examples of som nozzles h v ng
good or b d orifice

TABLE 7

A summar of inportant parameters to produce continuous four to five meters of metallic glass ribbons of six to seven milimeter width and twenty five to thirty five microns thickness.

Parameter	Description	Range	One particular convenient value	Remark
Material	Single nozzle shaped pellets without any oxidized layer or undissolved impurity	Nozzle out-side diameter 12 mm, inside diameter 10 mm sample weight 10 to 15 gms.	–	The higher the amount of material melt spun better is the product.
Nozzle dimension for 6 mm orifice	Fused silica tube for nozzle material	Angle with horizontal –exact range unknown but $60o > \angle > 80o$	76 12 mm outside diameter nozzle and 6 mm orifice length	–
Orifice geometry	–	As of Figure 17	–	–
Ejection pressure	–	Not less than 0.6 Kgf/cm^2	0.6 Kgf/cm^2	–
Distance between chill block and nozzle	–	Less than 2mm in upper limit, lower limit in the used set up is 0.3 mm.	1 mm	–
Nozzle position	–	Vertical	–	–
Super heating	–	68 div. , of input power to 80 div. of input power	75turns of input power	–
Velocity of substrate	–	See Table 6	480.8	–
Polish and cleanness of the substrate	–	Matte finish	Matte finish	–

IV 2 Characterization

The metallic glass ribbons so produced are studied to see whether the amorphous nature has been achived by X-ray and TEM X-ray results are given in Fig 49 and TEM results are given in Fig 50 given at end

Tne ribbons are then studied by electrical resistance vs temperature measurements with or without different types of heat treatment The crystallization studies have been given in Fig 18 and 19 The structural relaxation behaviour is given in Fig 20 and Fig 21 The Table 8 correlates the Figure numbers with the experiment and describes for each experiment the conditions and other relevent facts No figures are plotted below 60oC as the initial stabilization of the samples may show spurious effects at the start of the experiment

Similarly Fig. 44 to 48 give the Curie temperature and magnetization/ demagnetization measurements for the prepared samples And Table 11 correlates the Figure number with the experiments performed

Fig 22 to Fig 43 describes the results obtained by DSC measurements for samples with different types of heat treatments Table 10 correlates the Figure number with the corresponding experiment number And Table 9 correlates the experiment number with the corresponding experimental conditions Hence to find the necessary

experimental conditions for a particular figure, say Fig 23, we have to go to Table 10 to find the experimental number, i e experiment 8, and then from Table 9, find out the experimental conditions corresponding to say experiment 8

In DSC it is found that because of some equipment problems, the temperature axis is not uniform giving rise to unequal divisions in temperature Hence the temperatures are plotted manually and are recorded

In all the experiments, the samples are described by the nature of previous heat treatments For example in DSC, a sample refered to as, say 310oC/25 min/ 1st run means an as melt spun sample previously isothermally annealed at 310oC for 25 minutes is cooled to room temperature after annealing and is then dynamically heated in the DSC furnace A 100oC/25 min/ 2nd run sample means a 100oC and 25 minute annealed sample is given a dynamic thermal cycling through a temperature below the crystallization temperature and is then again dynamically heated up in the DSC at a fixed rate of heating Similarly for all the other tests, sometimes the samples are so referred

TABLE 8

Electrical resistance test for various samples with various heat treatments

Experiment Number	Sample condition	Experiment	Equipment and experimental conditions	Figure number	Figure characteristics
Crystallization studies					
1	As melt spun	Sample is heated up from room temperature to 556oC followed by furnace cooling	Chart speed=20/60 cm/minute Heating rate=2oC/minute Measuring current = 1 milliamp Argon gasflow=2 bubbles/minute μV meter sensitivity =100μV	18	X axis=Temperature in oC Y axis=Resistance at the temperature of measurement, R_T Resistance at 27oC,R_{27} Range= 240oC to 548oC
2a)	As melt spun	Sample is heated from room temperature to 300oC followed by furnace cooling	Chart speed #4/10 cm/minute Heating rate = 2oC/minute Measuring current =1 milliamp Argon gas flow = 2 bubbles/minute μV meter sensitivity = 30μV	–	–

2b)	As after 2a)	ample is heated from room temper-ature to 550oC	Chart speed = 4/10 cm/minute Heating rate = 2oC/minute Measuring current = 1 milliamp Argon gas flow = 2 bubbles/minute μV meter sensitivity =30μV upto 350oC 300μV after 350oC	19	Y and Y axis same as above Range =200oC to526oC
Structural relaxation studies					
3a)	As melt spun	Sample is heated up from room temperature to 300oC followed by furnace cooling	Chart speed =8/30cm/minute Heating rate=2oC/minute Measuring current =1 milliamp Argon gas flow =2 bubbles/minute μV meter sensitivity = 30μV	20	X and Y axis same as above Range = 60oC to296oC
3b)	As after 3a)	Sample is heated from room temper-ature to 300oC, followed by furnace cooling	same as above	21	same as above

1060

1030

1000

300   400   500   K

TEMP C →

970

$\dfrac{R_T}{R_{27}} \times 1000$

940

910

880

850

820

740
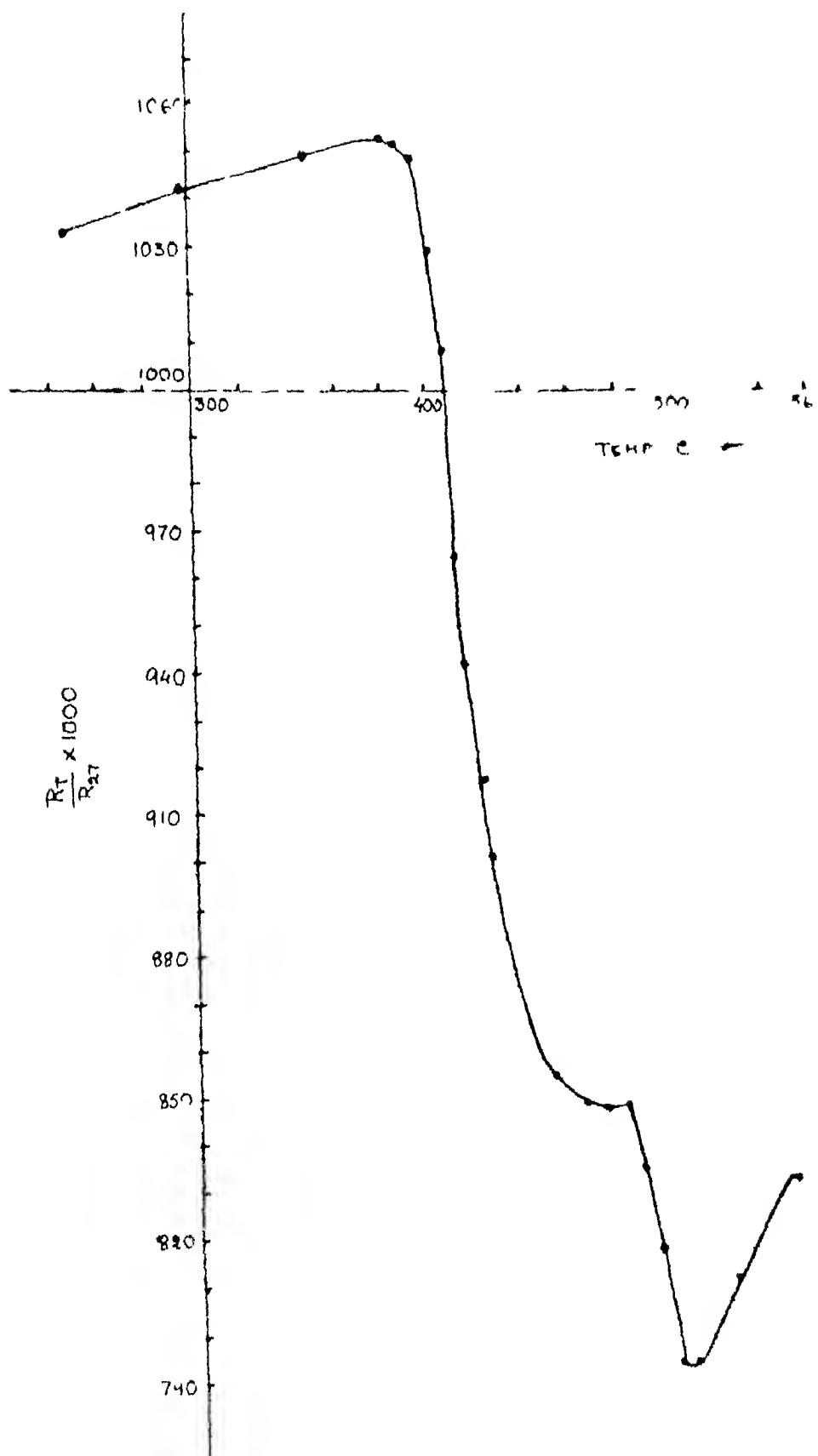
FIGURE 18 Crystallization of amorphous antimony/ first run, change in resistance
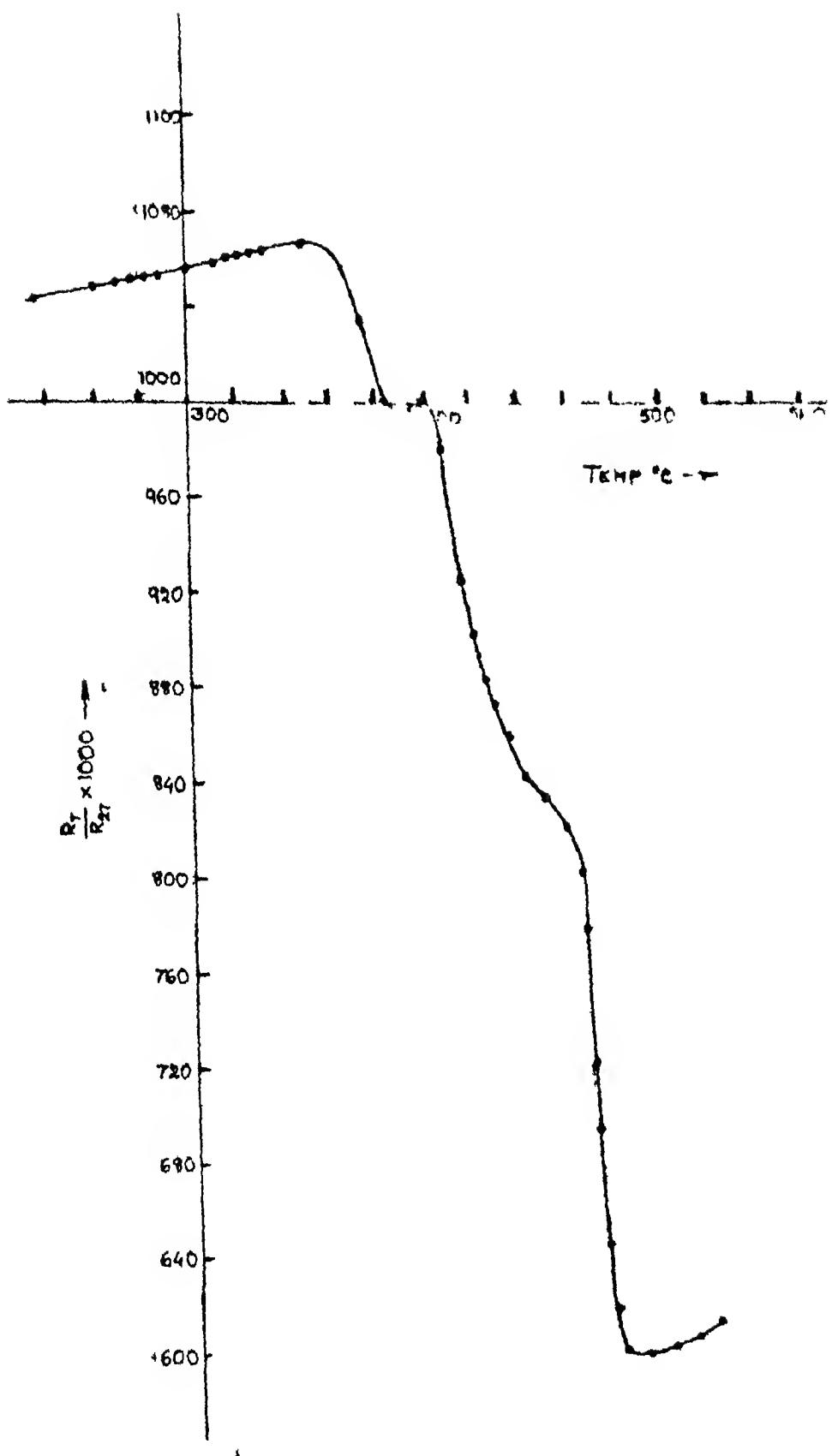
Figure 19 Crystallization studies of 'as melt spun/
second run' sample by electrical resistance
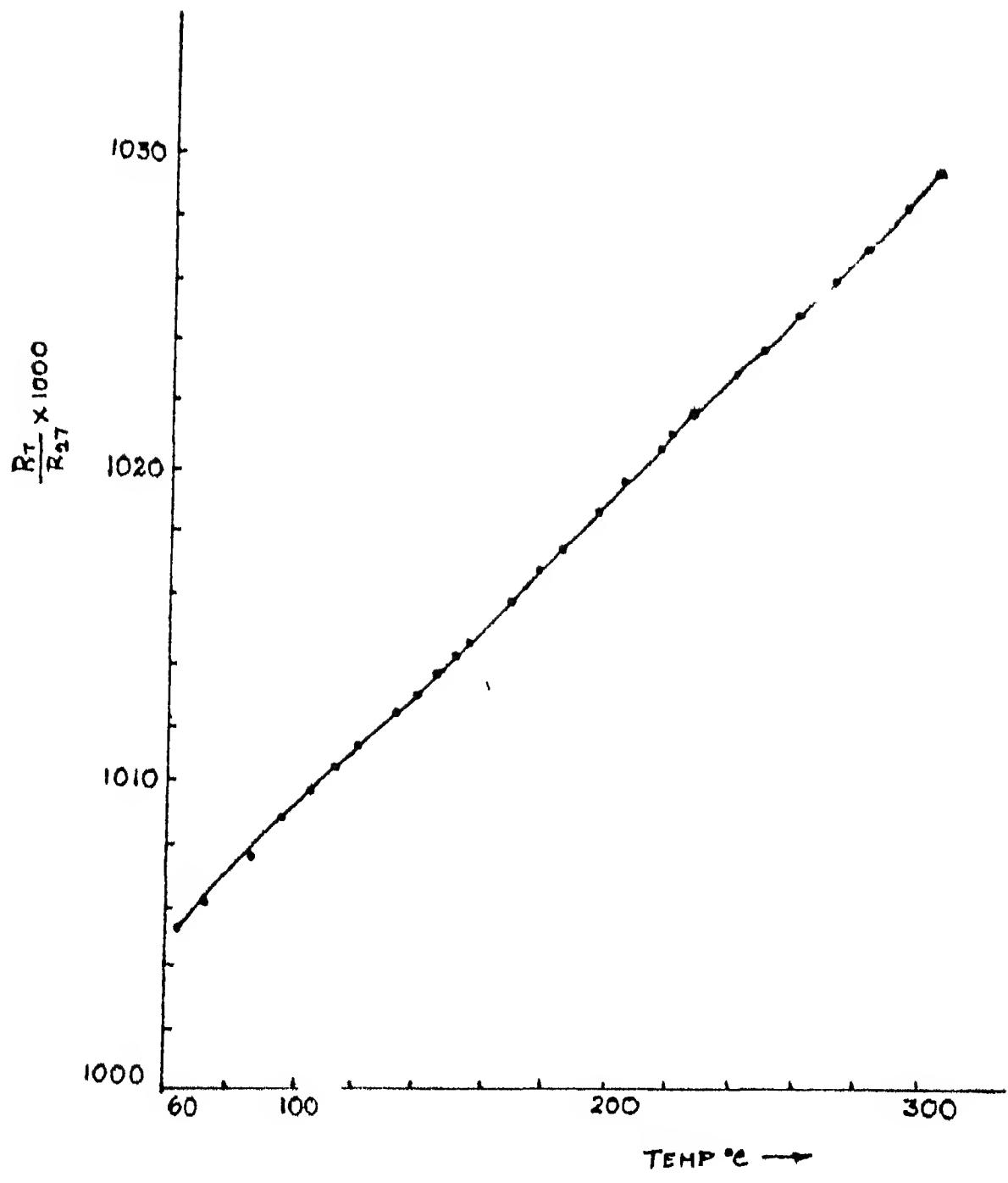
Figure 20 Structural relaxation studies of ' as melt spun/
first run' sample by electric l resistance.
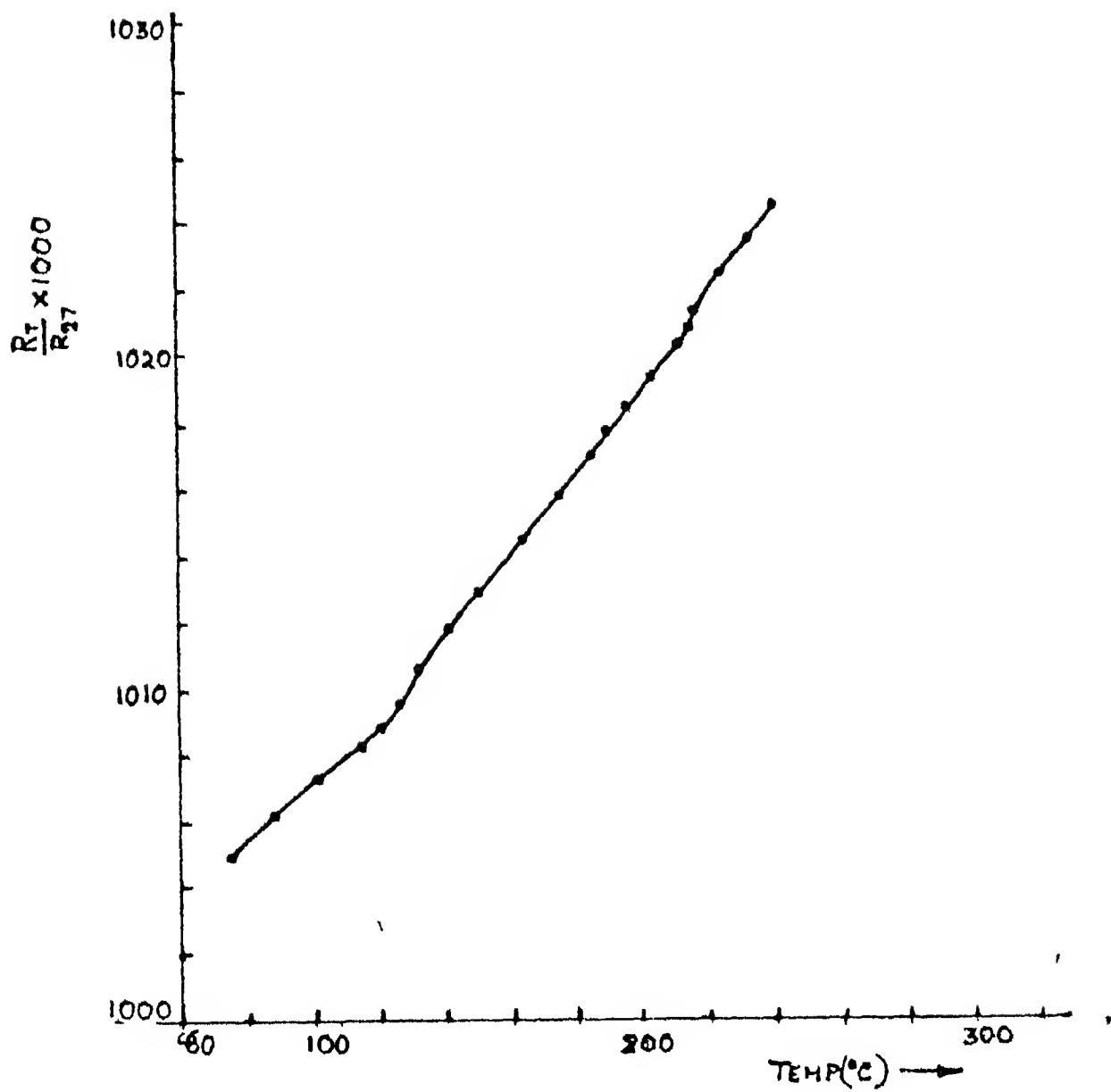
Figure 21   Structural relaxation studies of 'as melt spun/second run' sample by electrical resistance

DSC tests of various samples with various treatments

Experi-ment No	Sample conditions	Experiment	Equipment sensitivity			
			DSC sensiti-vity (xX)	Recorder sensitivity		
				Q (V)	dQ/dT (V)	
1	As melt soun in air	In single run upto 610oC	10X upto 333oC 1X upto 610oC	1	0 1	
2	As melt spun in Argon	a) 1st run upto 317oC followed by furnace cooling	10	1	0 1	
	As after 2 a)	b) 2nd run upto 322oC followed by furnace cooling	10	1	0 1	
	As after 2 b)	c) 3rd run upto 317oC followed by furnace cooling	10	1	0 1	
3	As melt spun	a) 1st run upto 331oC followed by furnace cooling	10	1	0 1	
	As after 3 a)	b) 2nd run upto 331oC followed by furnace cooling	10	1	0 1	
	As after 3 b)	c) 3rd run upto 331oC followed by furnace cooling	10	1	0 1	
	As after 3 c)	d) 4th run upto 610oC	10	1	0 1(upto 331oC) 1 0(from 331oC–610oC)	

Contd

4	As melt spun sample heated rapidly to 310oC in vaccun atmosphere in an annealing furnace and kept for 25 mi-nutes followed by uniform cooling to room temperature in 24 hours	a) 1st run upto 331oC furnace cooling	10	O 1	O 1	C 1
	As after 4 a)	b) 2nd run upto 331oC followed by furnace cooling	10	O 1	O 1
	As after 4 b)	c) 3rd run upto 331oC followed by furnace cooling	10	O 1	O 1
	As after 4 c)	d) 4th run upto 331oC followed by furnace cooling	10	O 1	O 1
	As after 4 d)	e) 5th run upto 610oC	10	O 1 (upto 331oC) 10 (331oC -610oC)	O 1 (upto 331oC) 10 (331oC-610oC)

No.	Sample preparation	Treatment			
5	As melt spun sample heted rapidly in vaccum to 310oC in an annealing furnace and kept for 25 minutes followed by uniform cooling to room temperature in 24 hours	a) 1st run upto 350oC followed by furnace cooling	1	0 1	0 1
		b) 2nd run to 610oC As after 5 a)	1	1	0 1
6	As melt spun sample heated rapidly to 310oC in vaccum atmosphere in DSC furnace and kept for 60 minutes followed by uniform cooling to room temperature	a) 1st run upto 331oC followed by furnace cooling	1	0 1	0 01
		b) 2nd run upto 331oC followed by furnace cooling As after 6 a)	1	0 1	0 01
		c) 3rd run upto 331oC followed by furnace cooling As after 6 b)	1	0 1	0 01

Contd

					C Cl (upto 331oC) O 1 (C31oC-61oC)
	d) 4th run upto 610oC	1			0 1
7	As melt spun	1st run upto 610oC	1	1	O 1
8	As melt spun heated in furnace rapidly to 310oC in vaccum and kept for 25 minutes followed by uniform cooling to room tempera- ture in 24 hours	a) 1st run upto 610oC followed by furnace cooling	1	1	O 1
	b) 2nd run upto 295oC	1	1	O 1
9	As melt spun heated rapidly in DSC furnace to 100oC, kept for 25 minutes followed by uniform cooling to room temperature in 45 minutes	1st run upto 610oC	1	1	O 1
10	As melt spun	1st run to 610oC	1	0 1	O Ol

Contd

11	As melt spun heated rapidly to 600oC in DSC furnace in Argon atmos-phere, kept for 10 minutes followed by uniform cooling to room tenpera-ture in 45 minutes	1st run to 500oC	1	0 1	0 01
12	As melt spun heated rapidly to 310oC in DSC furnace in Argon atmos-phere, kept for 60 minutes followed by uniform cooling to room tempera-ture in 45 minutes	1st run to 452oC	1	0 1	0 01

In 3rd column of the Table the DSC furnace is used, in 2nd column except where specifically mentioned the experiments are done in an annealing furnace, in DSC experiments heating rate of 10oC / minute is used

TABLE 10

DSC figures representing DSC experiments mentioned in Table 9

Figure No	Experiment No
General Curves	
22	10
23	8
24	6
25	11
26	8,9,7
Crystallization Studies	
27	8,4
28	10,3
29	9
30	5
31	12
Relaxation Studies	
32	3
33	4
34	6
35	3
36	4
37	6
38	3
39	4

Contd   TABLE   10

| Figure No	Experiment No
40	6
41	3
42	4
43	6
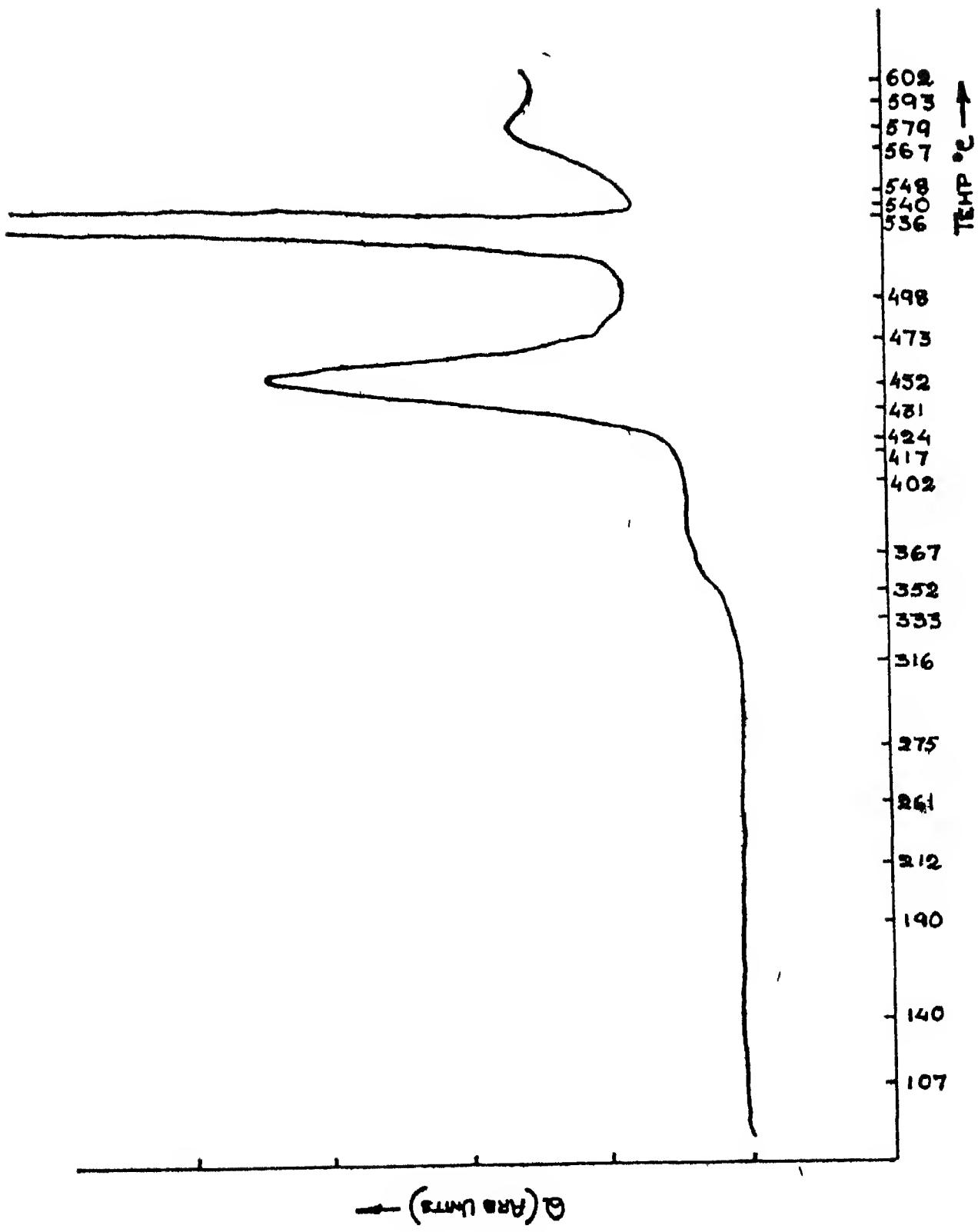
Figure 22 General DSC curve for 'as melt spun first run' sample
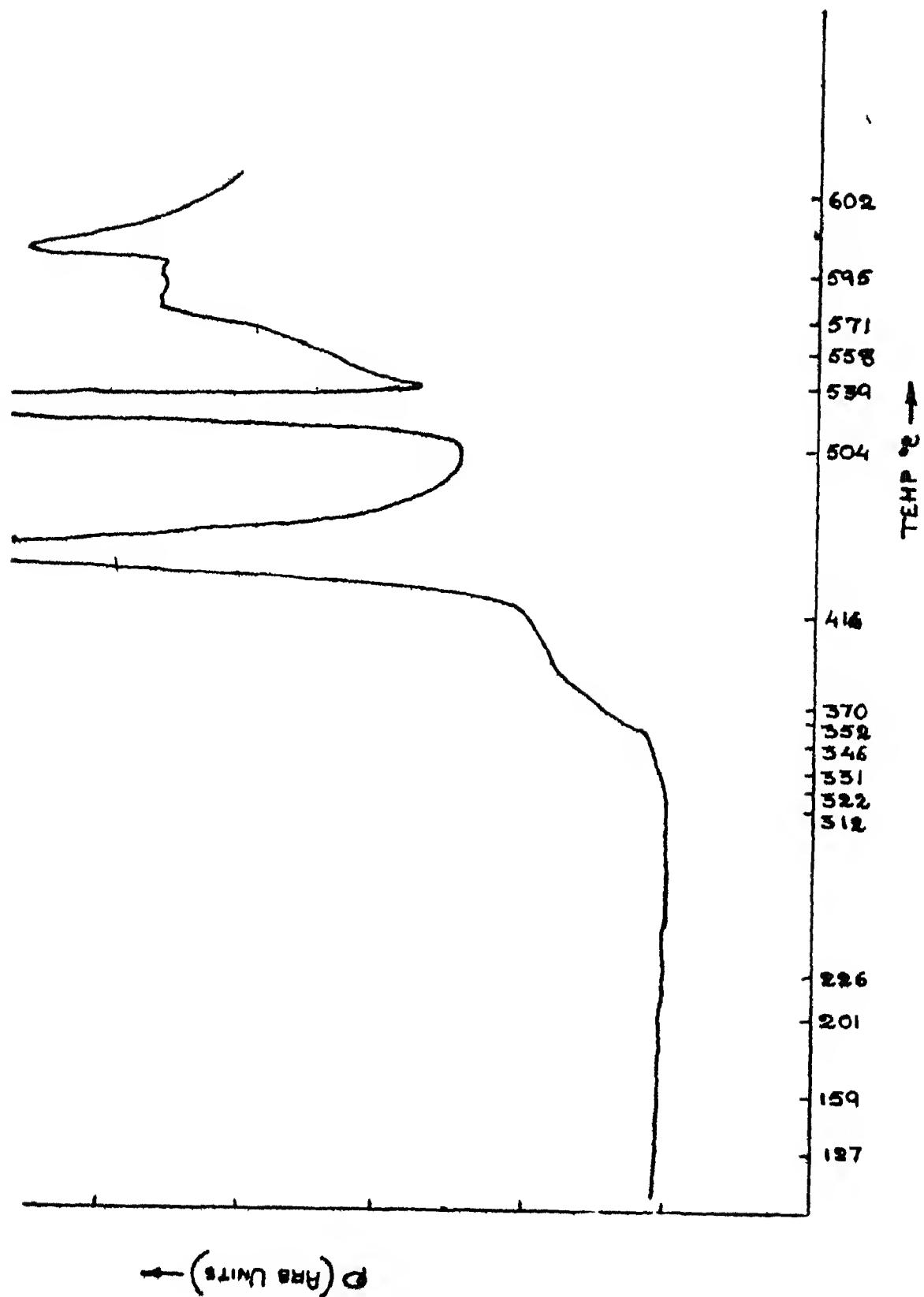
Figure 23   General DSC curve for ' 310°C/25 min/first run' sample
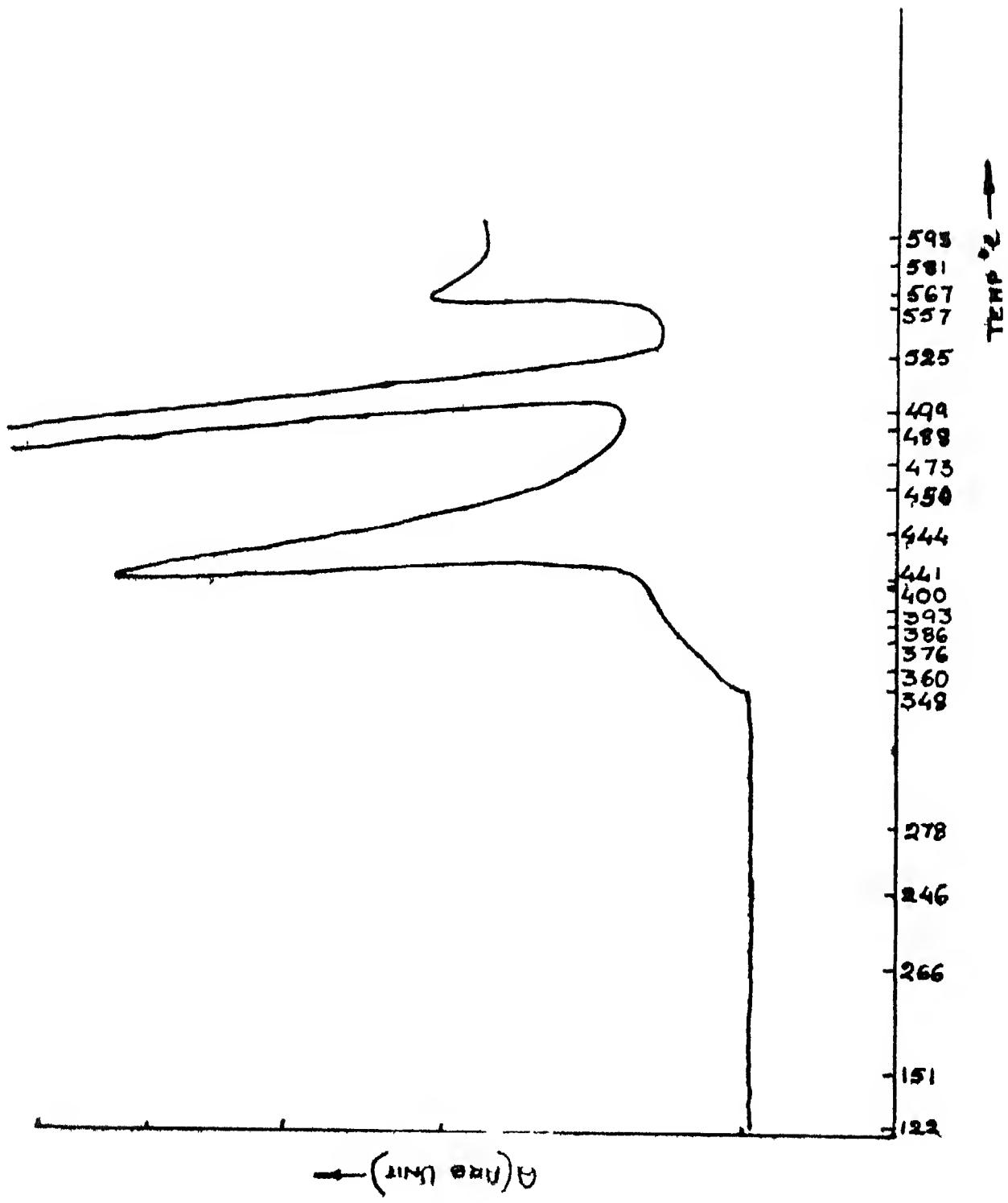
Figure 24 General DSC curve for '310°C/60 min/ fourth run' sample
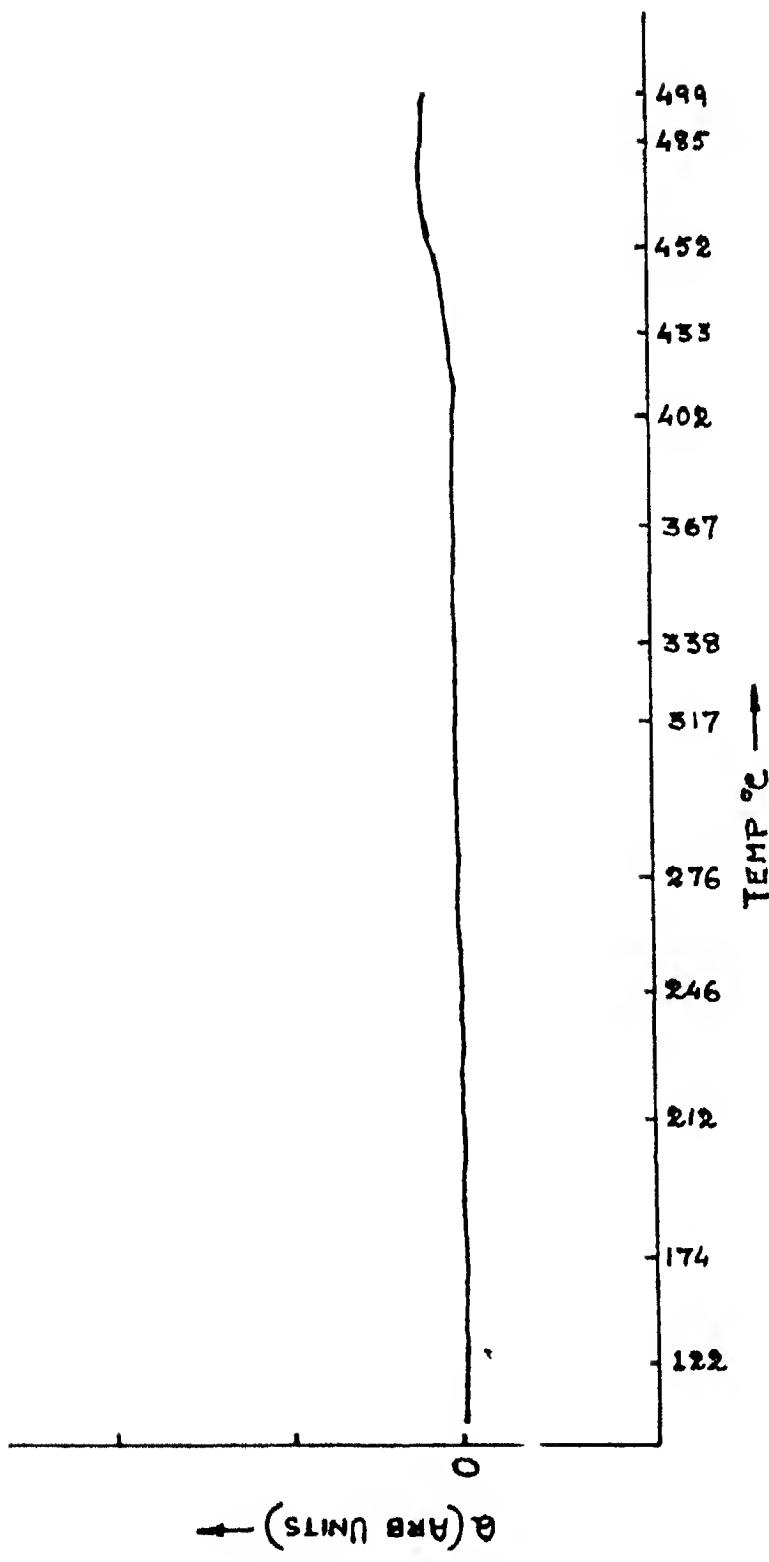
Figure 25 General DSC curve for ' 600°C/10 min/first run'
sample
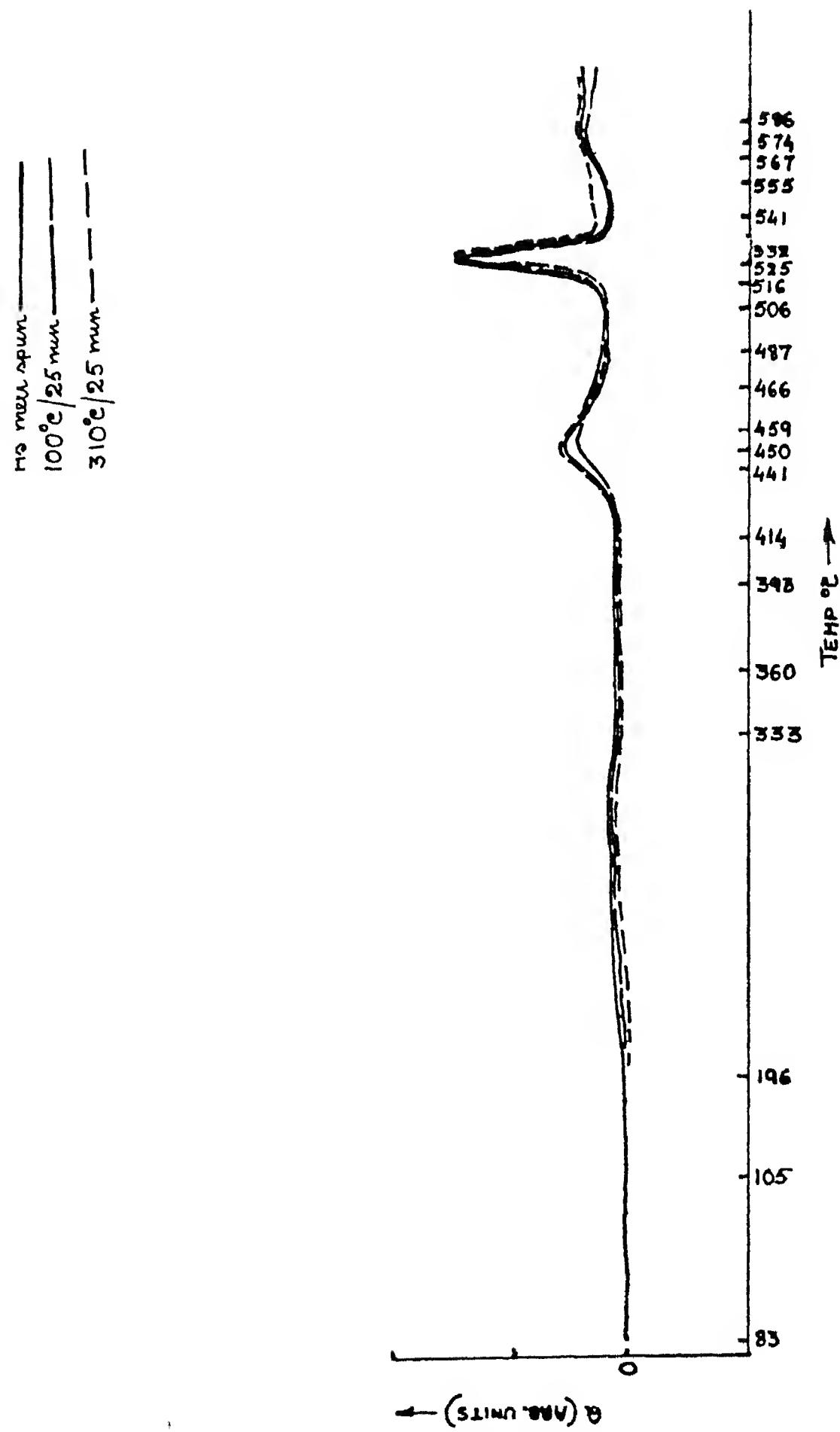
Figure 26 General comparison studies in DSC of
'as melt spun ','100°C/ 25 min',
'310ºC/25 min'-all first run samples
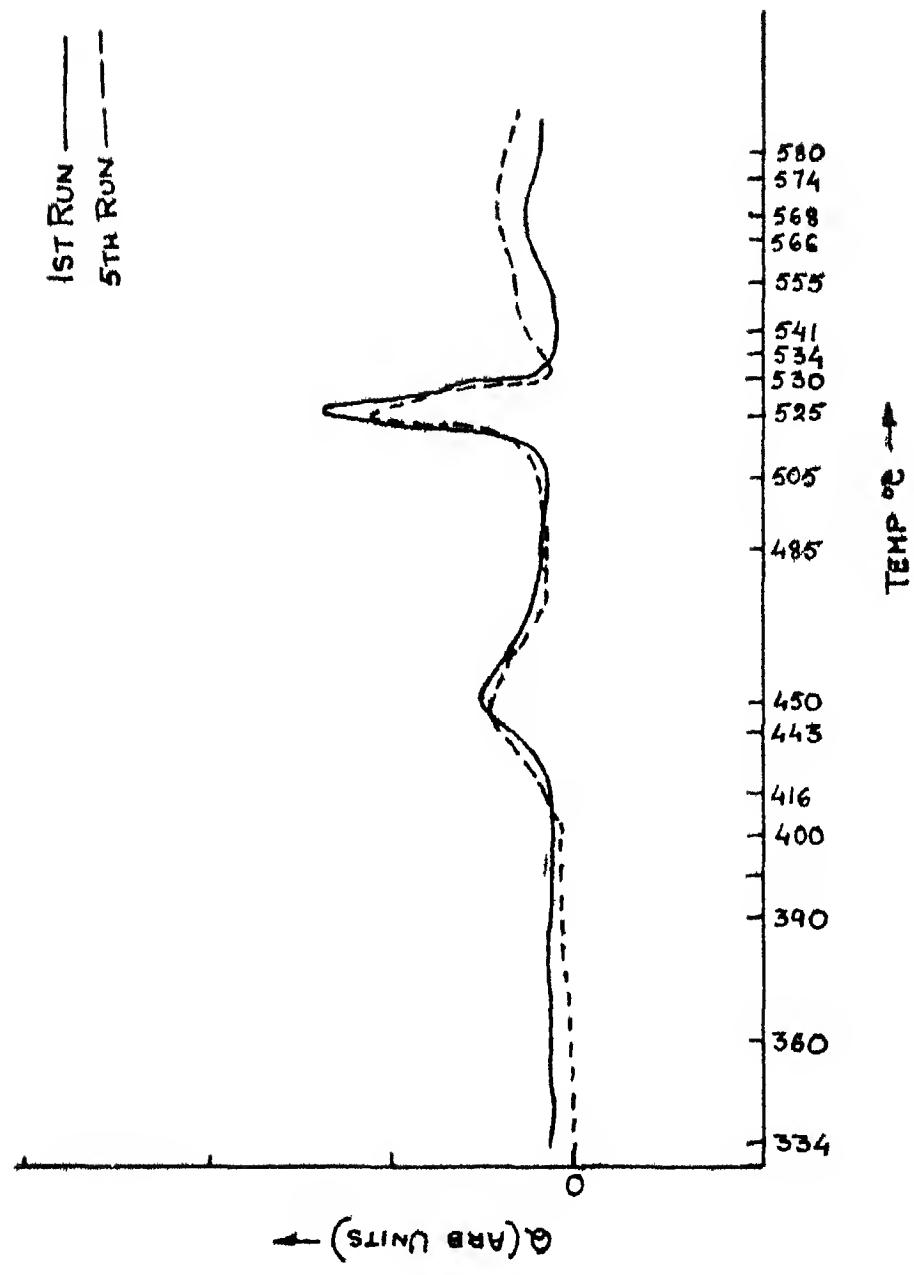
Figure 27   Crystallization comparison studies
in DSC of 310°C/25 min/ 1st and 310°C/25 min/
5th run samples
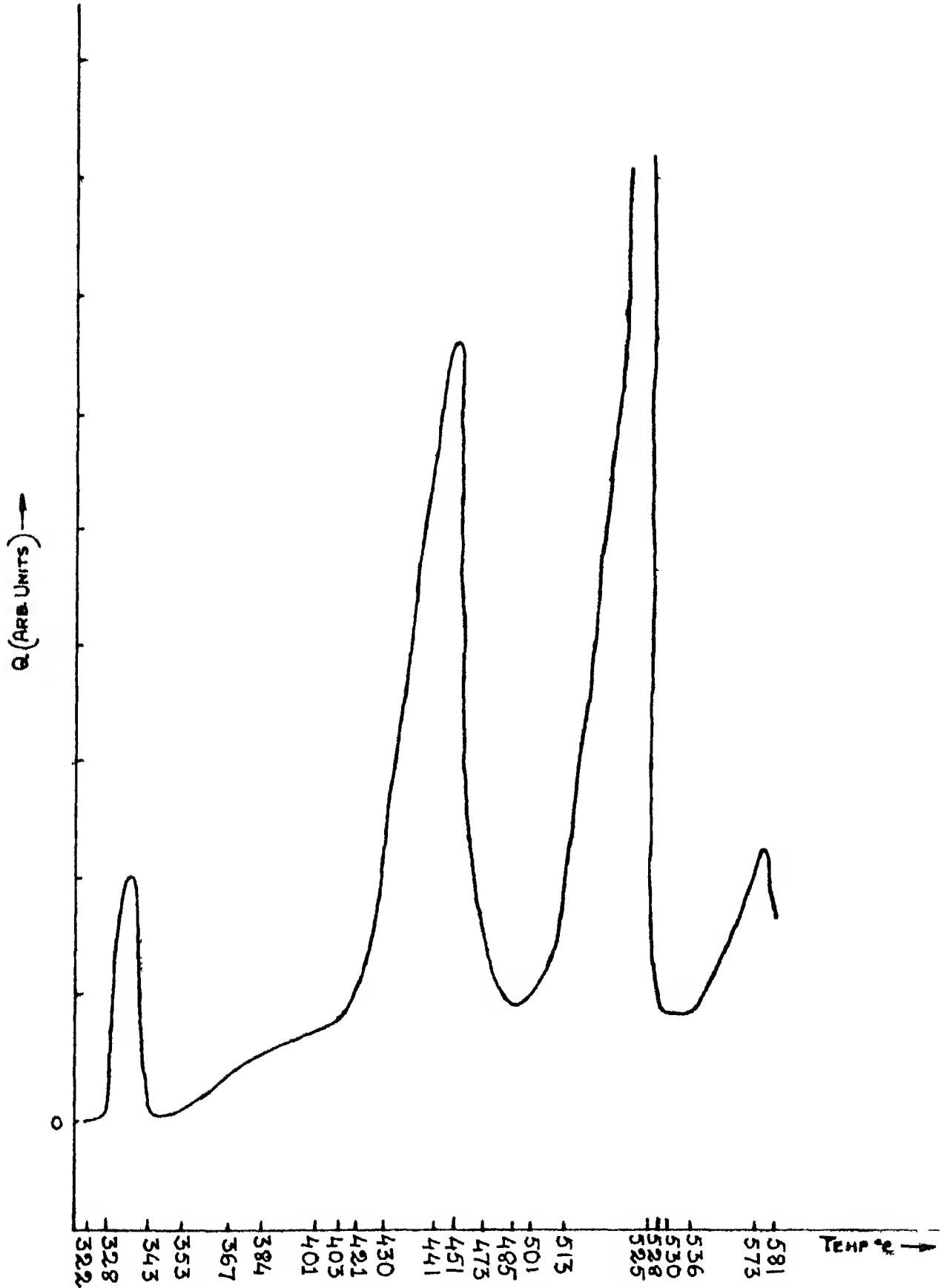
Figure 28 Crystallization studies of ' as melt spun/
4th run' sample in DSC
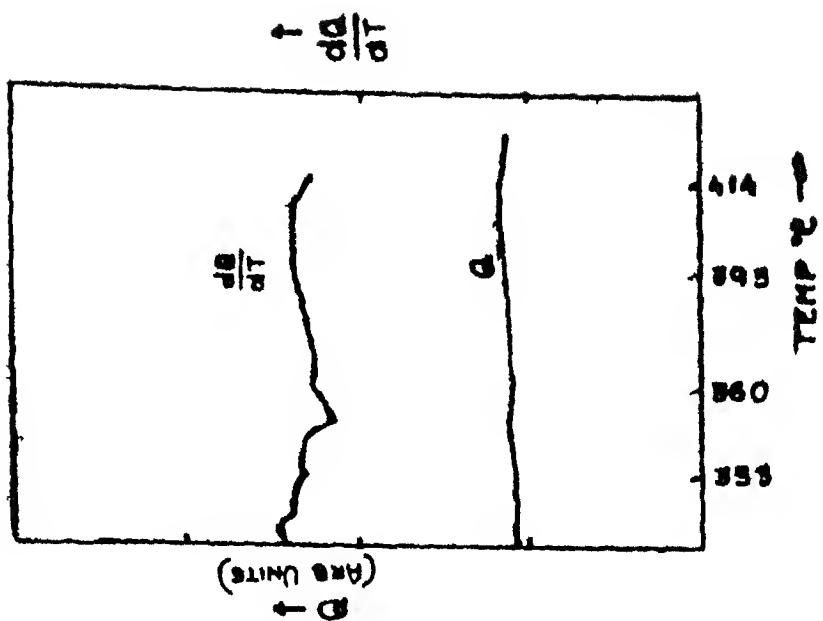
Figure 29 Crystallization studies of 100°C/25 min/1st run sample in DSC
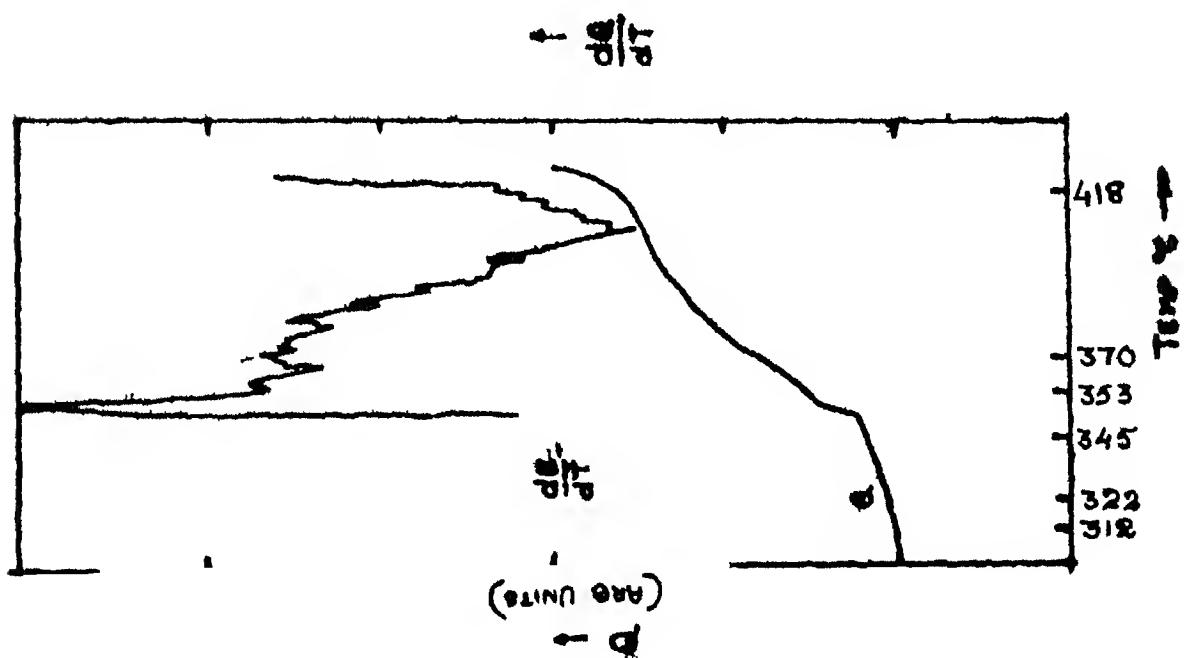
Figure 30 Crystallization studies of 310°C/25 min/2nd run sample in DSC
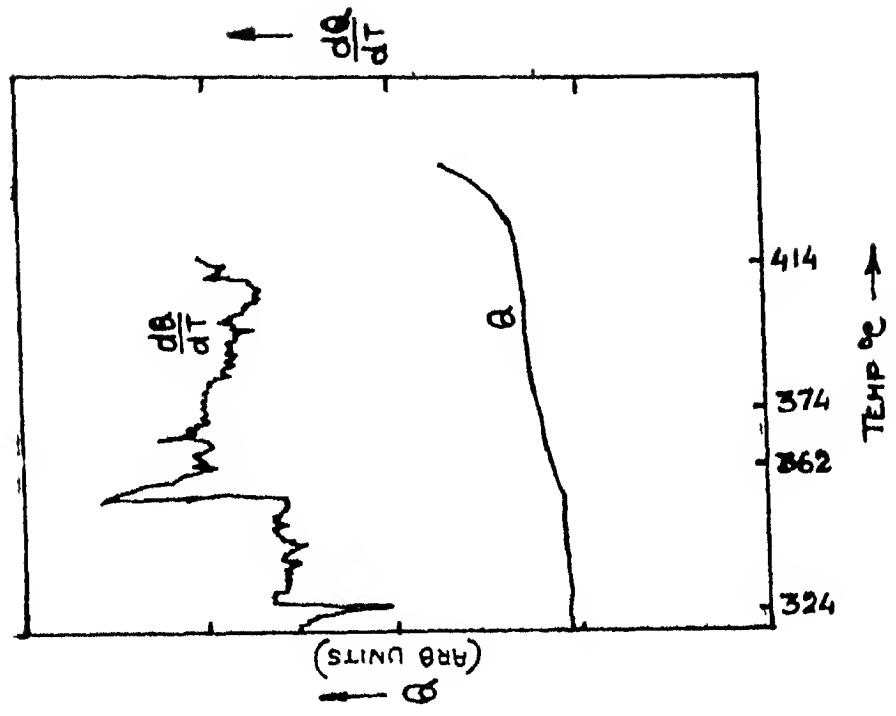
Figure 31   Crystallization studies of 310°C/60 min/1st
run sample in DSC
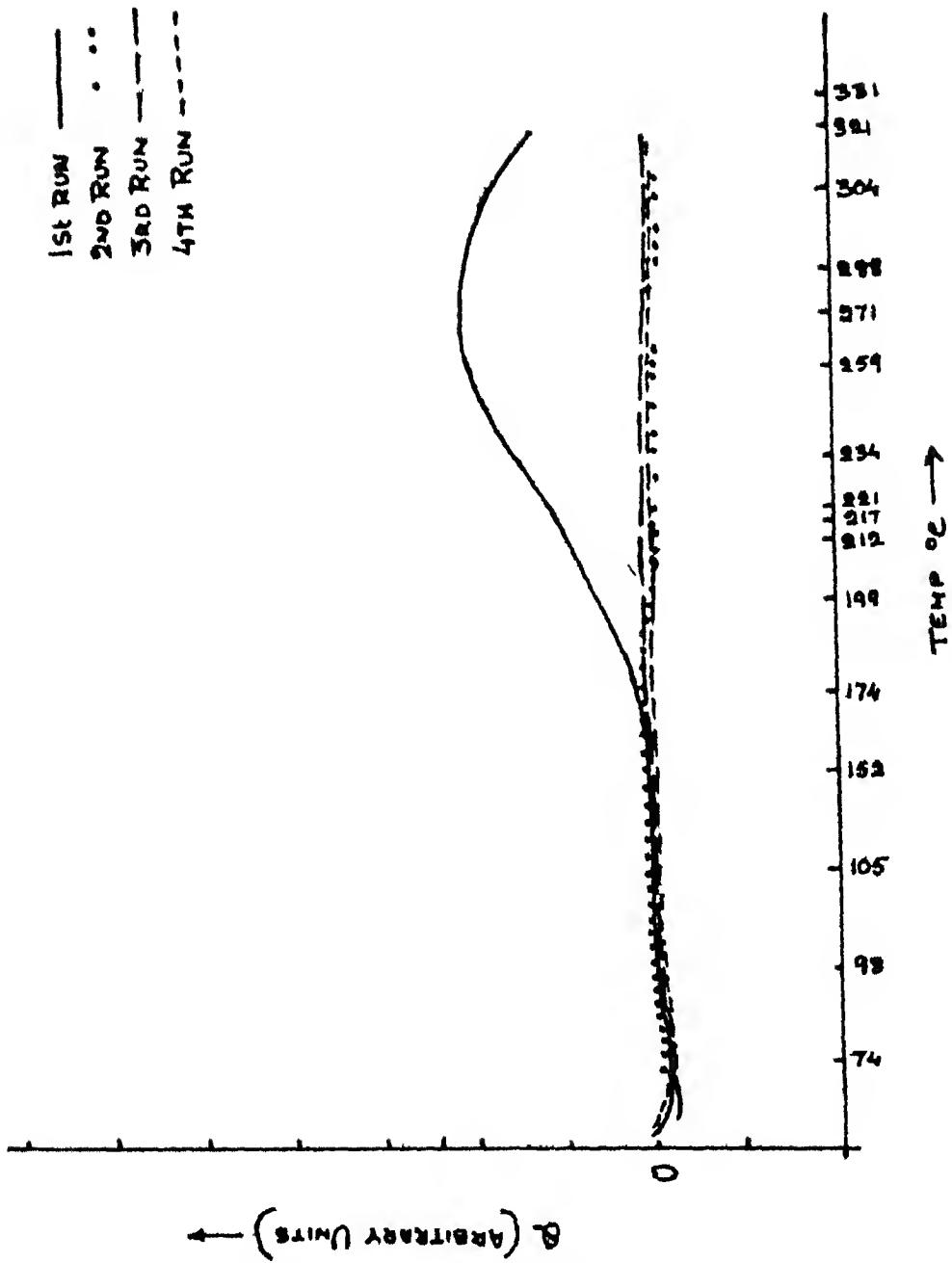
Figure 32   Structural relaxation studies of 'as
melt spun/first to fourth run' samples
in DSC
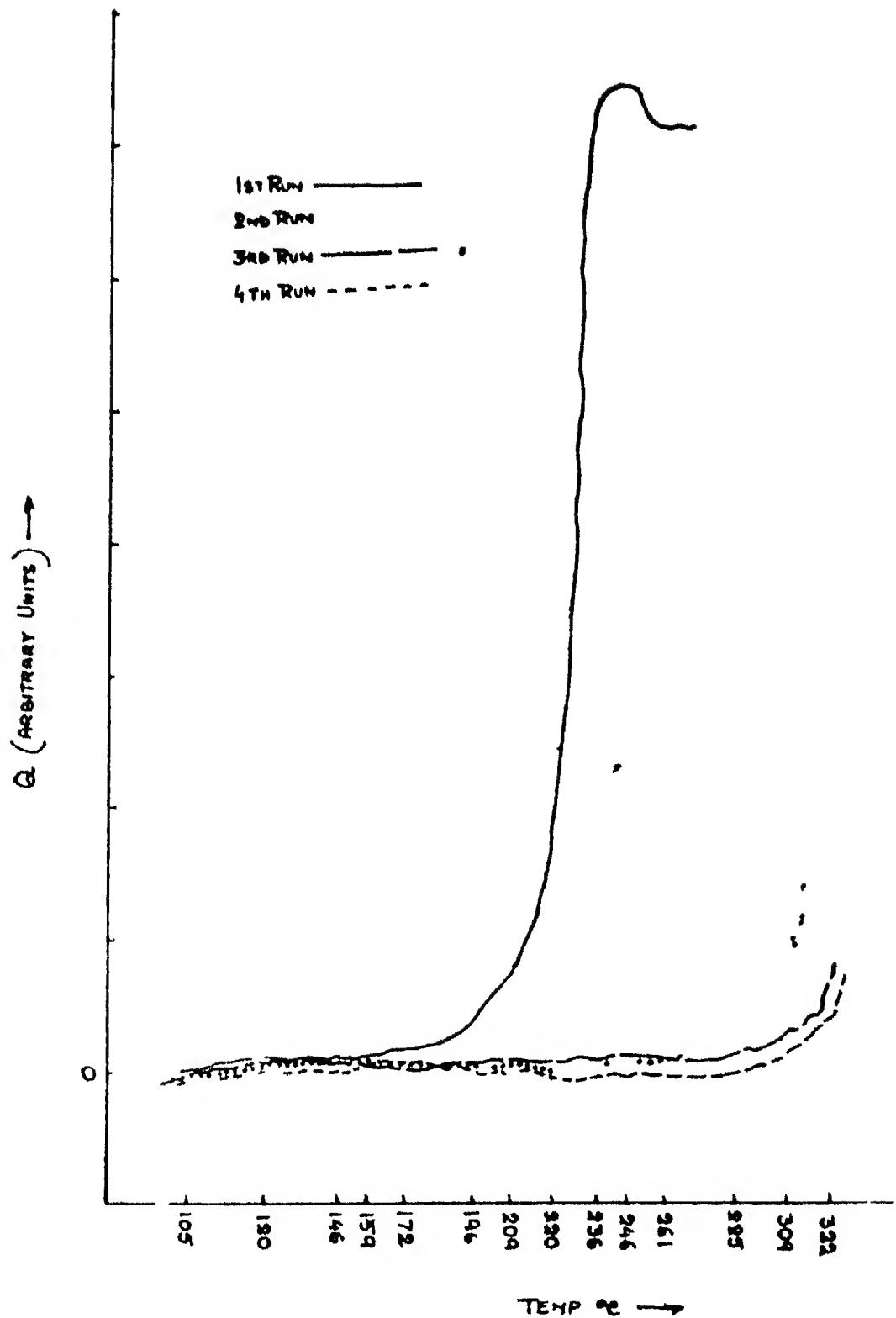
Figure 33   Structural relaxation studies of 310°C/25 min/
1st to 4th run samples in DSC
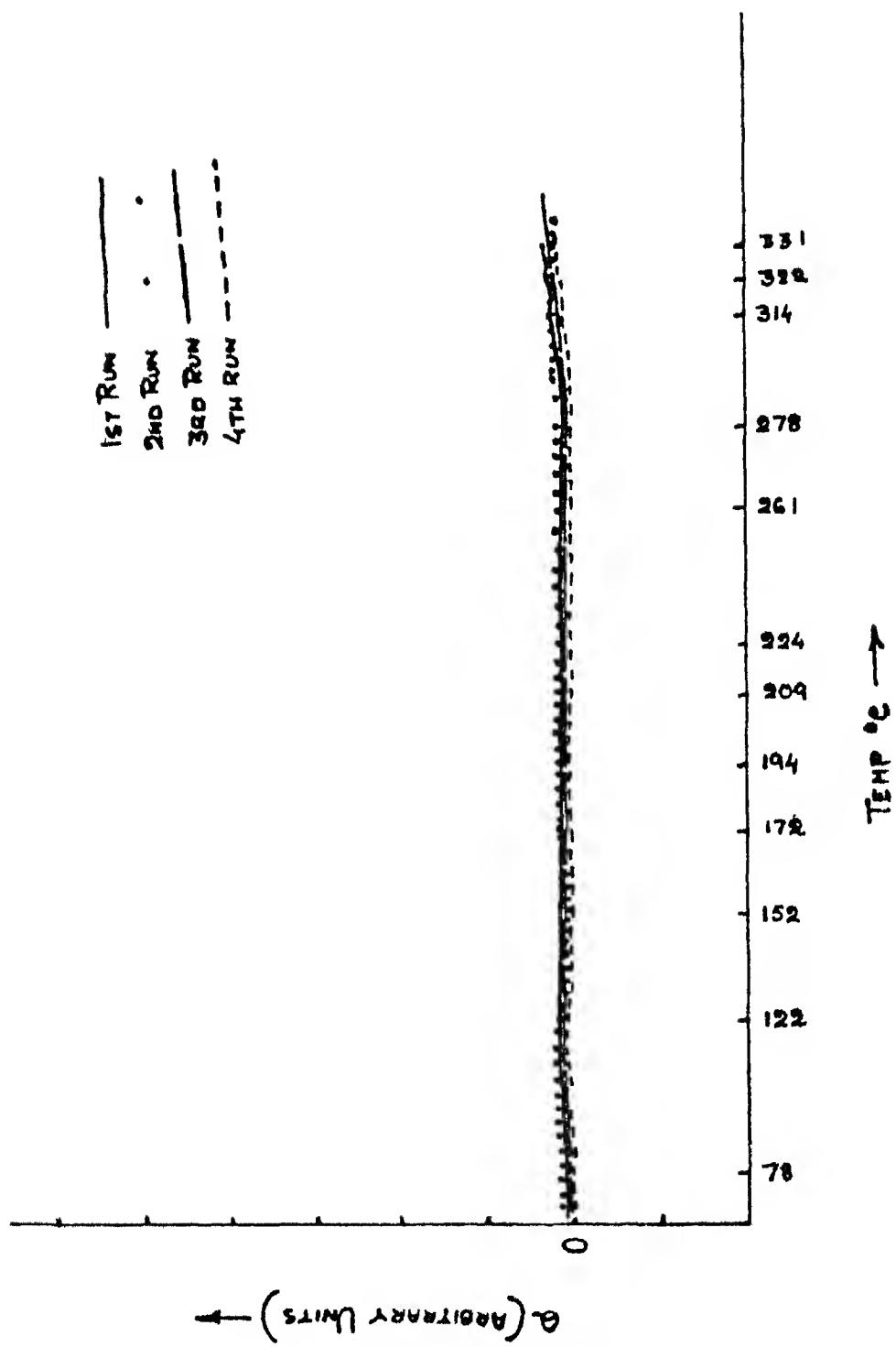
Figure 34 Structural relaxation studies of 310°C/60 min/
1st to 4th run samples in DSC

Figure 37

Fgirue 36
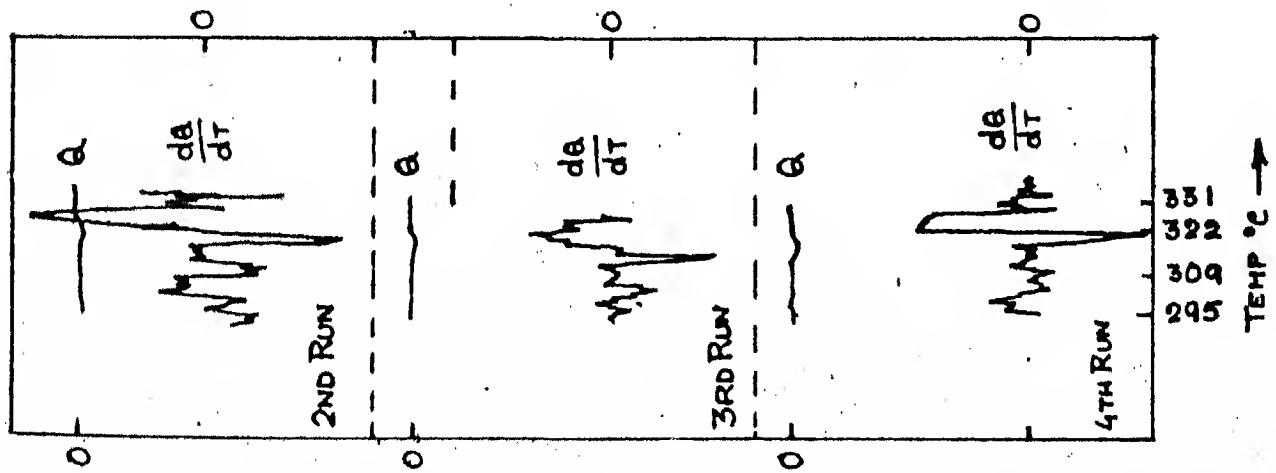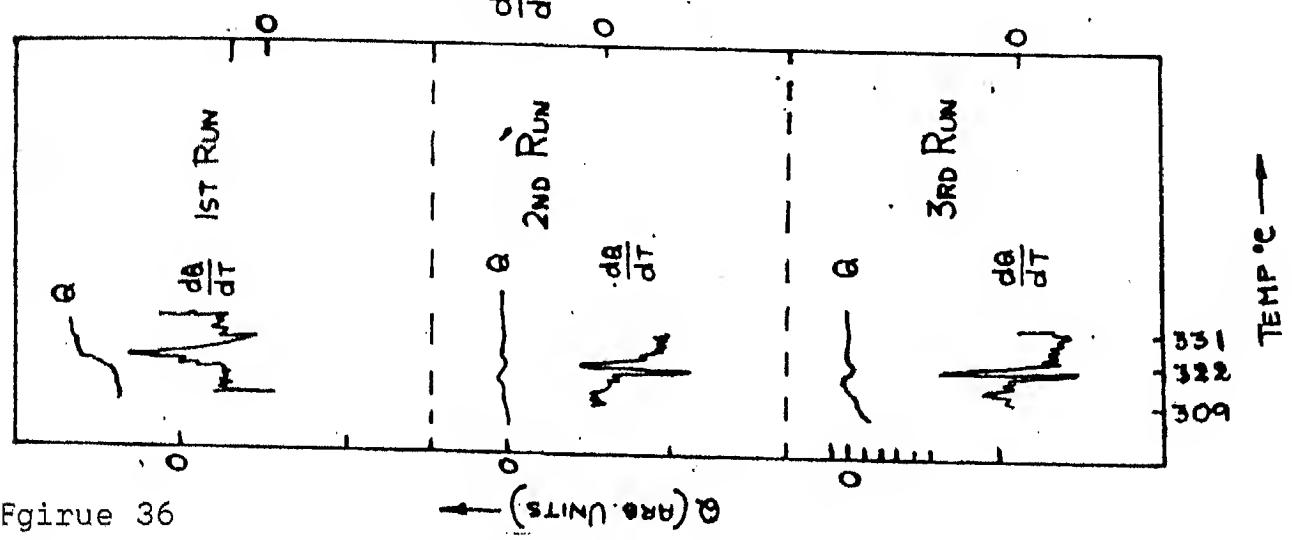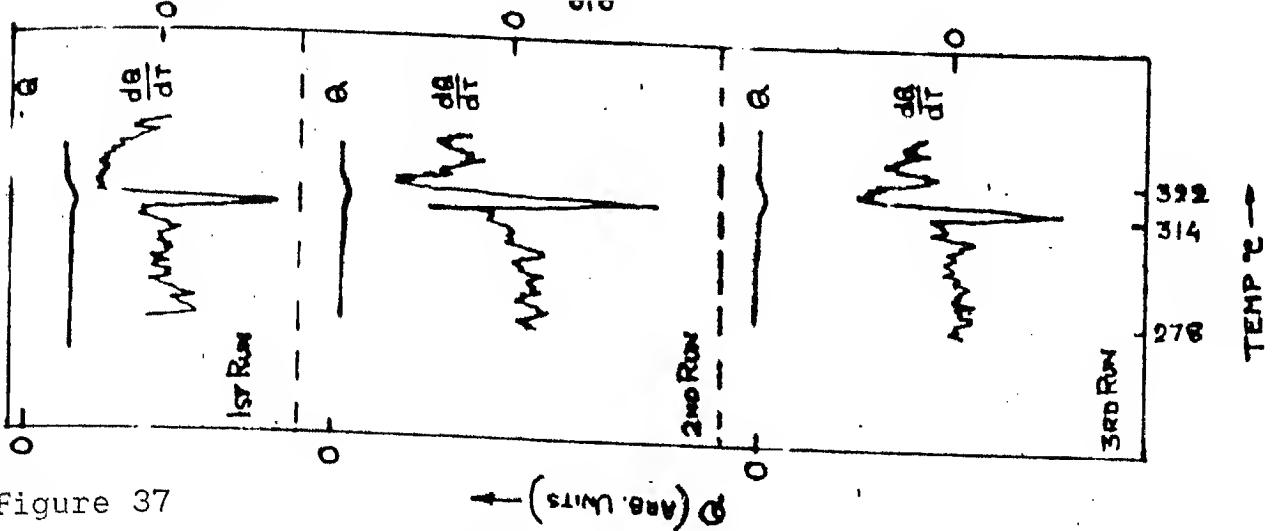
igure 35

igures 35 to 37. First reversible change studies of a) as melt spun/
2nd to 4th run samples - Fig. 35 b) 310°C/25 min/
1st to 3rd run samples - Fig. 36 c) 310°C/60 min/
1st to 3rd run samples - Fig. 37 in DSC.
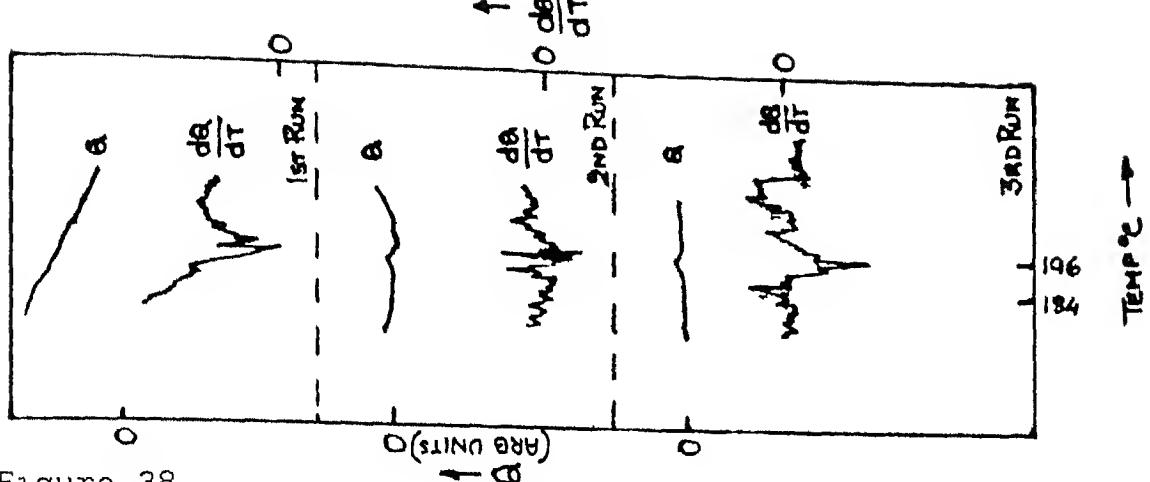
Figure 38
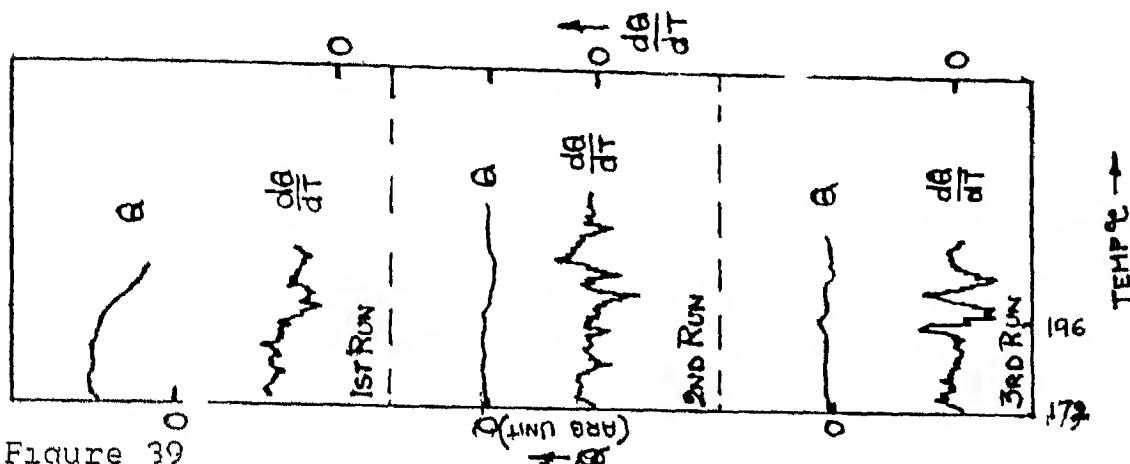
Figure 39
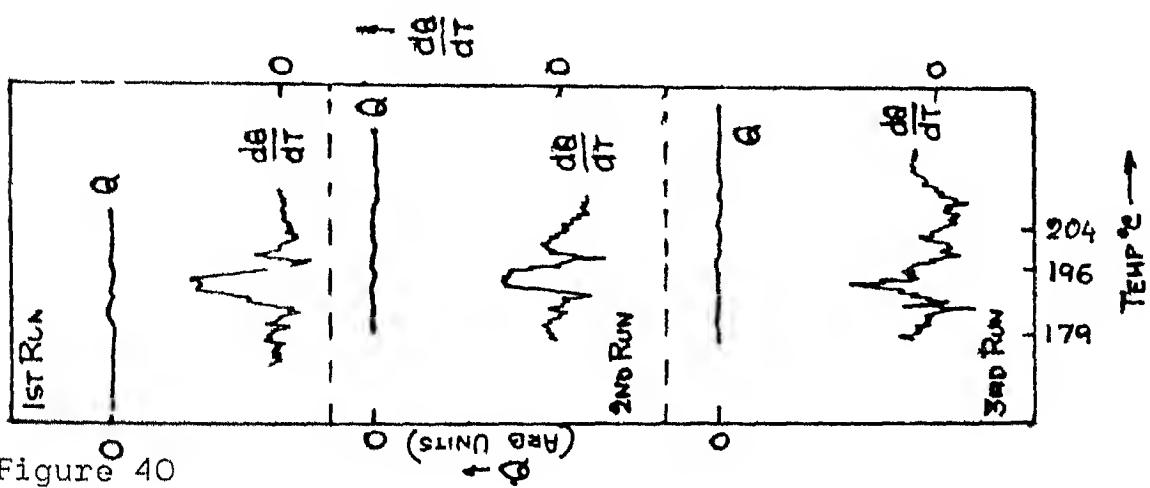
Figure 40

Figures 38 to 40   Second   reversible change studies of
                    a) as melt spun / 1st to 3rd run samples–Fig 38
                    b) 310°C/25 min / 1st to 3rd run samples–Fig 39
                    c) 310°C/60 min / 1st to 3rd run samples–Fig 40
                    in DSC
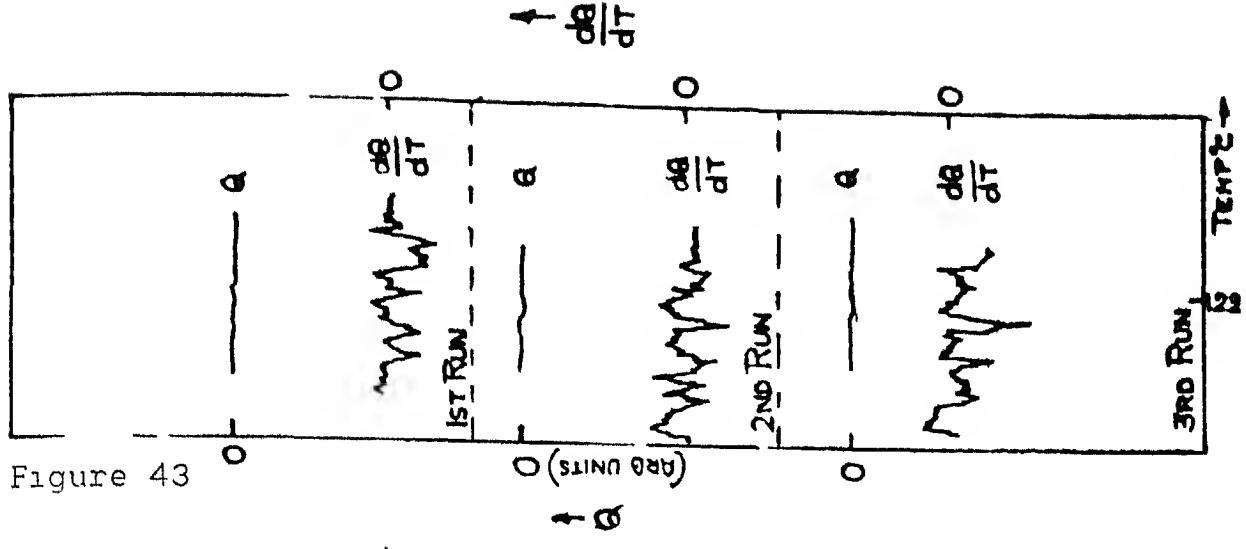
Figure 43
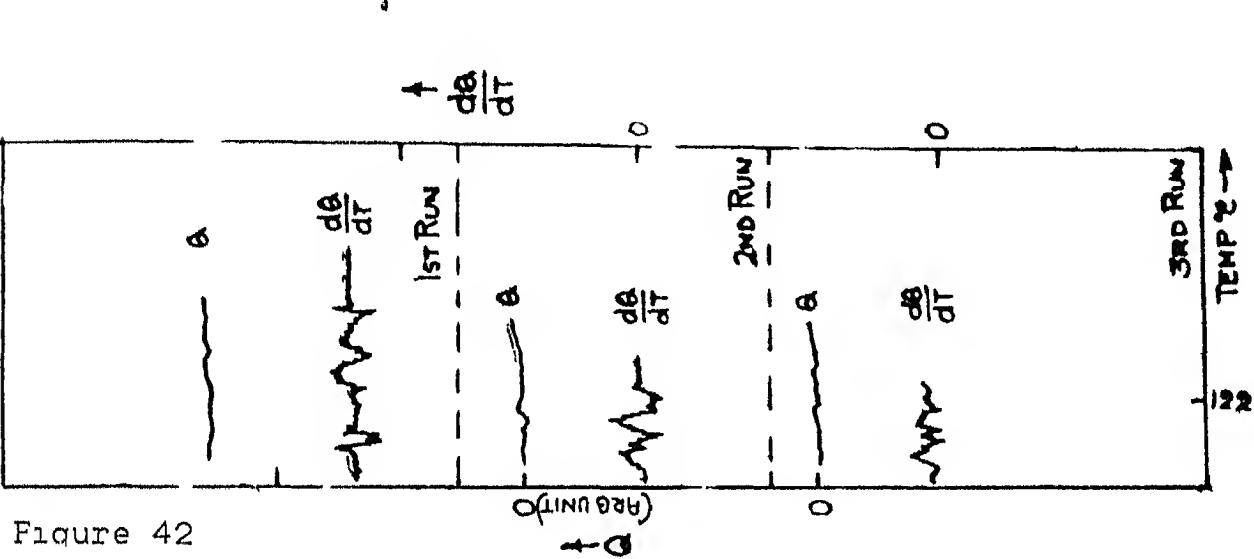
Figure 42
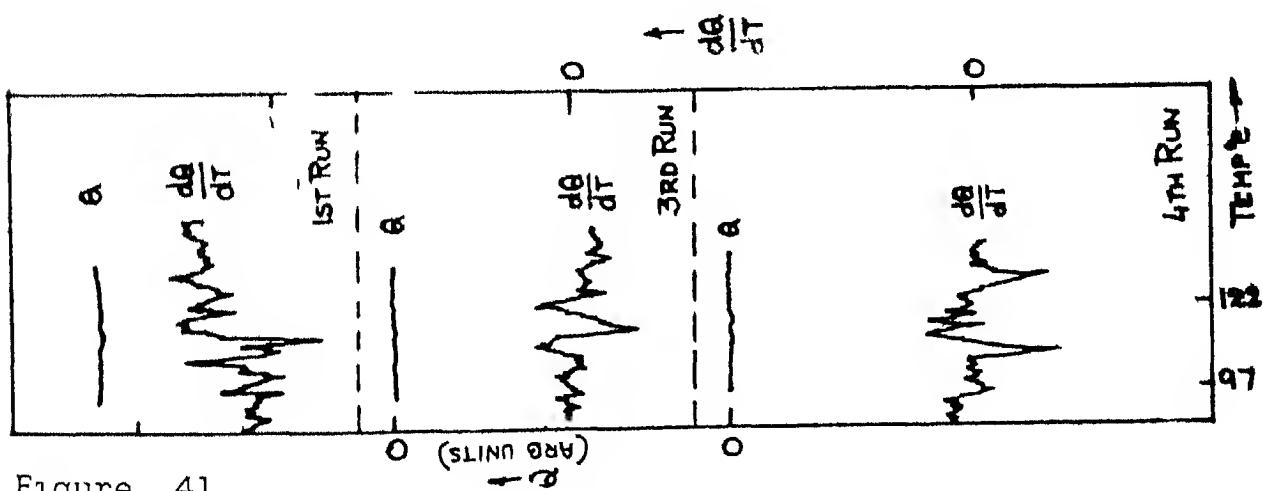
Figure 41

Figures 41 to 43 Third reversible change studies of
   a) as melt spun / 1st, 3rd, 4th run
      samples- Fig 41
   b) 310°C/25 min/1st to 3rd run samples-Fig 42
   c) 310°C/60 min/1st to 3rd run samples -Fig 43
      in DSC

Magnetic measurements for various samples

Curie temperature determination

Sample number and conditions	Experiment	Experimental and equipment conditions	Figure number
1) As melt spun	In single run from room temperature to 367oC	Room temperature = 22 5oC Field applied =50 Gauss Weight= 0 0052 gm Moment measured in scale = EMU Full scale (X1)	44
2) As after (1)	In single run from room temperature to 380oC	same as above	45

Magnetization measurements

3) As melt spun	-	Room temperature = 22 5oC Weight = 0 0052 gm Moment measured in scale = EMU Full scale (X1)	46
4) As after (1)	-	same as above	47
5) As after (2)	-	same as above	48

The results are plotted as follows
X axis = Temperature in oC
$Y \text{ axis} = \dfrac{\text{Moment}(\mu)}{\text{Weight of the sample}(gm)} = \dfrac{\mu}{g}$
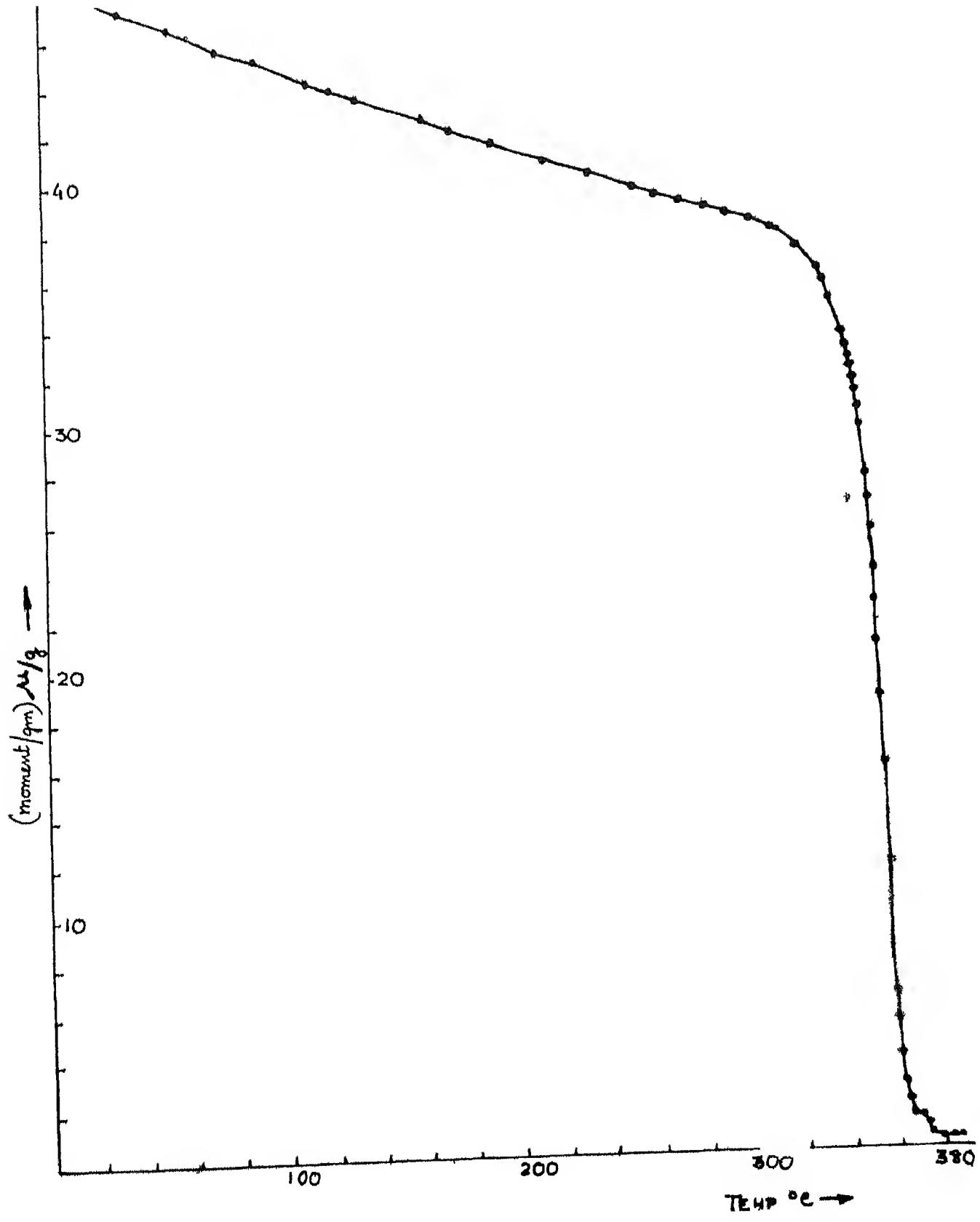
Figure 44   Curie temperature determination of 'as melt spun/first run' sample
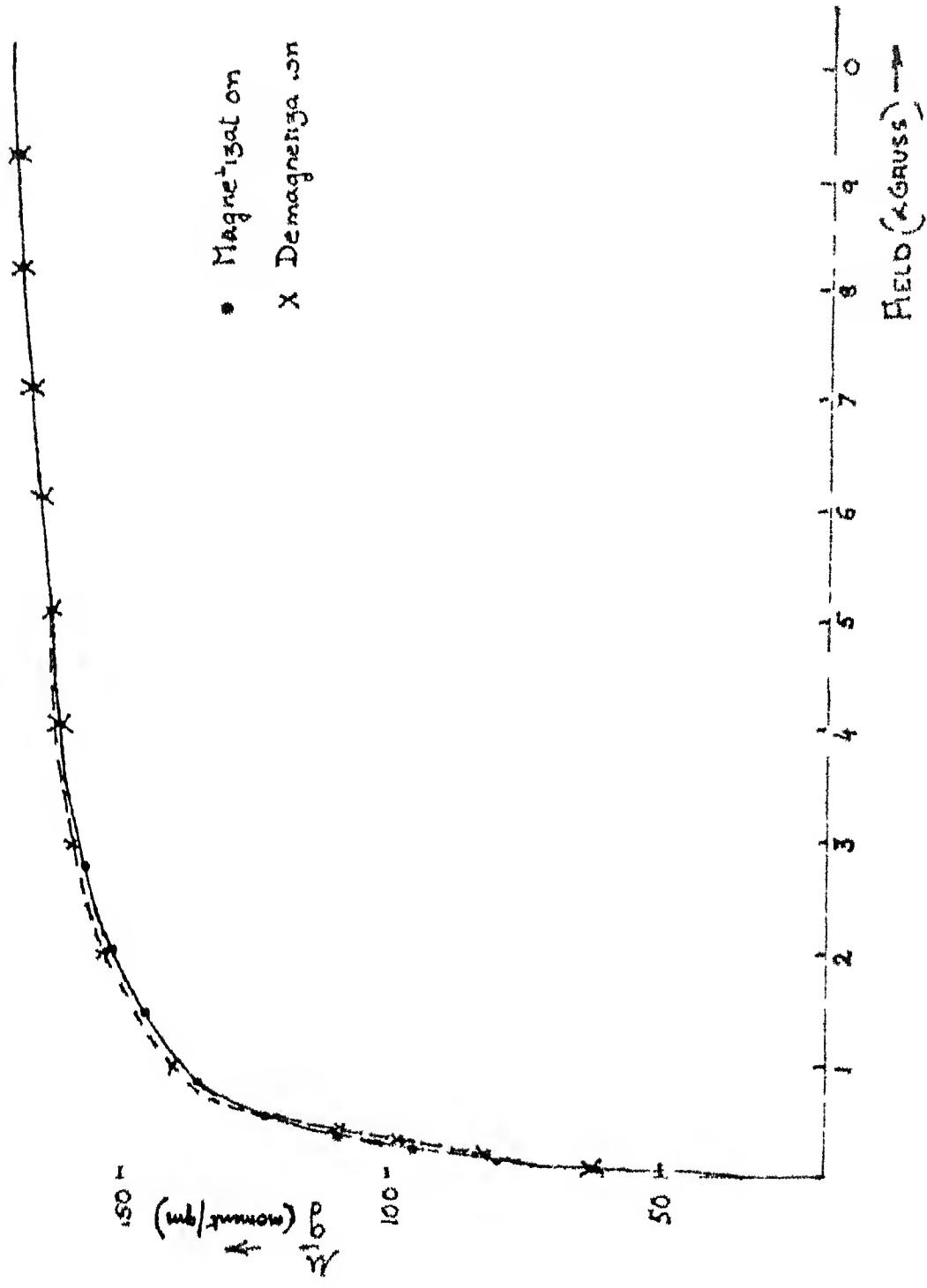
Figure 46 Magnetization studies of ' as melt spun' sample.

Magnetization

X Demagnetization

FIELD (KGAUSS) →

$\frac{M}{\rho}$ (moment/gm)

200

150

100

50

20
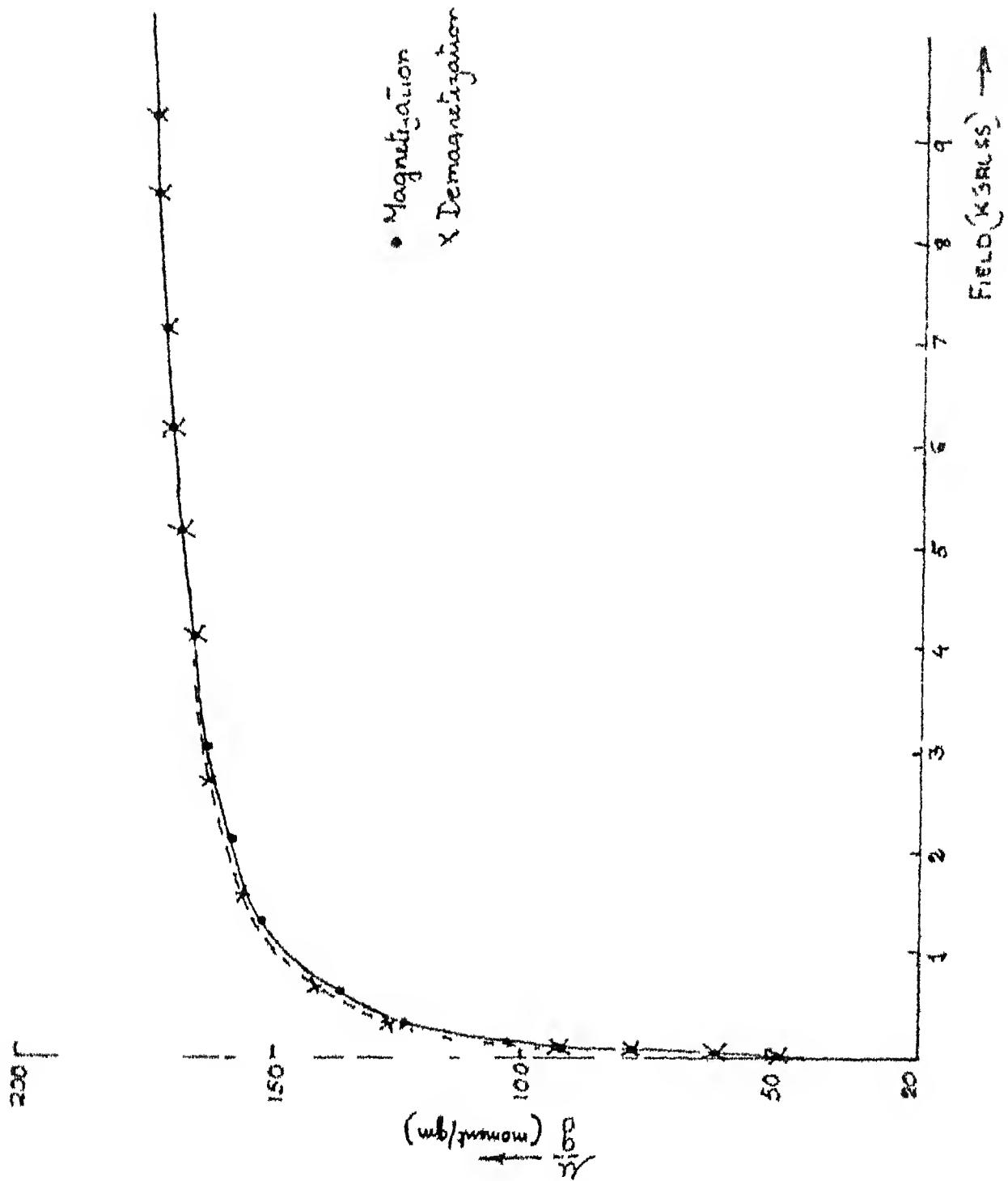
Figure 47 Magnetization studies of ' as melt spun/' first run' sample
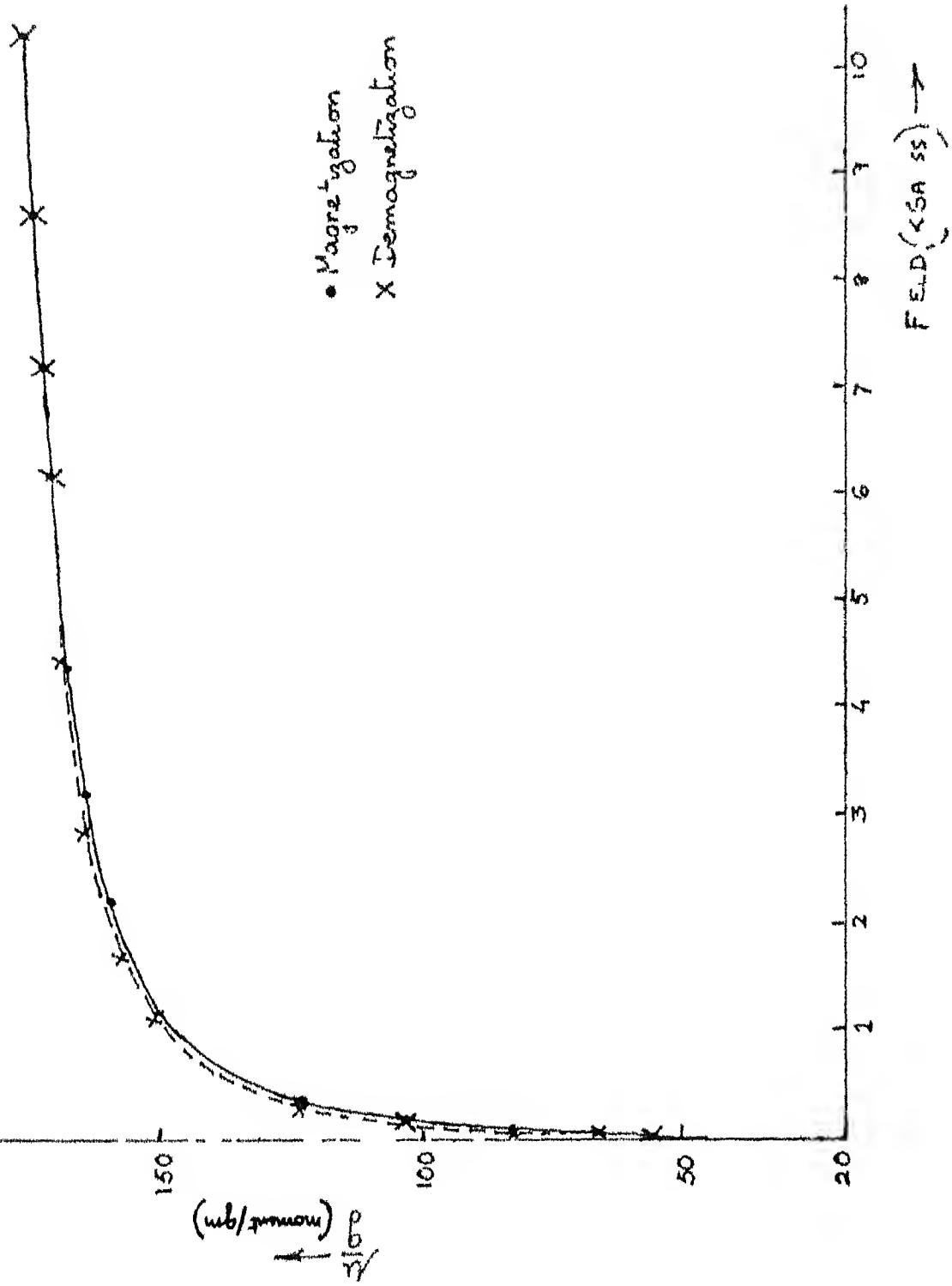
Figure 48 Magnetization studies of 'as melt spun/
second run' sample

Figure 49 X-ray diffraction pattern of as melt spun metallic glass ribbon equivalent to Metglas 2605 Sc as prepared in laboratory (showing latent onset ons)
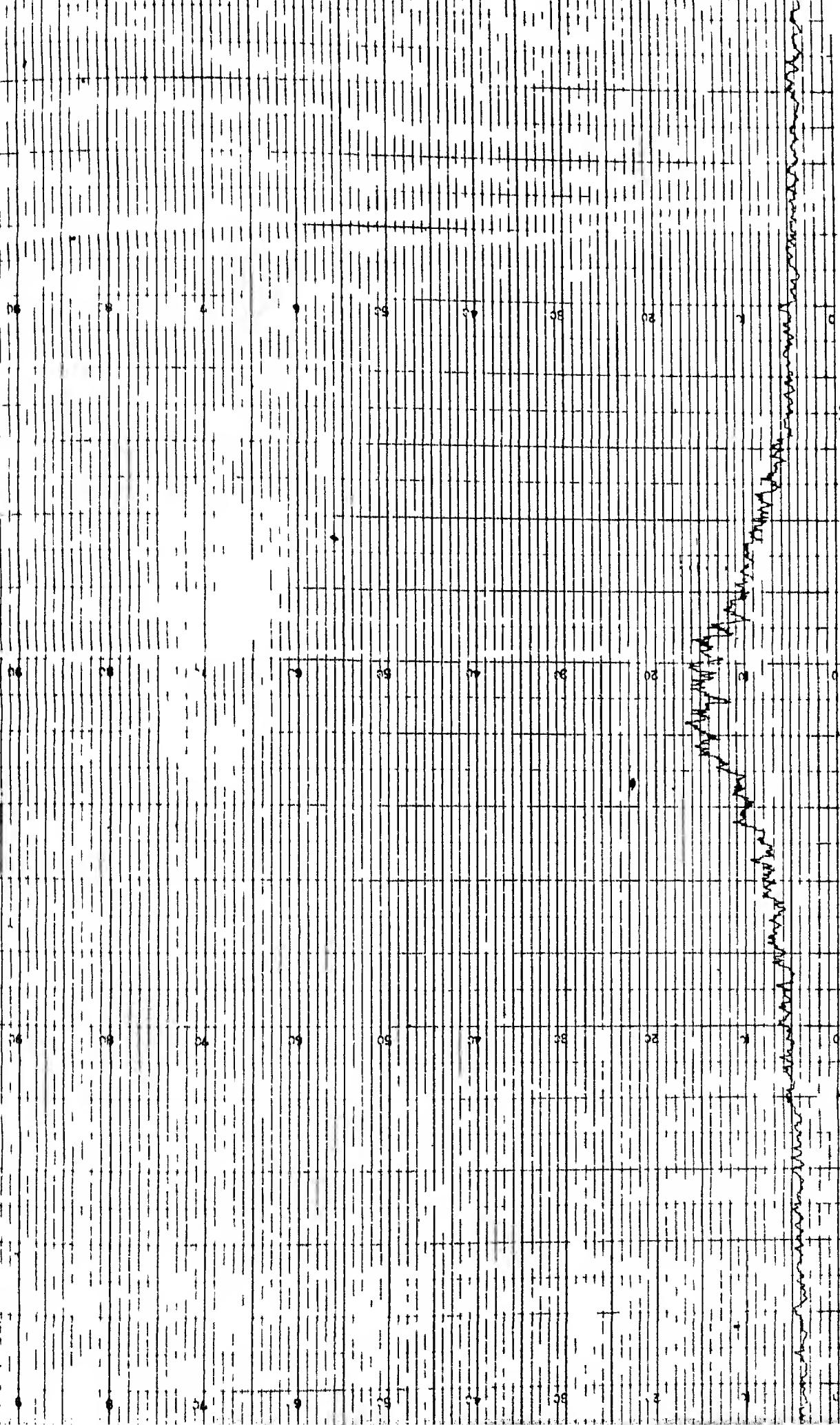
Figure 50 TEM diffraction pattern (SAD) and
microstructure of as melt spun metallic
glass ribbon equivalent to Metglas 2605Sc
as prepared in laboratory

CHAPTER V

DISCUSSION

V 1   Fabrication of Metallic glass

To obtain an amorphous ribbon and also a deoxidized one, the time required to cool the molten metal to the final ' room temperature structure' should be as small as possible as well as the distance between molten metal and cool substrate   And in the process, the important controlling parameters are the distance between chillblock and the nozzle, the amount of superheating as well as, in some cases, orifice geometry and even surface velocity of the wheel.   Agarwal and Chakachary [10] hold the view that the lesser is the distance between the chill block and nozzle, the lesser is the chance of melt oxidation and freezing   Our results also support this view   Upto a distance of 2 mm, the chances of ribbon production without oxidation is better while at a higher distance, namely 4 mm, results in completely oxidized ribbon.   However, Agarwal and Chakachary [10] proposed an optimum distance of 1 mm, while our experiments show that amorphous, deoxidized ribbons can be obtained even upto a distance of 2 mm

The fact that the path difference between the chill block and molten metal should be as small as possible also finds expression in orifice geometry   In nozzle (2) (Fig.17) the orifice extends upwards thereby increasing the

distance between chillblock and nozzle   That may be one
of the reasons why the nozzle is not suitable for melt
spinning

The results (see Chapter IV 1) show that if
no superheating is applied to the material, as is evident
from the case of melt cooling from the melting temperature
of the alloy, partly crystalline ribbons are formed Whereas
there will be some upper limit in the amount of superheat
above which crystalline material again forms   The results
can be rationalized as follows   Enough superheating is
required to compensate for the cooling of the alloy during
its passage through the relatively cold part of the nozzle
and the air gap between nozzle top and cold substrate   On the
other hand, at the highest limit, since the dwell time of the
substrate is short and fixed for a fixed speed, the ribbons
are not cooled below the temperature of glass formation and
are ejected from the surface   Thereby they will follow the
natural air cooling, resulting in the formation of crystalline
product.

The same rationalisation can be done when the
surface speed of the cold substrate is very high. For example,
the results (Table 5 in Chapter IV 1) show that at a high
surface speed corresponding to 270 volts, crystalline material
formation takes place.

The jet turbulence of the molten metal jet
seems to be an important factor in determining whether

uniform, continuous ribbons can be obtained or not It is found that the nozzles where the angle with the horizontal (Table 2 of Chapter IV 1) is varied from 60o to 80o even edge continuous ribbon formation is taking place Whenever the angle is too low, for example 35o, or too high, for example 8°o, uneven and discontinuous ribbon formation takes place

Nozzles with serrations, i e nozzle (3), (Fig. 17 of Chapter IV 1), nozzles where the orifice does not extend full distance lengthwise i e nozzle (4) (Fig 17) probably cause turbulence, resulting in uneven ribbons having holes and cracks From the results of Table 3 (Chapter IV 1), it can be observed that there is a limit of ejection pressure below which uneven and discontinuous ribbon formation takes place However, after an upward value, no further effect of increasing pressure is observed This view is also supported by Huang (Fig 3) [11]

As is expected increasing surface velocity results in decreasing the thickness of the ribbon produced.

The above discussion shows that the time required to cool the metal to glassy state is an important factor to determine whether a deoxidized uniform and continuous amorphous metallic glass ribbon will be obtained Also the jet turbulence probably plays an important part in determining the physical characteristics of the ribbons

However further experimentation is required to show whether the above factors do affect the ribbon formation or not and if so to what extent

V 2 Characterization

The characterization of the general nature of the as fabricated metallic glass is done in two ways First the fabricated ribbons are examined by TEM and X-ray to find whether amorphous stiucture has been achieved or not   The presence of the hallo characteristic of amorphous materials as well as the absence of any grains in the microstructural results of TEM (Fig.50) confirms that the amorphous state has been achieved   Similarly in Y-ray (Fig 49) the presence of the broad peaks suggest that the ribbons examined are amorphous in nature   Secondly, the thermal stability of metallic glasses so obtained is studied with different types of experiments as discussed in the Experimental Procedure (Chapter II) and the results obtained (Chapter IV) are discussed as follows

i) Structural relaxation

The literature survey shows that the as obtained Metglas 2605SC crystallizes giving rise to thermal effects in the temperature region at least above 330oC (Chapter II 2) As discussed in the literature survey, the changes occurring in the low temperature region can be considered to be due to atomic rearrangements arising out of the highly disordered

and metastable states of the amorphous alloys   These
changes are attributed to TSRO or CSRO (Refer II 3)
Fig 32 to 34 shows the effect of one or more thermal
cycling on as melt spun and heat treated specimens of the
prepared Fe-B-Si-C alloy   Fig 32 shows that a broad exother-
mic peak appears in the first run of the as melt spun sample
in the range of $\sim 160o$C and $\sim 330o$C
in the first heating itself   But after this first run of
                    followed by furnace cooling to room temperature
is completed, subsequent runs do not show the presence of this
broad exothermic peak   Of the two possibilities of low tem-
perature changes, TSRO and CSRO, only TSRO is irre versible,
hence the disappearance of this peak in the second and subse-
quent runs suggest that the changes occurring in between
$\sim 160o$C to $\sim 330o$C are due to structural relaxation of the
specimen because of TSRO

            The trace of Fig 33 has been obtained with
Y axis (Q) ten times more sensitive than that in Fig 32   If
the peak heights are considered to approximately give the
intensity of thermal effect, the preheattreated specimen of
Fig 33 shows somewhat less thermal effect than the as melt
spun sample in Fig 32 Fig 33 also shows that the heat
treated sample has no more thermal effect after the first
run, as that of Fig 32   The observed small rise in the
upper level of temperature in the second or subsequent runs
are due to base line characteristics of the apparatus at

the high sensitivity level   It is surprising that inspite
of the 25 minute isothermal anneal at 310oC given to the
sample of Fig 33, the specimen does not go through complete
structural relaxation   Whereas the same sample, after even
a single thermal recycling through ← 320oC, almost completely
structurally relaxes (Fig 33)   This severe effect of thermal
cycling is also found for as melt spun specimens   (Fig 32)
The question comes to mind is why 25 minute isothermal annea-
ling at high temperature (at 310oC) followed by very slow
cooling (sample withdrawn from hot zone to room temperature
in 24 hours) would not relax the sample more easily and
effectively then the dynamic heating (at the rate of $10^{o}C$ /
min) upto↙ 320oC followed by comparatively quick furnace
cooling in the DSC apparatus (approximately about three
quarter of an hour to come down to $50^{o}C$)   Further work is
necessary in detailed to understand this behaviour

The relaxation studies of 310oC/60 minute annealed
sample (Fig 34) shows that this isothermal heat treatment
causes almost complete structural relaxation as the broad
exothermic peak is absent in the first run itself   From this
result it can be qualitatively said that the effect of one
thermal recycling is somewhere in between but at least greater
than 25 minutes but less than 60 minutes isothermal annealing
of a sample at 310oC

(i) Crystallization

The crystallization behaviour of the metallic glass of present study by electrical resistance are shown in Fig. 18 and 19 The general nature of the shape of the curve obtained in the study of change in electrical resistance with temperature (Fig 18 and Fig 19) tallies well with the data obtained with Metglas 2605Sc by Bhanu Prasad et al([19] and Fig 8) but differ considerably in the temperature regions of transformations as well as in fine details The temperature regions of transformations observed in this investigation agree reasonably well with the different transformations determined by Sageusa and Moris [17,18] through Mossbauer spectroscopy Bhanu Prasad et al [19] have found that first a linear increase in electrical resistivity (Fig 8) occurs followed by a rapid and continuous decrease in electrical resistivity which starts at around 452oC The decrease in electrical resistivity is followed again by a uniform increase of resistivity starting at around 535oC The decrease in electrical resistivity from 452oC has been correlated with crystallization and the next increase in electrical resistivity from 535oC is correlated with the normal increase in electrical resistivity of the crystallized product The present results suggest that both for the as melt spun sample heated to crystallization (Fig 18) and for the as melt spun sample heated to 300oC followed by furnace cooling to room

temperature and then heated to crystallization (Fig 19), the crystallization start and finish occur at much lower temperatures ($\sim$ 390oC to $\sim$ 500oC for the former and $\sim$ 350oC to $\sim$ 486oC for the latter). It is also seen that unlike the results obtained by earlier investigators [19], electrical resistance does not decrease in a continuous fashion but in steps An arlest in the decrease in electrical resistance at $\sim$ 460oC occurs for both the samples studies (Fig. 18 and Fig 19) Moreover, an additional arrest appears in the temperature range of 383oC and 400oC for the heat treated sample (Fig 19) Crystallisation temperature range of the as melt spun first run sample correlates more closely with the start and finish of crystallization temperatures of the as melt spun alloy data reported by Sageusa and Moris [17,18] One possible reason as to why there is so much discrepency in the results obtained by Bhanu Prasad et al (19) and others on the one hand and Saegusa and Moris [17,18] and the present investigation on the other is possibly due to the presence of microscopic variations in composition, variation in the state of stress present in the material etc

Comparision of the crystallization of melt spun sample (Fig 18) and as pre heat treated sample subjected to one thermal recycling through $\sim$ 300oC followed by crystallization (Fig 19) shows interesting changes

has been found by the structural relaxation discussion of the present study (Chapter V 1), that a dynamic heating to a temperature of ∽ 300oC followed by furnace cooling structurally relaxes a sample almost completely Hence the sample whose electrical resistance graph has been shown in Fig. 19 can be considered to be almost completely structurally relaxed wheieas the as melt spun sample of Fig. 18 is not The enhancement of start and finish of crystallization of the former (Fig 19) by∽ 15o to∼ 35oC shows that the structural relaxation helps in enhancing the crystallization process

In interpreting their results obtained through Mossbauer spectroscopy Sageusa and Moris [17,18] have argued that the amorphous state instead of changing directly to final crystallised products passes through a series of intermediate states occuring in the temperature range of ∼432o and∽457oC The present results (Fig 18 and 19) also shows a break in the electrical resistance vs temperature curve in the temperature range of∼436o and∽460oC and supports the interpretation of results of Sageusa and Moris Since no TEM and X-ray diffraction was done in the present inves- tigation ,the product phases, however, could not be identified The thermally relayed sample (Fig 19) also shows an addi- tional arrest in the electrical resistance-temperature curve in the temperature range of∼383o and∽400oC The presence of this additional arrest suggest the showing up

of a finer change which was either obsecured by the rapid
reaction occuring in the unrelaxed sample (Fig 18) or the
occurence of a structural relaxation induced new intermediate
state   Further work using TEM and X-ray diffraction is
necessary to throw light on the nature of this observed
change

        The crystallization behaviour of as melt spun
specimen by DSC is shown in Fig 22 All the thermal effects
(except the reversible changes discussed before) are exother-
mic and unlike Swartz et al ([16]and Fig 5), no endothermic
reaction with a clear break in the DSC curve, due to magnetic
transition of the specimen, can be seen

        The first exothermic plateau occurs in the
temperature region of about 316oC to 417oC and shows only
a small thermal effect   It is followed by an exothermic
peak between⌄417oC to⌄500oC, termed as the first exothermic
peak or first thermal effect and is followed by a very sharp
thermal effect between⌄500oC and⌄540oC, called the second
exothermic peak   Finally a small thermal effect, smallest
of the three and is called third exothermic peak, is observed
above 540oC but it does not go to completion as the experiment
was terminated at⌄600oC, the high temperature limit of the
DSC apparatus.   The nature of the exothermic peaks indicate
that there are at least four distinct processes evolving

different quantities of heat and the reactions overlap
each.

A specimen rapidly heated in the DSC aparatus
within 15 to 20 minutes to 600oC follwed by 10 minutes of
anneal is cooled to room temperature and then the DSC
curve is traced (termed as 600oC/10 min/1st run) (Fig 25)
A small thermal effect between 433oC and 499oC shows that
complete crystallization has not occured in the sample even
if it is heated to much higher temperature above the crysta-
llization temperature   Normally at a temperature higher
than the crystallization temperature one should expect such
a thin ribbon to crystallize completely in a short time

The nature of the DSC curves of the preheat treated
specimens, 310oC/25 min/1st run (Fig 23) and 310oC/60 min/
4th run (Fig 24) are very similar to the DSC curve of the
as melt spun specimen (Fig 22), the exothermic peaks
appear more or less at the same temperature regions However
it is observed that the start of the exothermic reactions
in Fig 24 appear at about 10 to 20oC lower temperatures
than that observed in the other two cases (Fig 22 and Fig 23)
From the discussion on structural relaxation, we have seen
that annealing at 310oC for 25 minute does not relax the
sample to a great extent as compared to the as melt spun/
first run specimen   In both the cases the temperature
regions corresponding to the start and finish of each of
the exothermic peaks are almost the same   Hence we may

conclude that whenever two samples are more or less in the same structurally relaxed condition, as is the case of as melt spun/first run and 310oC/25 min/1st run samples, the crystallization behaviour remains more or less the same However from structural relaxation data, we have seen that the 310oC/60 min/4th run sample has complete structural relaxation When this sample crystallizes, we see that the temperature region corresponding to the start and finish of each peak is shifted somewhat to lower temperatures of approximately within 10 to 20oC This indicates that stru-ctural relaxation enhances crystallization Further evide-nce of this can be obtained if we compare the crystalliza-tion behaviour of as melt spun/first run (Fig 22) and fourth run (Fig 28) samples as also 310oC/25 min/1st run and 310oC/25 min/5th run (Fig 27) samples Enhancement of crystallization start temperature for completely relaxed specimen is also shown in electrical resistance data where as melt spun samples are taken to crystallization in first run (Fig 18) and second run (Fig 19) respectively The electrical resistance data also shows an enhancement of crystallization Hence comparing the structural relaxation data, electrical resistance data (Fig 18 and 19) as well as the DSC data (Fig 22 to 24), we conclude that recyc-ling between room temperature to 320oC is more effective in enhancing the crystallization behaviour rather than isothermal annealing at 310oC for 25 minutes The most

important conclusion from these studies is that complete structural relaxation is obtained by _ven one cycle of heating to $\vee$ 320oC to cause enhancement of crystallization process This also disproves the common belief that the as melt spun specimens become completely relaxed during heating before crystallization starts

In the above discussion only the gross changes observed due to different isothermal or dynamic treatments of the samples are pointed out There are certain fine changes in the DSC curves for the different samples too (Fig 26 and 27) In the DSC curves of as melt spun, 100oC/ 25 minute and 310oC/25 minute—all first runs (Fig 26) show that there are shoulders on the tailends of both the first and second exothermic peaks. Which indicate that the thermal effects observed are possibly not due to two single processes The discussion of crystallization behaviour of electrical resistance shows also a break in the electrical resistance in both Fig 18 and 19 at 460oC Both the electrical resistance as well as the DSC results support the view that crystallization does not follow a single or two step process but rather a multistep process Sageusa and Moris [17,18] also found by Mossbauer spectroscopy that Metglas 2605Sc is going through a series of multistep reactions during crystallization, forming metastable intermediate products and the amorphous phase continuously rearranging itself throughout the entire crystallization

process Hence the observations suggest that crystallization is a series of overlapping reactions

Preheat treatment as well as dynamic heating appears to affect not only the start and finish of crystallization but also appears to affect the shape of the peaks For example, comparison of the first exothermic reaction giving rise to a small plateu just before the first exothermic peak for the as melt spun/1st run (Fig 22) ana 310oC/25 min/1st run (Fig 23) with those of 310oC/60 min/1st run (Fig.31), 310oC/60 min/ 4th run (Fig 24)and 310oC/25 min/ 2nd run (Fig 30) samples, shows that the starting of the plateu becomes more sharply defined for the heat treated specimens The fine structures in the DSC peak appear to be affected by heat treatment (Fig 26)   The DSC curves of 1st and 5th run of 310oC/25 min samples (Fig 27) show some new variations in the DSC plots for structurally relaxed sample. The comparison of the as melt spun/first run (Fig 22) and as melt spun/4th run shows the presence of an additional peak in the temperature region of~3280C to~ 343oC   This is however, not consistant with our observation of structural relaxation ana its effect on crystallization. Since the completely relaxed specimen (310oC/60/min/ 4th run) (Fig 24) does not show anv extra thermal effect in the corresponding temperature region, it is rather hard to explain why the as melt spun/4th run sample, which is also a completely relaxed specimen, should not have the

thermal effect   Some spurious effect can not be ruled out and this is particularly suspected because this expriment was carried out only once, whereas for all the others, the experiments were repeated at least twice   From our electrical resistance plots we have seen that structural relaxation is throwing up new arrests during crystallization (Fig 18 and Fig 19)   From this, we can possibly conclude that either structural relaxation is showing up clearly a reaction already present or some new reactions involving the formation of new intermediate states are taking place

One importan observation is that all the as melt spun samples, 100oC/25 min   annealed samples, 310oC/25 min   samples with or without one or more thermal recycling through a temperature below crystallization (<330oC) do not become brittle   As the literature survey suggests (Chapter III 2) some glasses become brittle if subjected to some heat treatments below crystallization   Davis [44] observed that there is a relation between the final crystallized product and the corresponding amorphous phase in the matter of brittleness Further identification with the final products in the present study may show whether the relationship extends to the present system too

iii) Reversible change

Figs 35 to 43 show three specific temperature regions of DSC thermogram for metallic glass samples with different heat treatments   From both the Q and $\frac{dQ}{dT}$ plots,

it is apparent that there is a sharp and small endothermic
dip in the temperature region of ∨ 315oC to ✦ 322oC (Fig 35
to 37) (termed 1st reversible change), another exothermic
small and sharp change at a temperature region just above
∨ 197oC (Fig. 38 to 40) (termed second reversible change)
and most probably a third endothermic dip at a temperature
region just below ∨ 122oC (Fig 41 to 43) (termed third
reversible change) The presence of the second and third
reversible changes is also found in the electrical resis-
tance temperature curve of the structurally relaxed sample
as small decrease in electrical resistance in more or less
the same temperature regions (Fig 21)   These changes are
reversible in nature and do not change their position when
the samples are subjected to both isothermal and dynamic
heat treatments and hence do not depend on the state of
structural disorder (Figs 35 to 43).

There may be two kinds of reversible changes in
metallic glasses One is the expected magnetic change due
to Curie temperature transformation Any of the observed
changes are not due to the magnetic transformation The
prepared specimens show T_c of 352oC for unrelaxed samples
and 368oC for relaxed samples The reason why it is not
possible to observe the reversible magnetic change in DSC
traces is that these values of Curie temperature falls within
the temperature region where an exothermic change has been
observed.

The literature suggests that the nature of the changes obtained talies well with that of CSRO In some cases of the unrelaxed first run specimens, these changes are not shown up clearly This is probably because of the camouflage of such small changes by structural relaxation However in second or subsequent runs the changes show up more clearly The possibility of such camouflaging in electrical resistance had been suggested by Ballanzat et al and others [33] Hence they had suggested further studies by different methods particularly calorimetric tests to detect such changes. The fact that the other investigators who worked with the as obtained Metglas 2605SC [16 to 19] did not find these changes in electrical resistivity, DTA or DSC measurements may also be because of the structural relaxation The results of electrical resistance (Fig 21) also shows the changes in electrical resistance corresponding the second and third change in DSC The first change can not be detected by electrical resistance is because no such experiment has been done in that temperature narrow Whether these cchanges, which are occuring in very narrow temperature regions, are due to CSRO requires to be further investigated

iv) Magnetic properties

Curie temperature determination studies have been carried out with as melt spun ribbons (Fig 44) and ribbons relaxed by a cyclic heating of few degrees of centigrade per minute upto~367oC followed by furnace cooling in air in

The results show an increase
in Curie temperature by about 11oC for the structurally
relaxed sample (Fig 45) than that of structurally unrelaxed
sample T_c is 352oC (Fig 44)   Since structural relaxation
of specimen increases T_c and the T_c of the specimen lies
in the temperature range in which crystallisation appears
to have started, it is possible that the T_c of unrelaxed
sample is not of the lowest limit value

The Curie temperature obtained in this investi-
gation is considerably different from that reported by
other researchers [16 to 19]   Even the values of T_c given
by Sagousa and Moris [17 and 18],   whose results in case
of crystallization is talying closely with us, is very
different   This probably is because of microscopic differ-
ence in composition for different samples   However the
general idea that structural relaxation or TSRO enhances
Curie temperature is supported by the findings of present
study. The magnetization and demagnetization curves obtained
by the present study for as melt spun (Fig 46), as melt
spun after 1st run (Fig 47) and as melt spun sample with
two thermal cycles (Fig 48) show that the that the sample
follows the general characteristics shown by soft magnetic
materials   However, they do not reach the saturation even
after a high field   But the structurally relaxed sample
(Fig.47 and Fig 48) shows a high value of moment per gram
with a small field than the structurally unrelaxed sample

(Fig 46) But onece the structural relaxation is achieved,
subsequent thermal cycling do not produce any further effect
as is evident from Fig 47 and 48

CHAPTER VI

CONCLUSION

The preparation an characterization of Metglas 2605Sc show the following

i)   The process of preparing reasonably wide (6 to 7 mm) ribbons by single roller melt spinning process has been developed and standardized.

ii)   The range of different process parameters on the preparation of ribbons has been established   The time and temperature path difference between the molten metal state and the final amorphous state is important in achieving an amorphous structure and the jet turbulence of the molten metal decides the physical characteristics of the ribbon It is difficult, under existing conditions, to get an amorphous state from the liquidous temperature only and some superheat is found to be necessary

iii) The amorphous to crystalline transformation seems to be the net effect of a series of overlopping reactions   The alloy is rearranging itself throughout the transformation region through a series of steps, probably precipitating intermediate products   This continuous rearrangement extends not only at the finish of crystallization, but well beyond to it

iv)   Structural relaxation enhances crystallization by enhancing the start and finish or crystallization temperature It also shows up additional variations in calorimetric and electrical resistance tests indicating either old reactions camouflaged by structural disorder are showing up or crystallization takes a slightly different path for structurally relaxed sample

v)   The thin metallic glass samples structurally do not relax much when compared to as melt spun samples up to an isothermal anneal of 310oC and 25 minute severity   whereas an isothermal anneal at 310oC for 60 minute relaxes it completely

vi)   One dynamic thermal recycling with a few degrees per minute of heating rate through a temperature near but not far below crystallization start almost completely structurally relaxes a sample   Hence the effect on structural relaxation of an dynamic annealing is equivalent to an isothermal anneal at 310oC for a time not less than 25 minute but not greater than 60 minute

vii)   The as melt spun thin samples do not crystallize completely even after annealing to a temperature higher than crystallization temperature for several minutes,

viii) The ductile as melt spun ribbons do not lose their ductility even after isothermal annealing (upto 310oC) for some time (25 minutes) and / or subjected to one or more

thermal cycling through a temperature below crystallization starting temperature

ix) The presence of CSRO changes in this composition has been detected The detection has been done by electrical resistivity and particularly calorimetric tests. There are more than one but two and most probably three CSRO changes in the alloy below crystallization

x) Structural relaxation enhances Curie temperature and easens magnetization process

REFERENCES

1 D Pavuna, J of Mat Sc , 16 (1981) 2419

2. S Kavesh, Metallic Glasses- American Society for Metals
    Metals Park, Ohio 44073, USA, 36

3 H A Davis, Phys and Chem of Glasses, (1976) 17

4 H A Davis,J Aucote and J B Hull, ' Nature'- Phys Sc
    13 (1973) 246

5 H A Davis, and B G Lewis, Scripta Metall 9 (1975)1107

6 H S Chen, Acta Metall.22 (1974) 1505

7 H H Liebermann, Mat Sc Engg 43 (1980) 203

8 D Pavuna, J Non Cryst Sol 37 (1980) 133

9. D Pavuna, J Non Cryst. Sol 37 (1980) 417

10. D.C Agarwal and E A Chakachary, Bulletin of Mat Sc 7,
    No.2 (July, 1985) 137

11 S. Huang, Proc. 4th Int Conf on Rapidly Quenched
    Metals,The Japan Institute of Metals,1 (1982) 65

12. U. Koster and U Herold, Topics in Applied Physics,
    46, H J. Gunterford and H. Beck ed , Springer and
    Verlag (1981) 225

13 S Ranganathan and S Banerjee, Metallic Glasses, T R
    Anatharaman ed, Trans Tech Publication (1984) 147

14. U. Herold and U Koster, Proc. 3rd Int Conf on
    Rapidly Quenched Metals, The Metals Society London (1978) 81.

15. U Koster and U Herold, Topics in Applied Physics,
    46, H J. Gunterford and H Beck ed, Springer and Verlag
    (1981)253.

16 J C Swartz, R Kossowsky, J J Haugh and R ᵋ Crause , J. Appl Phys 52 No 5 (May 1981) 3324

17 N Sageusa and A H Moris, Phys Review B, 27,No 7 (April, 1983) 4027

18 N Sageusa and A H Moris, Phys Review B, 26, No 1 (July 1982) 305

19 B Bhanu Prasad, A K. Bhatnagar and R Jagannathan,J Appl Phys 54,No 4 (April 1983) 2019

20. C L Violet and D N Pipkorn, J Appl Phys 42 (1971)4339

21. M Goldstein, Modern aspectsof the Vitrious state, J D Mackenji ed Buttersworth Washington (1960)Vol 3, 90

22. S E Petrie, Polymorphic Materials, ASM ed (1975) 55

23 A J Kovaes, R A Stratton and J D Ferry, J Phys Chem 6-7 (1963) 152.

24. T Egami, J of Mat Sc 13 (1978) 2587-2599

25 M h Cohen and D Turnbull, J. Chem Phys 31 (1959) 1164

26. R Madin and T Masumoto, Mat Sc Engg 9 (1972)153

27. R. Williams and T Egami, ICLE Trans Mag Mag 12 (1976)927

28. T. Sochiroda, M Kavira and T. Masumoto, J Non Cryst Sol . 21 (1976) 688

29. H.H Liebermann, C D Graham Jr and P J Flanders,IEEE trans. Mag Mag 13(1977) 1541

30. E. Ballanjat,Scripta Metall 14 (1980) 173

31. A.V.D. Beukel and S. Radelaar, Acta Metall31 (1983) 419

32. T. Egami, Mat Res. Bull 13 (1978) 557-62

33   C Ballanjat, J T Stanley, C Mairy and J Hillbert ,
      Acta Metall 33 No 5 (1985) 785

34   J M Ziman, Phil Mag 6 (1961) 1013

35   T Egami, Mat Res Bull 13 (1978) 557

36.   H S Chen, Proc 4th Int Conf on Rapidly Quenched
      Metals, The Japan Institute of Metals, 1 (1982) 495

37   K.F Kelton and F Spapean, Proc 4th Int Conf on
      Rapidly Quenched Metals, The Japan Institute of Metals,
      1 (1982) 527

38   C.P.P. Chau and D Turnbull J Non Cryst Sol 17 (1975)
      169

39   F E. Lubrosky, J J   Backer, and R O McCary, IEEE Trans
      Mag Mag 11 (1975) 1644.

40.   S.S. Chen, R.C Sherwood and L M Greorgy, IEEE Trans
      Mag. Mag 13 (1977) 1538

41.   T Egami and R J Flanders, AIP Conf Proc 29 (1976)220

42.   F E. Lubrosky, R O McCary and J J Beker, Proc 2nd
      Int Conf on Rapidly Quenched Metals, MIT (1975)

43   J.L. Waller, F Baco and F E Lubrosky, Mat Sc Engg.
      24 (1976) 239

44.   G Hunger, K.D Ward and H A. Davis, Zeitschrift fur
      Metallkunde 70 (1979) 714.

45.   T. Mihara, S Otake, H Fukushima and M Doyama, J Phys
      F 11 (1981) 727

98038

MSP- 1906-m-ROY- FAB